REMARKS

Claims 1-116 were pending in the application. Claims 1-29, 36-73, 75-88 and 95-115 were withdrawn from consideration as directed to non-elected inventions. Claims 30-34 and 116 have been amended. Claims 74 and 89-94 have been cancelled without prejudice.

The title of the invention has been amended to more clearly describe the claimed invention. Support for this amendment can be found throughout the application as originally filed, including for example, in paragraph [00283].

Claim 30 was amended to incorporate the limitations of withdrawn claim 1, to recite specific levels of sequence identity, and to specify that the polypeptide encodes a potassium channel. Claims 31 and 32 were amended to recite specific levels of sequence identity and to remove reference to non-elected sequences. Claim 33 was amended to recite that the polypeptide encodes a human potassium channel. Claim 34 was amended to recite that the polypeptide encodes a human TREK-2 channel. Claim 116 was amended to remove reference to non-elected sequences and to recite that the chimeric receptor comprises a functional domain of TREK-2. Support for the amendments can be found throughout the application as originally filed including, in paragraphs [00010], [00050] and [00283].

No new matter has been added.

Upon entry of this amendment, claims 30-35 and 116 will be pending.

Priority

The Office Action alleges that "the applications upon which priority is claimed fails to provide adequate support under 35 U.S.C. 112 for claims 30-35, 74, 89-94 and 116 ..." Applicants do not agree.

As will be discussed in greater detail below in relation to the rejection under 35 U.S.C. §§ 101, 112, and 102, both the present application and U.S. provisional applications 60/203,305 and 60/216,893 satisfy the requirements of 35 U.S.C §§ 101 and 112, first paragraph. Pages 2-3 of U.S. provisional application 60/203,305 recites, *inter alia*, that the claimed receptor is a 4Tm-2P potassium channel and identifies closely related family members (TASK and TREK-1). Page 37 of U.S. provisional 60/203,305

further recites that the claimed polypeptide is a human TREK-2 channel. Pages 40-41 of U.S. provisional 60/203,305 recites results of tissue expression profiling of the claimed sequences. Accordingly, Applicants assert that the applications upon which priority is claimed do provide adequate support under 35 U.S.C. §112 and that the present invention is entitled to the priority dates of U.S. provisional applications 60/203,305 and 60/216,893.

Rejection under 35 U.S.C. §112, second paragraph

Claims 30-35, 74, 89-94 and 116 stand rejected under 35 U.S.C. §112, second paragraph, as allegedly indefinite. The Office alleges that the claims "recite or encompass SEQ ID NO: sequences which are not elected ..." (Office Action, page 4). Although Applicants do not agree, Applicants have amended the claims to remove reference to non-elected sequences, thereby rendering the rejection moot.

Rejection under 35 U.S.C. §101

Claims 30-35, 74, 89-94 and 116 stand rejected under 35 U.S.C. § 101 because the claimed invention allegedly "is not supported by either substantial asserted utility or a well established utility" and that "further research to identify or reasonably confirm a 'real world' context of use is required." (Office Action, pages 2-3). (Office Action, page 2). Applicants respectfully disagree. The claimed invention is supported by a substantial asserted utility ***and*** a well established utility.

The specification discloses that the claimed receptor is a 4Tm-2P potassium receptor and, more specifically, identifies the receptor as a TREK-2 receptor. (see, for example, paragraph [00283]). As set forth in the specification, 4Tm-2P receptors are "postulated to be responsible for the background potassium ion currents that are thought to set the resting membrane potential (Lesage F and Lazdunski M, (1999). "Potassium Ion Channels, Molecular Structure, Function, and Diseases" in Current Topics in Membranes 46; 199-222 ed. Kurachi, Y., Jan, LY., and Lazdunski, M.) (*see* paragraph [00010] of specification). The specification further asserts that because 4Tm-2P receptors are "activated by volatile general anesthetics such as chloroform halothane and isoflurane (Patel *et al.*, Nature Neuroscience, **1999**, 2:422-426) ... [the] channels [are

implicated] as a site of activity for these anesthetics. In addition, compounds that modify the activity of these channels may also be useful for the control of neuromotor diseases including epilepsy and neurodegenerative diseases including Parkinson's and Alzheimer's. Also compounds that modulate the activity of these channels may treat diseases including but not limited to cardiovascular arrhythmias, stroke, and endocrine and muscular disorders. (*see* specification at paragraph [00111]. Therefore, specific, substantial and credible utilities exist for the claimed receptors.

Utility Examination Guidelines

The Utility Examination Guidelines (the "Guidelines") require that a claimed invention have a specific, substantial and credible asserted utility, or, alternatively a well-established utility. Applicants have asserted that the claimed polypeptides are useful, *inter alia*, to generate antibodies specific for the claimed polypeptides.

As discussed in greater detail below, the claimed polypeptides share about 97% sequence identity with a potassium channel with known and proven function.[1] In fact, Applicants point out that the receptor with known and proven function is the same receptor as asserted by Applicants in the application as originally filed. The fact that the claimed polypeptides share 97% sequence homology with a receptor with known function supports the assignment of the same specific, substantial, and credible utilities of known 4Tm-2P receptors to the claimed polypeptides. The utilities asserted are art-established: those skilled in the art would readily acknowledge that the claimed polypeptides are useful within the meaning of 35 U.S.C. § 101.

Under the Guidelines, Office personnel are instructed to review the specification and claims of the application to determine if a specific and substantial utility that is credible is present. The Guidelines note that the specific and substantial requirement "excludes 'throw-away', insubstantial,' or 'nonspecific' utilities, such as the use of a complex invention as landfill." The Guidelines go on to note that an Examiner's "*prima facie* showing ***must*** establish that it is more likely than not that a person of ordinary skill in the art would not consider that any utility asserted by the applicant would be specific

[1] See alignment attached hereto.

and substantial." "If the applicant has asserted that the claimed invention is useful for any particular practical purpose (*i.e.*, it has a 'specific and substantial utility') and the assertion would be considered credible by a person of ordinary skill in the art, do ***not*** impose a rejection based on lack of utility." (Guidelines, emphasis added).

The Guidelines comment on the use of computer based analysis of nucleic acids to assign functions to a nucleic acid or polypeptide based upon homology to sequences found in databases. Specifically, the Guidelines state that the:

> suggestions to adopt a *per se* rule rejecting homology based assertions of utility ***are not adopted***. An applicant is entitled to a patent to the subject matter claimed unless statutory requirements are not met (35 U.S.C. 101, 102, 103, 112) . . .The inquiries involved in assessing utility are fact dependent, and the determinations must be made on the basis of scientific evidence. Reliance on the commenters' *per se* rule, rather than a fact dependent inquiry, is impermissible because the commenters provide no scientific evidence that homology-based assertions of utility are inherently unbelievable or involve implausible scientific principles. *See, e.g., In re Brana,* 51 F.3d 1560, 1566, 34 USPQ2d 1436, 1441 (Fed. Cir. 1995) (rejection of claims improper where claims did 'not suggest an inherently unbelievable undertaking or involve implausible scientific principles' and where ''prior art * * * discloses structurally similar compounds to those claimed by the applicants which have been proven * * * to be effective').
>
> A patent examiner ***must*** accept a utility asserted by an applicant unless the Office has evidence or sound scientific reasoning to rebut the assertion. The examiner's decision must be supported by a preponderance of all the evidence of record. *In re Oetiker,* 977 F.2d 1443, 1445, 24 USPQ2d 1443,1444 (Fed. Cir. 1992). More specifically, when a patent application claiming a nucleic acid asserts a specific, substantial, and credible utility, and bases the assertion upon homology to existing nucleic acids or proteins having an accepted utility, the asserted utility must be accepted by the examiner unless the Office has sufficient evidence or sound scientific reasoning to rebut such an assertion. ''[A] 'rigorous correlation' need not be shown in order to establish practical utility; 'reasonable correlation' is sufficient.'' *Fujikawa* v. *Wattanasin,* 93 F.3d 1559, 1565, 39 USPQ2d 1895, 1900 (Fed. Cir. 1996). The Office will take into account both the nature and degree of the homology.
>
> When a class of proteins is defined such that the members share a specific, substantial, and credible utility, the reasonable assignment of a new protein to the class of sufficiently conserved proteins would impute the same specific, substantial, and credible utility to the assigned protein. If the preponderance of the evidence of record, or of sound scientific reasoning, casts doubt upon such an asserted utility, the examiner should reject the claim for lack of utility under 35 U.S.C. 101. For example, where a class of proteins is defined by common structural features, but evidence shows that the

> members of the class do not share a specific, substantial functional attribute or utility, despite having structural features in common, membership in the class may not impute a specific, substantial, and credible utility to a new member of the class. When there is a reason to doubt the functional protein assignment, the utility examination may turn to whether or not the asserted protein encoded by a claimed nucleic acid has a well-established use. If there is a well-established utility for the protein and the claimed nucleic acid, the claim would meet the requirements for utility under 35 U.S.C. 101. If not, the burden shifts to the applicant to provide evidence supporting a well-established utility. There is no *per se* rule regarding homology, and each application must be judged on its own merits.

(Guidelines; emphasis added).

Preliminarily, Applicants remind the Office that specific and substantial utilities have been provided for the claimed polypeptides and that the asserted utilities are credible to one of skill in the art. The Office has failed to provide any evidence that "it is more likely than not that a person of ordinary skill in the art would not consider that any utility asserted by the applicant would be specific and substantial."

Art-Recognized Utility

The Utility requirement may also be satisfied by an "Art Established Utility" which means that "a person of ordinary skill in the art would immediately appreciate why the invention is useful based on the characteristics of the invention... and the utility is specific, substantial and credible." (M.P.E.P. §2107).

As discussed above, the claimed polypeptides are identified in the present application as TREK-2 channels, members of the 4Tm-2P family of potassium channels (see, for example, paragraphs [00010], [00011] and [00283]). Based on a BLAST alignment, SEQ ID NO:73 exhibited about 97% sequence identity with a known TREK-2 channel (see Accession No. NP_612191 sequence viewer attached hereto with copies of references cited therein (Gu et al., J. Physiol. (Lond.) 539 (Pt 3), 657-668 (2002); Goldstein et al., Nat Rev Neurosci 2 (3), 175-184 (2001); Lesage et al., J. Biol. Chem. 275 (37), 28398-28405 (2000); alignment of sequence with SEQ ID NO:73). The probability, therefore, that the claimed polypeptides' function and structure are related to those of the known potassium channel is, accordingly, extremely high. The Office has failed to provide any "countervailing evidence" required by the Utility Examination

Guidelines to show that the function asserted by Applicants or the relationship with known potassium channels does not exist.

Applicants respectfully point out that the functions and activities of such channels are well-known to those of skill in the art and include, *inter alia*, setting the resting membrane potential, the site of activity for certain anesthetics, controlling neuromotor diseases including epilepsy and neurodegenerative diseases including Parkinson's and Alzheimer's, and treating cardiovascular arrhythmias, stroke, and endocrine and muscular disorders. Applicants further point out that the Gu reference, for example, confirms that there are functional isoforms of the TREK-2 channel.

Because the claimed polypeptides share such significant sequence identity with known receptors, the probability, therefore, that the claimed polypeptides' function and structure are related to those of the known receptor is, accordingly, extremely high. The Office has failed to provide any "countervailing evidence" required by the Utility Examination Guidelines to show that the relationship does not exist.

Applicants note for the record that the Patent Office has issued patents in the field of ion channels for applications disclosing the same amount of information as is described in the present application. The Office has granted and apparently continues to grant patents to ion channel proteins, their encoding polynucleotides and antibodies directed to them ***in which no specific biological activity has been confirmed.*** Specifically, Applicants would like to bring the following US Patents which claim potassium channels to the Office's attention:

6,562,593 Merkulov *et al.* "Isolated human transporter proteins, nucleic acid molecules encoding human transporter proteins, and uses thereof" (Claims an isolated polynucleotide and method for producing polypeptide)

6,309,855 Duprat *et al.* "Family of mammalian potassium channels, their cloning and their use, especially for the screening of drugs" (Claims isolated polynucleotide)

6,087,488 Ganetzky *et al.* "Potassium ion channel genes and proteins" (Claims isolated polynucleotide)

5,710,019 Li *et al.* "Human potassium channel 1 and 2 proteins" (Claims an isolated polypeptide)

Applicants submit that these issued US Patents are evidence of an art recognized utility for ion channels. Upon review of the file histories of several of the above-identified patents, it is apparent that the present application provides at least as much functional data as the applications giving rise to the issued patents provided. For example, U.S. Patent 6,562,593 is directed to:

> An isolated nucleic acid molecule consisting of a nucleotide sequence selected from the group consisting of:
> (a) a nucleotide sequence that encodes a protein comprising the amino acid sequence of SEQ ID NO:2;
> (b) a nucleotide sequence consisting of the nucleic acid sequence of SEQ ID No:1; and
> (c) a nucleotide sequence that is completely complementary to a nucleotide sequence of (a)-(b).

(claim 1). The specification of the patent reveals that the claimed sequences were "related to the differentiation-associated Na-dependent inorganic phosphate cotransporter subfamily." (*see* column 11, lines 34-55). Apparently the activity of a known "differentiation-associated Na-dependent inorganic phosphate cotransporter" was imputed to the claimed sequence based on sequence similarity. The specification further provides sequence information, and the putative identification of structural elements including start codon, stop codon, and phosphorylation sites (*see* Figure 1).

The present application provides analogous information to that set forth by U.S. Patent 6,562,593. For example, the application indicates that the claimed polypeptides are TREK-2 channels. Sequence information relating to the claimed polypeptides is included throughout the specification and the appended sequence listing. Also, the present application provides expression data relating to the claimed polypeptides.

A brief review of commercially available antibodies reveals that an antibody specific for TREK-2 is available from Chemicon Inc. (product sheet attached hereto). The fact that such a product is commercially available proves that there is a well-established utility for the presently claimed polypeptides.

Accordingly there could be no better proof of the utilities of the claimed polypeptides -- such products are made by a manufacturer (who expects to sell them) for consumers (who expect to buy them). Any argument that there is no art-recognized utility for such polypeptides seems meritless.

Prior Art Cited by Examiner Confirms the Utility of the Claimed Invention

Applicants note that the Examiner has apparently acknowledged that related receptors disclosed in prior art applications have a "specific, substantial, and credible asserted utility, or a well established utility." As discussed in greater depth below, the Office has levied 35 U.S.C. § 102 rejections over the Meadows et al. application (WO 99/37762), the Meadows et al. patent (U.S. Patent 6,242,217) and the Guegler et al. application (WO 02/24748). Preliminarily, Applicants remind the Office that as set forth in M.P.E.P. 2121, "prior art is presumed to be operable/enabling", and, moreover, that issued U.S. patents are presumed to be valid, i.e., comply with the requirements of 35 U.S.C. §§ 101, 102, 103 and 112.

In the present Office Action, the Examiner rejected the claims under 35 U.S.C. § 112, first paragraph because "the claimed invention is not supported by either a specific, substantial or credible utility." The Office's citation of the Meadows application, the Meadows patent and the Guegler application as prior art, however, confirms that the Office considers that the cited references provide "a specific and substantial asserted utility or a well established utility". Indeed, Applicants remind the Examiner that the Meadows patent is an issued U.S. patent, presumed to be valid. The present disclosure provides proof of utility regarding the claimed invention that is similar to the utility disclosed in the cited references. Accordingly, the claimed potassium channels also provide "a specific and substantial asserted utility or a well established utility".

Rejections under 35 U.S.C. § 112, first paragraph

1. Enablement

Claims 30, 32-35, 74, 89, 91-94 and 116 stand rejected under 35 U.S.C. § 112, first paragraph, as allegedly "not supported by either a substantial asserted utility or a well established utility for the reasons set forth above, one skilled in the art clearly would not know how to use the claimed invention." Applicants do not agree.

As discussed above, the present invention ***is*** supported by a specific, substantial, and credible asserted utility as well as a well-established utility. Accordingly, Applicants respectfully request that the rejection be withdrawn.

2. Written Description

Claims 30, 32-35, 74, 89, 91-94 and 116 stand rejected under 35 U.S.C. § 112, first paragraph, as allegedly "containing subject matter which was not described in the specification in such a way as to reasonably convey to one skilled in the relevant art that the inventor(s), at the time the application was filed, had possession of the claimed invention." The Office alleges that the claims "encompass an isolated polypeptide and fragments of proteins without functional limitations." Applicants disagree.

Notwithstanding the foregoing, Applicants have amended the claims to recite that polypeptides have at least 98% sequence identity to SEQ ID NO:73 and to specify that the polypeptides encode a potassium channel.

Applicants respectfully assert that the claimed invention complies with the written description requirement of 35 U.S.C. §112, first paragraph. The claims, as amended, are analogous to the exemplary claim recited in Example 14 of the Written Description Guidelines set forth above. In the pending claims, homologs having at least 98% sequence identity to SEQ ID NO:73 are recited. The analysis set forth in the Guidelines states that "the genus of proteins that must be variants of SEQ ID NO: 3 does not have substantial variation since all of the variants must . . . have at least 95% identity to the reference sequence, SEQ ID NO: 3. . ." and that "[t]he single species disclosed is representative of the genus because all members have at least 95% structural identity with the reference compound and because of the presence of an assay which applicant provided for identifying all of the at least 95% identical variants of SEQ ID NO: 3 . . .". The Written Description Guidelines further state that "[o]ne of skill in the art would conclude that applicant was in possession of the necessary common attributes possessed by the members of the genus" and that "the disclosure meets the requirements of 35 U.S.C. §112 first paragraph as providing adequate written description for the claimed invention."

Applicants respectfully assert that the genera of proteins claimed comply with the written description requirement. The genera encompassed by the pending claims do not have substantial variation since all species within the genera must encode a potassium and because all must have at least 98% sequence identity to SEQ ID NO:73.

Applicants also provide methods for assaying for ion channel polypeptide-interacting proteins (Example 7), methods for analyzing protein-protein interactions involving ion channel polypeptides (Example 8), and assays to identify modulators of ion channel activity (Example 9).

The Office Action has failed to provide any evidence or reasoning why the specific species described, along with a description of the attributes and features of the polypeptides that comprise the claimed genera, does not constitute adequate description of the claimed subject matter. One of skill in the art would conclude that Applicants were in possession of the necessary common attributes possessed by the members of the genera and that the disclosure meets the requirements of 35 U.S.C. §112 first paragraph as providing adequate written description for the claimed invention.

University of California was cited to support the Office's assertion that the pending claims did not satisfy the Written Description requirement. Applicants respectfully assert that persons of ordinary skill in the art would recognize that Applicants were in possession of the claimed subject matter. As discussed above, the pending claims provide Written Description support for themselves as they are virtually identical to those originally filed.

University of California v. Eli Lilly and Co. is distinguishable from the present fact pattern. The Written Description Guidelines discuss the *University of California* scenario in Example 7 and state that the exemplary claim (An isolated DNA comprising SEQ ID NO: 16) does not satisfy the written description requirement because "[t]he present claim encompasses full-length genes and cDNAs that are not further described. There is substantial variability among the species of DNAs encompassed within the scope of the claims because SEQ ID NO:16 is only a fragment of any full-length gene or cDNA species. When reviewing a claim that encompasses a widely varying genus, the examiner must evaluate any necessary common attributes or features."

Again, as discussed in greater detail above, the pending claims do satisfy the written description guidelines because, *inter alia*, there is no "substantial variation among the species of polypeptides" – a minimum of 98% sequence homology is required to SEQ ID NO:73, and a functional limitation is set forth. Applicants respectfully point out that the facts relating to the pending claims are analogous to Example 14 of the "The Revised

Interim Written Description Guidelines Training Materials", in which the exemplary claim is said to satisfy the Written Description Requirement.

Rejections under 35 U.S.C. § 102

Claims 30, 32-35, 74, 89, 91-94 and 116 stand rejected under 35 U.S.C. § 102(b) as allegedly anticipated by Meadows et al. (WO 99/37762; hereinafter the "Meadows application"). The Office asserts that the Meadows application discloses a "potassium channel comprising SEQ ID NO:2 which is 64.3% best local similarity to the claimed polypeptide of SEQ ID NO:73."

Preliminarily, Applicants note that the claims have been amended to require at least 98% sequence identity to SEQ ID NO:73. Claims 74, 89 and 91-94 have been cancelled without prejudice. Because the Meadows application fails to teach or even suggest a polypeptide having at least 98% sequence identity to SEQ ID NO:73, the Meadows application fails to anticipate.

Claims 30, 32-35, 74, 89, 91-94 and 116 stand rejected under 35 U.S.C. § 102(e) as allegedly anticipated by Meadows et al. (U.S. Patent 6,242,217; hereinafter the "Meadows patent"). The Office asserts that the Meadows patent discloses a "potassium channel comprising SEQ ID NO:2 which is 64.3% best local similarity to the claimed polypeptide of SEQ ID NO:73."

Preliminarily, Applicants note that the claims have been amended to require at least 98% sequence identity to SEQ ID NO:73. Claims 74, 89, 91-94 have been cancelled without prejudice. Because the Meadows patent fails to teach or even suggest a polypeptide having at least 98% sequence identity to SEQ ID NO:73, the Meadows patent fails to anticipate.

Claims 30-35, 74, 89, 91-94 and 116 stand rejected under 35 U.S.C. § 102(e) as allegedly anticipated by Guegler et al. (WO 02/24748; hereinafter the "Guegler application"). The Office asserts that the Guegler application discloses a potassium channel which is 100% identical to the claimed polypeptide of SEQ ID NO:73."

Preliminarily, Applicants note that the Guegler application is not prior art against the present application. According to 35 U.S.C. § 102(e)(1), "an international application filed under the treaty defined in section 351(a) shall have the effects for the purposes of this subsection of an application filed in the United States ***only*** if the international application designated the United States and was published ... in the English language." (Emphasis added).

Applicants respectfully point out that the Guegler application, although published in English, does not designate the United States. Accordingly, the Guegler application is only available as prior art as of its publication date, March 28, 2002. This date is after the claimed priority date of the present application and also after the filing date of the present application. Accordingly, the Guegler application is not prior art against the present application.

In view of the foregoing, Applicants respectfully request the reconsideration and withdrawal of the rejections under 35 U.S.C. § 102.

The examination of these claims and passage to allowance are respectfully requested. An early Notice of Allowance is therefore earnestly solicited. Applicants invite the Examiner to contact the undersigned at (215) 665-6904 to clarify any unresolved issues raised by this response.

Respectfully submitted,

Gwilym John Owen Attwell
Registration No. 45,449

Date: **October 4, 2004**
COZEN O'CONNOR, P.C.
1900 Market Street
Philadelphia, PA 19103-3508
Telephone: (215) 665-6904
Facsimile: (215) 701-2004

Attachments:

-Accession No. NP_612190 sequence viewer
-Gu et al., J. Physiol. (Lond.) 539 (Pt 3), 657-668 (2002)
-Goldstein et al., Nat Rev Neurosci 2 (3), 175-184 (2001)
-Lesage et al., J. Biol. Chem. 275 (37), 28398-28405 (2000)
-EMBL-EBI Alignment of sequence with SEQ ID NO:73
-TREK-2 Chemicon Inc. Product Sheet

EMBOSS-Align **Results**

Water Results	
Matrix	Blosum62
Open gap penalty	10.0
Gap extension penalty	0.5
Water output	water-20040921-18375936735599.output
SUBMIT ANOTHER JOB	

```
########################################
# Program:  water
# Rundate:  Tue Sep 21 18:38:02 2004
# Align_format: srspair
# Report_file: /ebi/extserv/old-work/water-20040921-18375936735599.output
########################################
#=======================================
#
# Aligned_sequences: 2
# 1: SID73
# 2: Bang
# Matrix: EBLOSUM62
# Gap_penalty: 10.0
# Extend_penalty: 0.5
#
# Length: 544
# Identity:     520/544 (95.6%)
# Similarity:   529/544 (97.2%)
# Gaps:           7/544 ( 1.3%)
# Score: 2659.5
```

```
#
#
#=======================================

SID73             1 MKFPIETPRKQVNWDPKVAVPAAA-PVCQPKSATNGQPPAPAPTPTPRLS     49
                    ||||||||||||||||||||||| |||||||||||.      .|.||||
Bang              1 MKFPIETPRKQVNWDPKVAVPAAAPPVCQPKSATNGH------HPVPRLS     44

SID73            50 ISSRATVVARMEGTSQGGLQTVMKWKTVVAIFVVVVVYLVTGGLVFRALE     99
                    |||||||||||||.||||||||||||||||||||||||||||||||||||
Bang             45 ISSRATVVARMEGASQGGLQTVMKWKTVVAIFVVVVVYLVTGGLVFRALE     94

SID73           100 QPFESSQKNTIALEKAEFLRDHVCVSPQELETLIQHALDADNAGVSPIGN    149
                    |||||||||||||||||||||:|||||||||||||||||||||||:||
Bang             95 QPFESSQKNTIALEKAEFLRDHICVSPQELETLIQHALDADNAGVSPVGN    144

SID73           150 SSNNSSHWDLGSAFFFAGTVITTIGYGNIAPSTEGGKIFCILYAIFGIPL    199
                    |||:||||||||||||||||||||||||||||||||||||||||||||||
Bang            145 SSNSSSHWDLGSAFFFAGTVITTIGYGNIAPSTEGGKIFCILYAIFGIPL    194

SID73           200 FGFLLAGIGDQLGTIFGKSIARVEKVFRKKQVSQTKIRVISTILFILAGC    249
                    ||||||||||||||||||||||||||||||||||||||||||||||||||
Bang            195 FGFLLAGIGDQLGTIFGKSIARVEKVFRKKQVSQTKIRVISTILFILAGC    244

SID73           250 IVFVTIPAVIFKYIEGWTALESIYFVVVTLTTVGFGDFVAGGNAGINYRE    299
                    ||||||||||||||||||||||||||||||||||||||||||||||||||
Bang            245 IVFVTIPAVIFKYIEGWTALESIYFVVVTLTTVGFGDFVAGGNAGINYRE    294

SID73           300 WYKPLVWFWILVGLAYFAAVLSMIGDWLRVLSKKTKEEVGEIKAHAAEWK    349
                    ||||||||||||||||||||||||||||||||||||||||||||||||||
Bang            295 WYKPLVWFWILVGLAYFAAVLSMIGDWLRVLSKKTKEEVGEIKAHAAEWK    344

SID73           350 ANVTAEFRETRRRLSVEIHDKLQRAATIRSMERRRLGLDQRAHSLDMLSP    399
                    ||||||||||||||||||||||||||||||||||||||||||||||||||
Bang            345 ANVTAEFRETRRRLSVEIHDKLQRAATIRSMERRRLGLDQRAHSLDMLSP    394

SID73           400 EKRSVFAALDTGRFKASSQESINNRPNNLRLKGPEQLNKHGQGASEDNII    449
                    ||||||||||||||||||||||||||||||||||||||||||||||||||
Bang            395 EKRSVFAALDTGRFKASSQESINNRPNNLRLKGPEQLNKHGQGASEDNII    444

SID73           450 NKFGSTSRLTKRKNKDLKKTLPEDVQKIYKTFRNYSLDEEKKEEETEKMC    499
                    |||||||:|||||||||||||||||||||||||||||||:|||||||
Bang            445 NKFGSTSKLTKRKNKDLKKTLPEDVQKIYKTFRNYSLDEEKKEDETEKMC    494

SID73           500 NSDNSSTAMLTDCIQQHAELENGMIPTDTKDREPENNSLLEDRN    543
                    ||||||||||:||||.||:||||:|.||||:..||||||||||
Bang            495 NSDNSSTAMLTECIQQQAEMENGMVPMDTKDQGLENNSLLEDRN    538

#---------------------------------------
#---------------------------------------
```

Page maintained by EBI Support

View Printer-friendly version of this page.

1: NP_612191. potassium channel...[gi:20143946] BLink, Links

LOCUS NP_612191 543 aa linear PRI 23-AUG-2004
DEFINITION potassium channel, subfamily K, member 10 isoform 3; TWIK-related K+ channel 2; 2P domain potassium channel TREK2; outward rectifying potassium channel protein TREK-2; potassium channel TREK-2 [Homo sapiens].
ACCESSION NP_612191
VERSION NP_612191.1 GI:20143946
DBSOURCE REFSEQ: accession NM_138318.1
KEYWORDS .
SOURCE Homo sapiens (human)
ORGANISM Homo sapiens
Eukaryota; Metazoa; Chordata; Craniata; Vertebrata; Euteleostomi; Mammalia; Eutheria; Primates; Catarrhini; Hominidae; Homo.
REFERENCE 1 (residues 1 to 543)
AUTHORS Gu,W., Schlichthorl,G., Hirsch,J.R., Engels,H., Karschin,C., Karschin,A., Derst,C., Steinlein,O.K. and Daut,J.
TITLE Expression pattern and functional characteristics of two novel splice variants of the two-pore-domain potassium channel TREK-2
JOURNAL J. Physiol. (Lond.) 539 (Pt 3), 657-668 (2002)
PUBMED 11897838
REMARK GeneRIF: Expression pattern and functional characteristics of two novel splice variants of the two-pore-domain potassium channel TREK-2.
REFERENCE 2 (residues 1 to 543)
AUTHORS Goldstein,S.A., Bockenhauer,D., O'Kelly,I. and Zilberberg,N.
TITLE Potassium leak channels and the KCNK family of two-P-domain subunits
JOURNAL Nat Rev Neurosci 2 (3), 175-184 (2001)
PUBMED 11256078
REFERENCE 3 (residues 1 to 543)
AUTHORS Lesage,F., Terrenoire,C., Romey,G. and Lazdunski,M.
TITLE Human TREK2, a 2P domain mechano-sensitive K+ channel with multiple regulations by polyunsaturated fatty acids, lysophospholipids, and Gs, Gi, and Gq protein-coupled receptors
JOURNAL J. Biol. Chem. 275 (37), 28398-28405 (2000)
PUBMED 10880510
REFERENCE 4 (residues 1 to 543)
AUTHORS Bang,H., Kim,Y. and Kim,D.
TITLE TREK-2, a new member of the mechanosensitive tandem-pore K+ channel family
JOURNAL J. Biol. Chem. 275 (23), 17412-17419 (2000)
PUBMED 10747911
COMMENT REVIEWED REFSEQ: This record has been curated by NCBI staff. The reference sequence was derived from AF385399.1.

Summary: This gene encodes one of the members of the superfamily of potassium channel proteins containing two pore-forming P domains. The message for this gene is highly expressed in the kidney and pancreas. This channel is an open rectifier which primarily passes

outward current under physiological K+ concentrations. The protein is stimulated strongly by arachidonic acid and to a lesser degree by membrane stretching, intracellular acidification, and general anaesthetics. Three transcript variants have been identified for this gene.

Transcript Variant: This variant (3) has a different first exon than variant 1. Isoform 3 has a unique N-terminus, longer by 5 aa than that of isoform 1.

```
FEATURES             Location/Qualifiers
     source          1..543
                     /organism="Homo sapiens"
                     /db_xref="taxon:9606"
                     /chromosome="14"
                     /map="14q31"
     Protein         1..543
                     /product="potassium channel, subfamily K, member 10
                     isoform 3"
                     /note="TWIK-related K+ channel 2; 2P domain potassium
                     channel TREK2; outward rectifying potassium channel
                     protein TREK-2; potassium channel TREK-2"
     Region          <134..204
                     /region_name="Ion transport protein"
                     /note="Ion_trans"
                     /db_xref="CDD:25532"
     Region          159..180
                     /region_name="pore-forming domain"
     Region          268..294
                     /region_name="pore-forming domain"
     CDS             1..543
                     /gene="KCNK10"
                     /coded_by="NM_138318.1:123..1754"
                     /note="isoform 3 is encoded by transcript variant 3;
                     go_component: membrane fraction [goid 0005624] [evidence
                     NR];
                     go_component: integral to plasma membrane [goid 0005887]
                     [evidence NR];
                     go_function: potassium channel activity [goid 0005267]
                     [evidence TAS] [pmid 10880510];
                     go_function: voltage-gated ion channel activity [goid
                     0005244] [evidence IEA];
                     go_process: ion transport [goid 0006811] [evidence IEA];
                     go_process: signal transduction [goid 0007165] [evidence
                     NR] [pmid 10880510];
                     go_process: potassium ion transport [goid 0006813]
                     [evidence IEA]"
                     /db_xref="GeneID:54207"
                     /db_xref="LocusID:54207"
                     /db_xref="MIM:605873"
ORIGIN
        1 medgfkgdrt egcrsdsvav paaapvcqpk satngqppap aptptprlsi ssratvvarm
       61 egtsqgglqt vmkwktvvai fvvvvvylvt gglvfraleq pfessqknti alekaeflrd
      121 hvcvspqele tliqhaldad nagvspigns snnsshwdlg safffagtvi ttigygniap
      181 steggkifci lyaifgiplf gfllagigdq lgtifgksia rvekvfrkkq vsqtkirvis
      241 tilfilagci vfvtipavif kyiegwtale siyfvvvtlt tvgfgdfvag gnaginyrew
      301 ykplvwfwil vglayfaavl smigdwlrvl skktkeevge ikahaaewka nvtaefretr
      361 rrlsveihdk lqraatirsm errrlgldqr ahsldmlspe krsvfaaldt grfkassqes
      421 innrpnnlrl kgpeqlnkhg qgasedniin kfgstsrltk rknkdlkktl pedvqkiykt
      481 frnysldeek keeetekmcn sdnsstamlt dciqqhaele ngmiptdtkd repennslle
      541 drn
```

//

Sep 10 2004 06:44:09

Journal of Physiology (2002), **539.3**, *pp.* 657–668
© The Physiological Society 2002

DOI: 10.1013/jphysiol.2001.013432
www.jphysiol.org

Expression pattern and functional characteristics of two novel splice variants of the two-pore-domain potassium channel TREK-2

Wenli Gu *, Günter Schlichthörl †, Jochen R. Hirsch ‡, Hartmut Engels *, Christine Karschin §, Andreas Karschin §, Christian Derst †, Ortrud K. Steinlein * and Jürgen Daut †

** Institut für Humangenetik, Universität Bonn, Wilhelmstrasse 31, D-53111 Bonn, † Institut für Physiologie, Universität Marburg, Deutschhausstrasse 2, D-35037 Marburg, ‡ Experimentelle Nephrologie, Universität Münster, Domagstrasse 2, D-48149 Münster and § Institut für Physiologie, Universität Würzburg, Röntgenring 9, D-97070 Würzburg, Germany*

Two novel alternatively spliced isoforms of the human two-pore-domain potassium channel TREK-2 were isolated from cDNA libraries of human kidney and fetal brain. The cDNAs of 2438 base pairs (bp) (TREK-2b) and 2559 bp (TREK-2c) encode proteins of 508 amino acids each. RT-PCR showed that TREK-2b is strongly expressed in kidney (primarily in the proximal tubule) and pancreas, whereas TREK-2c is abundantly expressed in brain. *In situ* hybridization revealed a very distinct expression pattern of TREK-2c in rat brain which partially overlapped with that of TREK-1. Expression of TREK-2b and TREK-2c in human embryonic kidney (HEK) 293 cells showed that their single-channel characteristics were similar. The slope conductance at negative potentials was 163 ± 5 pS for TREK-2b and 179 ± 17 pS for TREK-2c. The mean open and closed times of TREK-2b at −84 mV were 133 ± 16 and 109 ± 11 μs, respectively. Application of forskolin decreased the whole-cell current carried by TREK-2b and TREK-2c. The sensitivity to forskolin was abolished by mutating a protein kinase A phosphorylation site at position 364 of TREK-2c (construct S364A). Activation of protein kinase C (PKC) by application of phorbol-12-myristate-13-acetate (PMA) also reduced whole-cell current. However, removal of the putative TREK-2b-specific PKC phosphorylation site (construct T7A) did not affect inhibition by PMA. Our results suggest that alternative splicing of TREK-2 contributes to the diversity of two-pore-domain K^+ channels.

(Received 22 October 2001; accepted after revision 26 November 2001)
Corresponding author J. Daut: Institut für Physiologie, der Universität Marburg, Deutschhausstrasse 2, 35037 Marburg, Germany. Email: daut@mailer.uni-marburg.de

The family of two-pore-domain potassium (K_{2P}) channels is defined by their common structural features: the individual subunits have four transmembrane domains, two pore domains and a large M1–P1 linker (reviewed by Lesage & Lazdunski, 2000; Goldstein *et al.* 2001; Patel & Honore, 2001). Using homology analysis, five subfamilies of K_{2P} channels have been identified, the TWIK subfamily (Lesage *et al.* 1996*a*; Chavez *et al.* 1999; Salinas *et al.* 1999; Patel *et al.* 1999*b*), the THIK subfamily (Rajan *et al.* 2001), the acid-sensitive subfamily comprising TASK-1, -3 and -5 (Duprat *et al.* 1997; Kim *et al.* 1998, 2000; Rajan *et al.* 2000; Kim & Gnatenco, 2001; Karschin *et al.* 2001), the mainly alkaline-sensitive subfamily comprising TALK-1, TALK-2 and TASK-2 (Reyes *et al.* 1998; Decher *et al.* 2001; Girard *et al.* 2001), and the mechanosensitive subfamily comprising TREK-1, TREK-2 and TRAAK (Fink *et al.* 1996, 1998; Maingret *et al.* 1999*a,b*; Lesage *et al.* 2000*a,b*; Bang *et al.* 2000).

Most of the 14 mammalian K_{2P} channels identified so far are abundantly expressed in the brain (Talley *et al.* 2001). Since K_{2P} channels have been identified quite recently, less is known about their function compared with other K^+ channels. Nevertheless, four aspects that may be relevant for neuronal function have now become clear. (i) Some of the K_{2P} channels are modulated by changes in intracellular pH and may therefore play a protective role during cerebral ischaemia (Maingret *et al.* 1999*b*). (ii) Some of the K_{2P} channels are activated by volatile anaesthetics (Patel *et al.* 1999*a*; Gray *et al.* 2000; Lesage *et al.* 2000*b*; Sirois *et al.* 2000) and this may represent one of the major mechanisms responsible for the anaesthetic effect of halothane, chloroform, isoflurane and related drugs. (iii) Some of the K_{2P} channels can be activated by polyunsaturated fatty acids and by lysophospholipids (Fink *et al.* 1998; Lesage *et al.* 2000*a,b*; Maingret *et al.* 2000). It has been postulated that the release of polyunsaturated fatty acids following receptor-mediated stimulation of phospholipases may modulate synaptic transmission in the CNS (Fink *et al.* 1998). (iv) Some of the K_{2P} channels have been shown to be inhibited by activation of G-protein-coupled receptors, for example the M_3 muscarinic receptor (Millar *et al.*

2000), the thyrotrophin-releasing hormone receptor TRH-R1 (Talley *et al.* 2000) or the metabotrophic glutamate receptor mGluR1 (Lesage *et al.* 2000). Thus, K_{2P} channels could be the effectors of excitatory postsynaptic potentials elicited by activation of receptors coupled to G-proteins of the $\alpha_{q/11}$ subtype. Other transmitters that have been postulated to modulate the activity of K_{2P} channels include serotonin, noradrenaline (norepinephrine) and substance P (Talley *et al.* 2000).

The K_{2P} channel TREK-2 shares all of these functions (i–iv) and may therefore participate in many regulatory processes in the brain. Here we characterize two novel human splice variants of TREK-2, denoted TREK-2b and TREK-2c, which are differentially expressed in brain, kidney and pancreas. Since previous investigations of the related channel TREK-1 had shown that it can be modulated by protein kinase A (PKA) and protein kinase C (PKC) (Patel *et al.* 1998) we studied the possible function of the PKA and PKC phosphorylation sites of TREK-2b and TREK-2c using site-directed mutagenesis.

METHODS

Cloning of two splice variants of human TREK-2

A basic local alignment search tool (BLAST) search with the TREK-1 cDNA in the high throughput genomic sequences (HTGS) DNA database revealed a genomic fragment AL122021 (locus CNS01DSW) from human chromosome 14 that shares partial homology with TREK-1. The chromosomal localization of TREK-2 was confirmed by fluorescence *in situ* hybridization (data not shown). Reverse transcription-polymerase chain reaction (RT-PCR) was performed with human fetal brain total RNA (Clontech, Palo Alto, CA, USA) using the Titan One Tube RT-PCR system (Roche Molecular Biochemicals, Mannheim, Germany) and the primers:

5′-CCAAGTTGGTCTCCAATTCCAGCC-3′ (forward)

and 5′-GCGGGAGTCAGTCCAATAGGAAA-3′ (reverse).

The partial TREK-2 PCR product was cloned into the vector TOPO PCR2.1 (Invitrogen, Groningen, Germany) and sequenced. To obtain the entire TREK-2 cDNA, 5′ and 3′ rapid amplification of cDNA ends (RACE) was performed using Marathon-ready cDNA (Clontech) from human fetal brain and human kidney. Two 3′ nested primers:

5′-GCGGGAGTCAGTCAATAGGAAA-3′

and 5′-CAGCAGCCACTGGGACCTCGGCAG-3′

and two 5′ nested primers:

5′-CCTTCAGTGCTCGGAGCAATATTCCC-3′

and 5′-TCTTCTGGCTGCTCTCAAAGGGCTGCTCCAATGC-CCGGAAGA-3′

were used for amplification. The amplified products were cloned into the TOPO PCR2.1 vector and sequenced.

Cloning of rat TREK-1 and TREK-2c cDNAs

Two EST clones encoding partial human TREK-1 (AA464375, IMAGE-Id: 810165) and TREK-2 (AI073392, IMAGE-Id:1640332) cDNAs were labelled with digoxigenin and used for a non-radioactive screening of a λ-ZAP2 rat brain cDNA library using standard hybridization procedures and disodium 3-(4-methoxy-spiro(1,2-dioxetane-3,2′-(5′-chloro)tricyclo[3,3.1.1^{3,7}]decan)-4-yl) phenyl phosphate (CSPD) as a chemiluminescence substrate. After two further screenings for plaque purification, pBSK+ plasmids containing the TREK cDNAs were excised using the Exassist helper phage and completely sequenced.

Tissue distribution of the TREK-2 splice variants in different human tissues

The expression of three TREK-2 splice variants in different human tissues was analysed by PCR. The multiple-tissue cDNA panels Human I and Human II (Clontech) were used as templates. Sense primers corresponding to the first exons of the different splice variants were combined with the antisense primer located within the shared exon 2. Amplification products were designed to be of similar length to facilitate quantitative comparison. A second amplification was performed using two primers from the shared region to analyse the distribution of total TREK-2 expression. The primers used for each transcript were as follows. For TREK-2b:

FORb (5′-GCAAGGCATGGAGCCTGCACTTT-3′)

with BACK (5′-ACACCGGTGCTGCG GGAACGGCCA-3′);

for TREK-2c:

FORc (5′-TTCCTCCACGAGCCAGTCCAAGGCT-3′) with BACK;

and for TREK-2a:

FORa (5′-GGAGACTTTGCTCCACGATGTT-3′) with BACK.

Primers

5′-GCGGGAGTCAGTCCAATAGGAAAC-3′

and 5′-CCAAGTTGGTCTC CAATTCCAGCC-3′

from the part common to all three splice variants were used to analyse the total expression level of TREK-2. PCR was performed for 25 cycles of 2 s at 94 °C and 3 min at 68 °C with the polymerase Advantage 2 (Clontech).

The expression of TREK-2a in human total brain was additionally tested by nested RT-PCR from human fetal (Promega, Mannheim, Germany) and adult brain RNA (Clontech). The first RT-PCR step was carried out using the Titan One Tube RT-PCR system (Roche, Mannheim) according to the protocol of the manufacturer with an annealing temperature of 65 °C. The primers were

5′-GTTGCCAGAGATGACTGGGGTTTTCGGG-3′ and BACK.

Zero point zero two microlitres of the product was amplified again with the second pair of primers

5′-CGCAGGAACGCTAGGCAGTCTCT-3′

and 5′-GAAGTCTGTGTAGAGAAAAAACATCC-3′

using *Taq* polymerase (Invitrogen) and standard PCR conditions with an annealing temperature of 68 °C. All primers used in the distribution assays and RT-PCR were tested in combination with an antisense primer using genomic DNA. They all gave strong specific amplifications.

RT-PCR analysis of isolated of human nephron segments

Healthy cortical kidney pieces were obtained (with written consent) from patients undergoing tumour-nephrectomy. Nephron

segments were isolated using the procedure described previously for rat and rabbit kidney (Schafer *et al.* 1997). Selected tubules of a total length of 200 mm or glomeruli (400 pieces) were lysed in a 4 M guanidinium chloride buffer and total RNA was isolated using the RNeasy kit (Qiagen). Isolated total RNA was incubated with 10 units DNAse I (Promega, Heidelberg, Germany) at 37 °C for 1 h to digest traces of genomic DNA. RNA and DNase I were then separated by an additional cleaning step using a new RNeasy column. First strand cDNA synthesis was performed in a total reaction volume of 30 μl containing 5 μg total RNA, 10 mM dNTP-Mix, 1 nM $p(dT)_{10}$ nucleotide primer (Roche) and 200 units Moloney murine leukaemia virus (MMLV) reverse transcriptase (Promega). One-thirtieth of each cDNA first strand reaction mixture was then subjected to a 50 μl PCR reaction using 20 pmol of each primer (also used for the tissue distribution) and 1 unit of *Taq* DNA polymerase (Qiagen). Reaction conditions were as follows: 3 min at 94 °C, 30 s at 53 °C and 1 min at 72 °C, 1 cycle; 30 s at 94 °C, 30 s at 53 °C and 1 min at 72 °C, 30 cycles; 30 s at 94 °C, 30 s at 53 °C and 10 min at 72 °C, 1 cycle. All PCR products were directly sequenced to confirm correct amplification. For negative controls reverse transcriptase was omitted. Additionally, to exclude contamination, appropriate water controls excluding cDNAs were performed.

In situ hybridization of rat brain sections

Wistar rats were decapitated under ether anaesthesia, their brains were removed and frozen on powdered dry ice. Tissue was stored at −20 °C until cutting. Sixteen micrometre sections were cut on a Cryostat, thaw mounted onto silane-coated slides and air dried. After fixation for 10 min in 4% paraformaldehyde dissolved in phosphate-buffered saline (PBS), slides were washed in PBS, dehydrated and stored in ethanol until hybridization.

Synthetic antisense oligonucleotides with least tendency of forming hairpins and self-dimers were chosen from the untranslated region and open reading frame (base positions on coding strand):

TREK-1,

(i) (125–172) 5′-CCCGCGAGGCGCTGGCAAGCATGAG-GCATGCAGCATTCAAAATGTTTG-3′,

(ii) (197–244) 5′-TGGAGTTCTGAGCAGCAGACTTGGGA-TCCAGCAAGTCAGGGGCCGCCA-3′,

(iii) (1262–1308) 5′-CACCGACAGGGTCCTCCTACATGGAG-TCAGTTCCTGGTTATGGTTAC-3′;

TREK-2c,

(i) (199–245) 5′-CTTGAAGTGGCTCGTGGGGAGCCCG-GGAGAAAGATAAGCGGGAAAAT-3′,

(ii) (344–391) 5′-CTTGGCGTCTCGATTGGAAATTTCAT-TGCTCCGTTGCCCACAGGGGGG-3′,

(iii) (1904–1952) 5′-CTCCAGCCCCTGGTCTTTGGTGTCCA-TGGGTACCATTCCATTCTCCATC-3′.

Three specific oligonucleotides corresponding to different 3′ and 5′ regions of the cDNAs were generated to exclude cross-hybridization between different K_{2P} subunits and to detect possible discrepancies related to the existence of additional N- or C-terminal splice variants.

Oligonucleotides were 3′ end-labelled with [^{33}P]dATP (New England Nuclear, Boston, MA, USA; 1000 Ci mmol^{-1}) by terminal deoxynucleotidyl transferase (Roche Diagnostics) and used for hybridization at concentrations of 2–10 pg μl^{-1} (4×10^5 c.p.m. (100 μl)$^{-1}$ hybridization buffer per slide). Control sections were (a) hybridized with sense oligonucleotide probes, (b) digested with RNase A (50 ng ml^{-1}) for 30 min at 37 °C before hybridization, and (c) hybridized with a mixed oligonucleotide probe containing a 20- to 50-fold excess of unlabelled probe. Slides were air dried and hybridized for 20–24 h at 43 °C in 100 μl buffer containing 50% formamide, 10% Dextran sulfate, 50 mM DTT, 0.3 M NaCl, 30 mM Tris–HCl, 4 mM EDTA, 1 × Denhardt's solution, 0.5 mg ml^{-1} denatured salmon sperm DNA, and 0.5 mg ml^{-1} polyadenylic acid and labelled oligonucleotide probe. Sections were washed 2 × 30 min in 1 × SSC plus 50 mM 2-mercaptoethanol, 1 h in 1 × SSC at 60 °C, and 10 min in 0.1 × SSC at room temperature. Specimens were then dehydrated, air dried and exposed to Kodak BIOMAX x-ray film for 16–21 days. For cellular resolution, selected slides were dipped in photographic emulsion, incubated for 6–10 weeks and then developed in Kodak D-19 for 3 min.

Expression of TREK channels in HEK 293 cells

The entire hTREK-2b and hTREK-2c coding regions were cloned into the expression vector pcDNA3.1 and transfected into HEK 293 cells using lipofectamine 2000 (Life Technologies). Electrophysiological recordings were made using with an Axopatch 200B amplifier (Axon Instruments). The sampling rate was usually 16 kHz and the cut-off frequency of the low-pass filter was 10 kHz (−3 dB). In some experiments the sampling rate was increased to 100 kHz. Pipettes with resistances of 5–8 MΩ were used for cell-attached and whole-cell measurements. The pipettes were coated with R6101 elastomer from Dow Chemicals. Single-channel measurements were performed with a pipette solution containing (mM): 140 KCl, 1 EGTA and 10 Hepes (divalent cation-free solution) or 145 KCl, 1 $MgCl_2$, 1 $CaCl_2$ and 5 Hepes (divalent cation-containing solution). The bath solution for the single-channel measurements contained (mM): 60 KCl, 85 NaCl, 1 $MgCl_2$, 0.33 NaH_2PO_4, 5 Hepes and 10 glucose. In this solution, the average membrane potential was approximately −4 mV. Whole-cell measurements were carried out with a pipette solution containing (mM): 65 potassium glutamate, 50 KCl, 10 KH_2PO_4, 7.9 $MgCl_2$, 5 EDTA, 5 Hepes, 1.9 K_2ATP and 0.2 Na_3GTP. The bath solution for the whole-cell measurements contained (mM): 5 KCl, 140 NaCl, 10 Hepes, 10 glucose, 1 $MgCl_2$, 1 $CaCl_2$, 0.33 NaH_2PO_4 and 2 sodium pyruvate. The membrane potential measurements were not corrected for the liquid junction potential, determined as described by Neher (1992), which was +2.8 mV.

RESULTS

Cloning of two novel human TREK-2 splice variants

Using a RACE strategy we isolated two novel human TREK-2 splice forms, denoted TREK-2b and TREK-2c, from human kidney and brain, respectively. The isolated cDNAs of 2438 base pairs (bp) (TREK-2b, GenBank accession number AF385399) and 2559 bp (TREK-2c, GenBank accession number AF385400) both code for proteins of 508 amino acids. At the amino acid level the proteins are 66% identical to human TREK-1 and 47% identical to human TRAAK. TREK-2b and TREK-2c differ significantly in their 5′-UTR and in the coding region for the first 17 amino acids. These regions also differ significantly from a previously isolated human TREK-2

splice variant (Lesage *et al.* 2000*b*; GenBank accession number: AF279890), here referred to as TREK-2a (Fig. 1*B*). The differences are due to alternative usage of the first exon. The alternative exons were localized by BLAST search in a human genomic database entry; the predicted gene structure is indicated in Fig. 1*A*. Interestingly, TREK-2b harbours a PKC phosphorylation site in the N-terminal part that is not present in the other two splice variants.

Cloning of rat brain TREK isoforms

cDNAs encoding the rat orthologues of TREK-1 and TREK-2c (rTREK-1 and rTREK-2c) were isolated from a rat brain cDNA library. The cDNAs of 3291 bp (rTREK-1, GenBank accession number AF385401) and 3056 bp (rTREK-2c, GenBank accession number AF385402) code for predicted proteins of 426 amino acids (rTREK-1) and 538 amino acids (rTREK-2), respectively, which were 60.7 % identical to each other at the amino acid level. Whereas the coding region of the rTREK-2c cDNA was identical to a recently described isoform (Bang *et al.* 2000), the rTREK-1 cDNA showed a 15 amino acid extension compared with the human TREK-1 sequences described previously (Fink *et al.* 1996; Meadows *et al.* 2000). However, another human GenBank entry (AF004711) encoding a TREK-1 isoform (named TPKC-1) from human brain shows a similar extension at the N-terminus and a different 5′ UTR compared with the shorter TREK-1 splice form (Bockenhauer *et al.* 2001). This may indicate alternative splicing of the human TREK-1 gene in which the start codon of the shorter splice form is split by an intron. A similar alternative N-terminal splicing may also take place in the TRAAK gene (compare Lesage *et al.* 2000*a* and GenBank entry AF247042).

Tissue distribution of human TREK-2 splice forms

The expression of TREK-2 splice variants in different human tissues was analysed by PCR of multiple-tissue cDNA panels Human I and II from Clontech. As shown in Fig. 2, TREK-2b is strongly expressed in kidney and pancreas. Only very faint signals could be observed in lung, liver and skeletal muscle. TREK-2c is strongly expressed in adult brain, while weak expression could also be observed in other tissues. In panel Human II, none of the three primers gave any PCR product (not shown). Using the same experimental procedure, no transcripts of TREK-2a could be identified in either cDNA panel, suggesting that it is not or very weakly expressed in these tissues (data not shown). Since TREK-2a was originally cloned from human brain RNA (Lesage *et al.* 2000*b*) we performed nested RT-PCR of both human fetal and adult brain RNA. TREK-2a primers amplified a splice variant-specific fragment of 139 bp which was subsequently confirmed by sequencing. Thus, TREK-2a is expressed in brain, but at a much lower level than TREK-2c.

Amplification with two primers from the shared part of the variants was used to estimate the total amount of TREK-2 expression. The strongest signal was observed in kidney, followed by brain and pancreas (Fig. 2). In all other

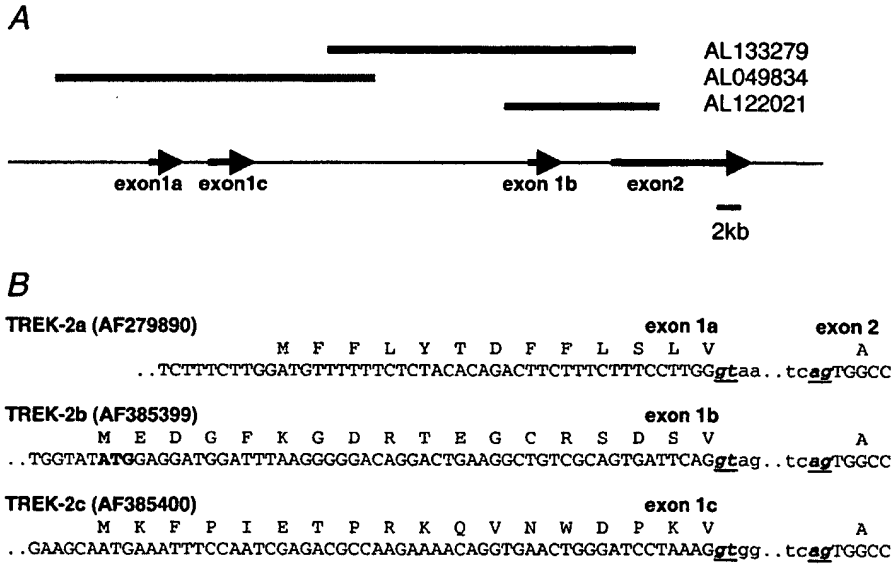

Figure 1. Sequence analysis of TREK-2 splice forms

A, relative orientation of the first exons of the splice variant identified in kidney (TREK-2b), fetal brain (TREK-2c) and the variant reported by Lesage *et al.* 2000*b* (TREK-2a). The corresponding genomic contigs are also shown. Exons are not drawn to scale. *B*, N-terminal cDNA and amino acid sequences of the human TREK-2 splice variants (accession numbers are given in brackets). The start codon (bold) and the splice sites of the first intron (underlined) are indicated. cDNA sequences are shown in capital letters, intronic sequences in lower case letters.

Table 1. Distribution of TREK-1 and TREK-2c mRNA in the adult rat brain

Brain region	TREK-2c	TREK-1	Brain region	TREK-2c	TREK-1
Olfactory bulb granule cell layer	+++	+	Thalamus: anteromedial nuclei	+++	+++
Olfactory tubercle	0	+++	Central grey	+	+++
Piriform cortex	+++	+++	Dorsal raphe nucleus	++	+++
Tenia tecta, Indusium griseum	0	++++	Interpeduncular nucleus	+	+++
N. of the lateral olfactory tract	++	+++	Cerebellum: deep nuclei	0	0
Neocortex	+	++	Cerebellum: Purkinje cells	0	0
Neocortex layer IV	+	+++	Cerebellum: granule cell layer	++++	+
Hippocampus dentate gyrus	+++	++	Pontine nucleus	+++	0
CA1 pyramidal cells	++	++	Medioventral periolivary n.	0	+++
CA2 pyramidal cells	++	++++	Trapezoid body	+++	0
CA3 pyramidal cells	++	0	Superior olivary nuclei	+	0
Caudate putamen	0	+++	Locus coeruleus	++++	0
Nucleus accumbens	0	+++	Dorsal tegmental nuclei	++	+++
Globus pallidus	0	0	Gigantocellular reticular n.	++++	0
Medial amygdaloid nuclei	+	++++	Spinal trigeminal nucleus	+++	±
Hypothalamus	+	++	Motor trigeminal nucleus	++	+++
Arcuate nucleus	+	+++	Facial nucleus	few+++	few+++
Preoptic nuclei	+	+++	Hypoglossus nucleus	++	++
Supraoptic nucleus	+++	+	Dorsal motor n. of the vagus	+++	+++
Habenula, medial nuclei	++	±	Solitary nucleus	++	+++
Thalamus: reticular nucleus	+	+++	Area postrema	+	++++
Thalamus: paraventricular nuclei	+++	+++	Inferior olive	0	++

In situ hybridization signals obtained for ^{33}P-labelled oligonucleotide probes on adult rat brain sections were rated according to the relative grain density: ++++, very abundant; +++, abundant; ++, moderate; +, low; ±, just above background; 0, no expression; few, only a few cells are labelled. Note that only selected brain regions with elevated expression levels or markedly differential expression patterns are included in the table.

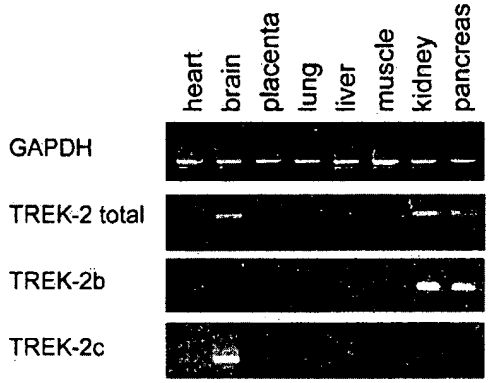

Figure 2. Tissue distribution of human TREK-2b and TREK-2c

Multiple-tissue cDNA panels from Clontech were used to study the tissue distribution of the three TREK-2 isoforms. To avoid possible genomic contamination, we used splice variant-specific primer pairs that included an exon–intron boundary fragment. In panel Human I, 180 bp fragments were amplified by specific TREK-2b and TREK-2c primers, whereas no PCR product could be observed with specific TREK-2a primers (not shown). Note that the TREK-2b signals in lung, liver and muscle were very faint. All cDNAs were also tested for GAPDH expression, and negative controls were performed with all RNA samples to exclude contamination.

tissues, weak but distinct expression could be seen. This result is in good agreement with the previously reported distribution pattern of TREK-2 expression. The strong expression of TREK-2 in kidney suggests that this K^+ channel may play a role in transepithelial transport. Therefore we analysed the expression of TREK-2b in different segments of human nephrons. In isolated human tubular fragments TREK-2b was strongly expressed only

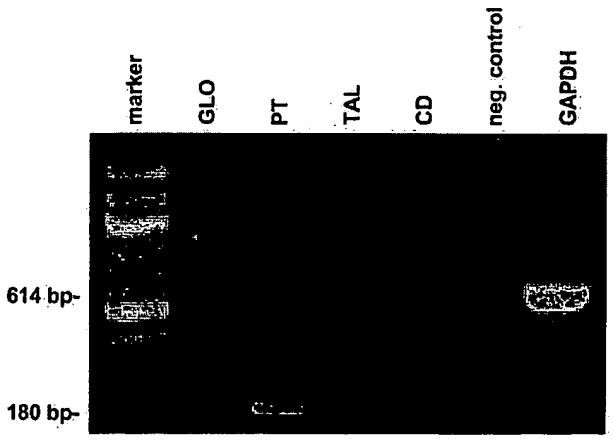

Figure 3. Expression of TREK-2b in human kidney

RT-PCR analysis of human glomeruli (GLO), proximal tubule (PT), thick ascending limb (TAL) and cortical collecting duct (CD). Molecular weight markers are shown in the left lane.

in the proximal tubule, as illustrated in Fig. 3. A faint expression was also detected in the collecting duct (not shown). No expression was found in the thick ascending limb and in glomeruli.

TREK-1 and TREK-2c localization in rat brain

Using *in situ* hybridization we compared the mRNA expression pattern of the brain-specific TREK-2c splice variant with the expression pattern of TREK-1 in the adult rat brain (Table 1, Fig. 4). In these experiments probe specificity was ensured by identical hybridization patterns of three oligonucleotides for each TREK-1 and TREK-2 in rat brain, as well as complete overlap with signals obtained from mouse-specific oligonucleotide probes in mouse brain.

As summarized in Table 1, TREK-2c hybridization signals were present throughout the brain. Of special note, high TREK-2c mRNA expression levels coincide with strong expression of TREK-1 mRNA in various nuclei, such as the nucleus of the lateral olfactory tract and the piriform cortex in the forebrain, the paraventricular and anteromedial thalamic nuclei, and in the brainstem the dorsal tegmental nuclei, solitary nucleus, and dorsal nucleus of the vagus. On the other hand, strong TREK-2c signals are also found in brain regions where TREK-1 mRNA is virtually absent. These include the granule cell layers of the cerebellum and olfactory bulb, as well as particular brainstem nuclei, e.g. pontine nucleus, trapezoid body, locus coeruleus, spinal trigeminal nucleus and gigantocellular neurons throughout the reticular formation. Note that vice versa many regions such as caudate putamen, nucleus accumbens, neocortex layer IV or interpeduncular nucleus specifically express only TREK-1 mRNA. Both TREK-1 and TREK-2b were found to be absent from fibre pathways, in which only glial labelling is expected.

Electrophysiological characterization of TREK-2 splice forms

For analysis of channel function TREK-2b and TREK-2c were heterologously expressed in HEK 293 cells. Single-

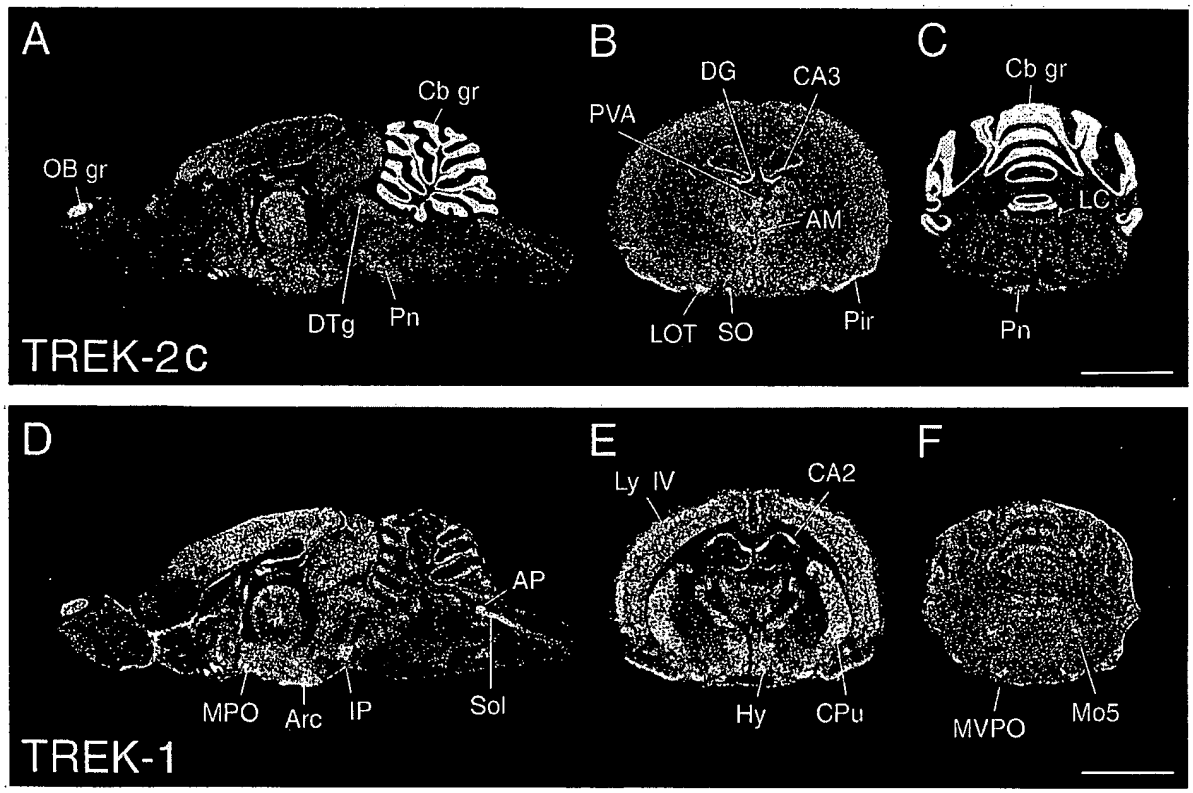

Figure 4. Distribution of TREK-2c and TREK-1 transcripts in rat brain

A–C, TREK-2c; *D–F*, TREK-1. X-ray film images show the differential expression patterns in adjacent midsagittal sections (*A* and *D*), and in coronal forebrain (*B* and *E*) and brainstem (*C* and *F*) sections. AM, anteromedial thalamic n.; AP, area postrema; Arc, arcuate n.; CA2 and CA3, hippocampal pyramidal cells of the corresponding region; Cb gr, cerebellar granule cell layer; CPu, caudate putamen; DG, hippocampus dentate gyrus; DTg, dorsal tegmental n.; Hy, hypothalamus; IP, interpeduncular n.; LC, locus coeruleus; LOT, n. of the lateral olfactory tract; Ly IV, neocortical layer IV; Mo5, motor trigeminal n.; MPO, medial preoptic n.; MVPO, medioventral periolivary n.; OB gr, olfactory bulb granule cell layer; Pir, piriform cortex; Pn, pontine n.; PVA, paraventricular thalamic n.; SO, supraoptic n.; Sol, solitary n., where n. stands for nucleus; scale bars represent 5 mm.

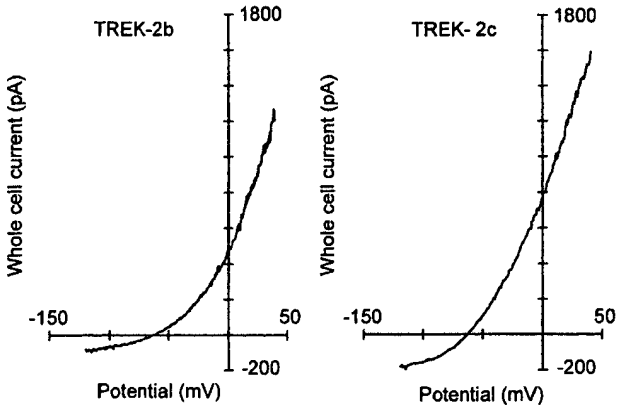

Figure 7. Whole-cell currents through TREK-2b and TREK-2c channels

Typical whole-cell currents in physiological salt solution (containing 5 mM K^+) observed after transfection of HEK 293 cells with TREK-2b or TREK-2c.

almost linear in the presence of divalent cations in the pipette solution (Fig. 6*A* and *B*). The slope conductance between −76 and −36 mV was found to be 163 ± 5 pS for TREK-2b and 179 ± 17 pS for TREK-2c. For both splice forms the slope conductance was significantly larger in the absence of external divalent cations, for TREK-2b it was 298 ± 16 pS and for TREK-2b it was 273 ± 35 pS. In all cases, the difference between the two splice forms was not statistically significant ($P > 0.05$; Fig. 6*C*). Our results clearly show that in divalent cation-free solution both TREK-2b and TREK-2c showed inward rectification at the single-channel level.

Whole-cell recordings of HEK 293 cells transfected with TREK-2 channels show strong outward rectification in physiological salt solution containing 5 mM K^+ and divalent cations, as illustrated in Fig. 7. Since TREK-2a has been shown to be activated by volatile anaesthetics (Lesage *et al.* 2000*a*) we tested the effects of isoflurane, chloroform and halothane on the whole-cell currents produced by the novel splice variants TREK-2b and TREK-2c (not illustrated). In the voltage range tested (−120 to +40 mV) the currents of the transfected cells were reversibly increased by isoflurane and halothane, in agreement with the results reported for TREK-2a. At 0 mV, the outward current produced by TREK-2b or TREK-2c was increased by 34.5 ± 5.5 % ($n = 5$) in the presence of 1 mM halothane and by 12.0 ± 6.7 % in the presence of 1 mM isoflurane ($n = 3$). No difference between TREK-2b and TREK-2c in the sensitivity to volatile anaesthetics was found. We also tested whether the novel splice forms of TREK-2 could be stimulated by externally applied lipids. In agreement with previous work on TREK-2a (Lesage *et al.* 2000*b*) we found that the whole-cell currents produced by TREK-2b and TREK-2c could be increased by application of 10 μM linoleic acid (60 ± 26 %; $n = 3$) or 10 μM arachidonic acid (62 ± 13 %; $n = 3$). These data suggest that the pharmacological properties of the TREK-2 channels are unaltered by the alternatively spliced N-terminus.

TREK-2c has a putative PKC phosphorylation site (at position 7) not present in TREK-2b and TREK-2a. Therefore we tested the effects of PKC phosphorylation (induced by application of phorbol-12-myristate-13-acetate, PMA) on TREK-2b and TREK-2c whole-cell currents (Fig. 8). The currents were inhibited by PMA in the voltage range tested, as illustrated in Fig. 8*B*. At 0 mV, 40 nM PMA decreased TREK-2b outward currents to 51 ± 5 % of control and TREK-2c currents to 57 ± 10 % of control. Exchange of the putative TREK-2c PKC phosphorylation site (TREK-2c T7A) did not change inhibition by PMA (Fig. 8*B*, *inset*), indicating that this effect is mediated by

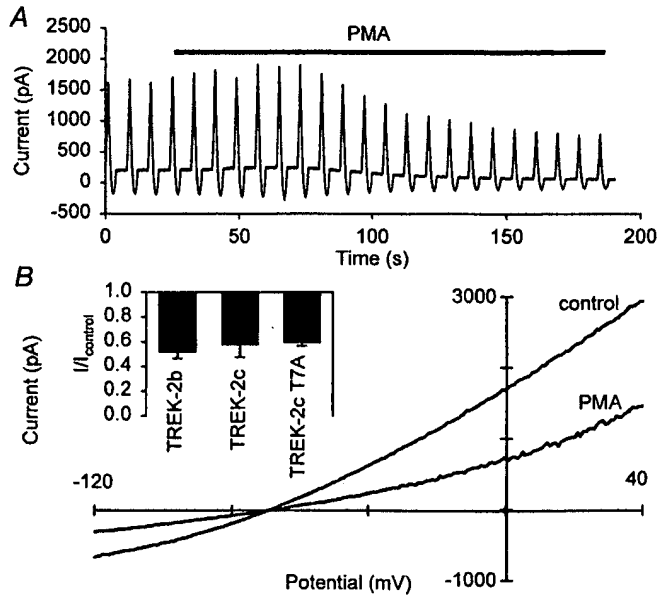

Figure 8. Effects of protein kinase C activation

A, typical recording of the effects of 40 nM PMA on the whole-cell current carried by TREK-2c; repetitive voltage ramps between −120 and +40 mV were applied. *B*, comparison of the current–voltage relation obtained under control conditions and in the steady state after application of PMA. *Inset*, comparison of the effects of 40 nM PMA on the currents produced by TREK-2b, TREK-2c and TREK-2c T7A.

channel recordings showed channels with the characteristic high-frequency flicker of two-pore-domain K^+ channels (Fig. 5*A*). The all-points histogram (Fig. 5*B*) illustrates that not all of the rapid closures could be resolved at a sampling rate of 16 kHz. The amplitude of the single-channel currents was determined using an algorithm which excludes the short events, as illustrated in Fig. 5*C*. This method allows precise determination of single-channel conductance even in channels with rapid kinetics. The longer closed times could not be determined because most patches contained more than one channel. The open and closed times responsible for the flicker could be analysed during episodes in which only one channel was open (Fig. 5*A*). Typical open and closed time distributions are shown in Fig. 5*D* and *E*. At −84 mV, the mean open time of TREK-2b was 133 ± 16 μs ($n = 4$), the short mean closed time of TREK-2b was 109 ± 11 μs ($n = 4$). Similar data were obtained for TREK-2a and in recordings in which the sampling rate was increased to 100 kHz ($n = 4$, not illustrated).

In symmetrical potassium solution the dependence of the single-channel current on potential was found to be

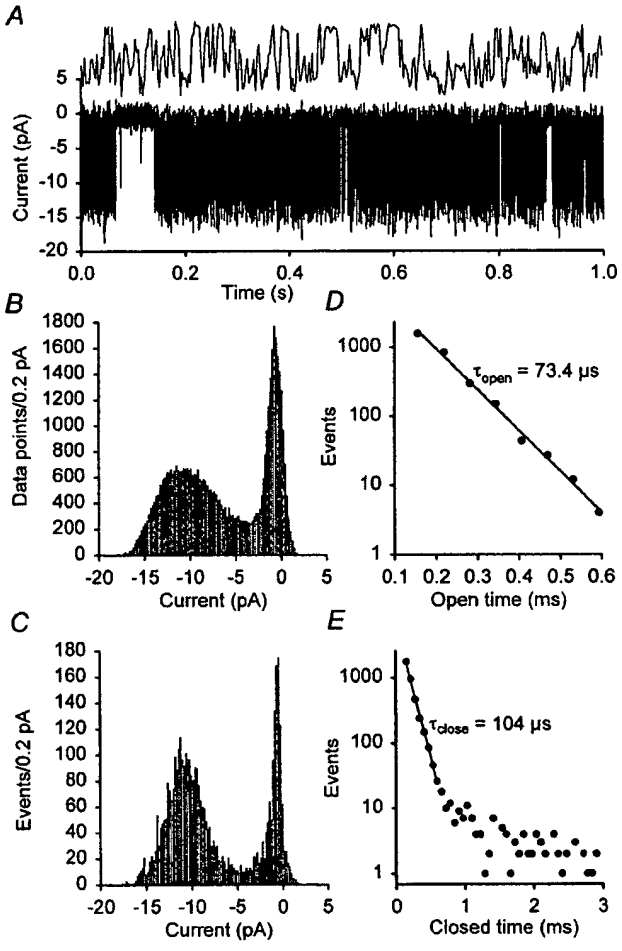

Figure 5. Single-channel recordings of TREK-2c

A, typical cell-attached recording of a TREK-2c channel expressed in HEK 293 cells. The top trace shows the first 20 ms of the lower trace at 50 × higher time resolution. *B*, all-points amplitude histogram of a typical cell attached record form a patch containing only one TREK-2c channel. *C*, event amplitude histogram constructed from the same set of data using an algorithm that excludes very short events, i.e. only events with a duration of more than 0.3 ms (> 5 data points) were included. *D*, typical open time distribution. *E*, closed time distribution of the same recording. In *A*–*E* the transmembrane potential (inside–outside) was −84 mV, the sampling rate was 16 kHz, and the pipette solution contained no divalent cations.

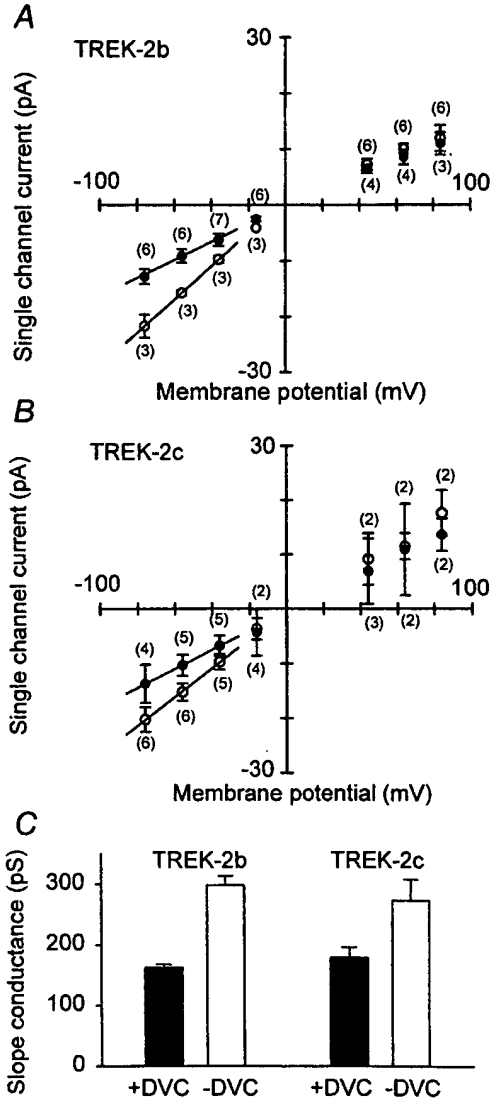

Figure 6. Dependence of single-channel conductance on external Ca^{2+}

A, single-channel current–voltage relation of TREK-2b and TREK-2c in the presence (●) and in the absence (○) of external divalent cations. *B*, mean values of the slope conductance of TREK-2b and TREK-2c, determined between −80 and −40 mV in the presence (●) and in the absence (○) of external divalent cations. *C*, the slope conductance of TREK-2b and TREK-2c measured in the presence (+DVC) and in the absence (−DVC) of external divalent cations.

one or more PKC phosphorylation sites shared by both splice forms.

It has been shown previously that the TREK-1 current amplitude is also down-modulated by PKA phosphorylation at the serine residue at position 333 (Patel *et al.* 1998; Lesage *et al.* 2000*b*). Since this PKA site is conserved in TREK-2 (serine 364) we tested the effects of PKA phosphorylation induced by forskolin (Fig. 9). Application of 10 μM forskolin produced a significant decrease in whole-cell current in both TREK-2b (to 57 ± 7% of control) and TREK-2c (to 64 ± 13% of control). When the single PKA phosphorylation site was removed (TREK-2c S364A) treatment of the cells with forskolin had no effect (95 ± 7% of control) as illustrated in Fig. 9*B inset*. These data suggests a direct effect of the phosphorylation of residue 364 on TREK-2b and TREK-2c channels.

DISCUSSION

Tissue distribution of TREK-2 channels

The two novel splice forms of TREK-2 reported here showed a clearly distinct expression pattern: whereas TREK-2b is strongly expressed in kidney and pancreas, TREK-2c is mainly expressed in brain. This may indicate differentially regulated alternative splicing of the TREK-2 pre-mRNA in different tissues. We were not able to detect the originally described splice form, TREK-2a (Lesage *et al.* 2000*b*), in any of the multiple-tissue cDNA panels tested. However, RT-PCR of human RNA indicated a very low level of expression of TREK-2a in fetal and adult brain, which was only detectable after re-amplification of the original RT-PCR products.

We have found a differential expression pattern for TREK-1 and TREK-2c mRNAs in rat brain (Fig. 4 and Table 1). In some areas of the brain the transcripts of TREK-1 and TREK-2c were found to have an overlapping distribution, whereas in other areas only transcripts of one of the channels could be detected. The expression pattern of TREK-2c described here may be compared with the *in situ* hybridization data obtained very recently by Talley *et al.* (2001) with non-specific TREK-2 oligonucleotides that did not discriminate between different splice variants. Despite quantitative differences, the results of Talley *et al.* (2001), which probably also represent the regional distribution of the splice variant TREK-2c, are in reasonable agreement with our data in many brain regions. However, there are also some remarkable discrepancies. In our analysis, for example, various brainstem nuclei, e.g. the dorsal motor nucleus of the vagus, solitary nucleus and hypoglossus nucleus were found to contain high levels of TREK-2c transcripts. Furthermore, we detected strong expression levels of TREK-2c in the paraventricular and anteromedial thalamic nuclei as well as in the pontine nucleus. Another striking difference is that in our study strong TREK-2c signals were observed in the locus coeruleus, whereas Talley *et al.* report signals very close to background in this area. The locus coeroleus contains most of the noradrenergic neurons of the CNS with a broad efferent network, thus providing a well-characterized neural system suitable for the functional characterization of TREK-2c.

It is generally agreed that quantitative comparison of expression levels of different channels is difficult because the hybridization efficiencies of oligonucleotide and RNA probes may depend not only on the design of the probe and methodological details but also on local cellular factors. In view of these experimental limitations it is gratifying to see that by and large the results obtained by Talley *et al.* (2001) and by our group are consistent.

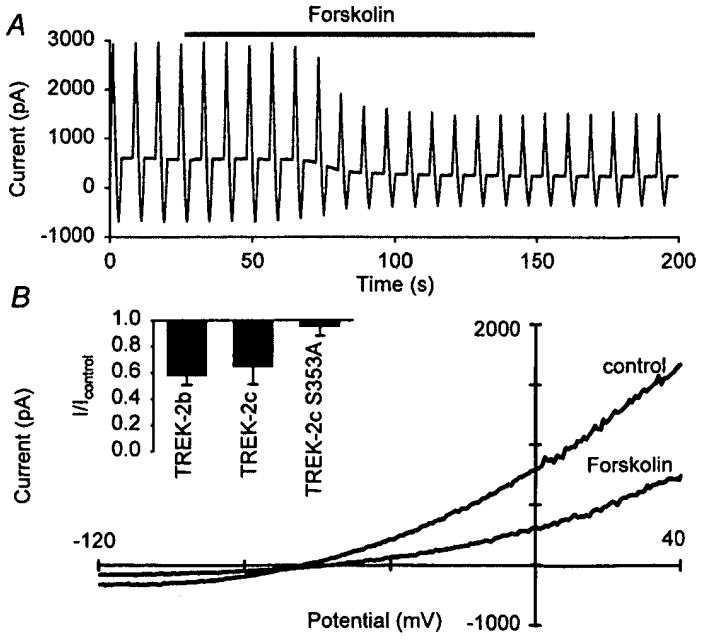

Figure 9. Effects of protein kinase A activation

A, typical recording of the effects of 10 μM forskolin on the whole-cell current carried by TREK-2c; repetitive voltage ramps between −120 and +40 mV were applied. *B*, comparison of the current–voltage relation obtained under control conditions and in the steady state after application of forskolin. *Inset*, comparison of the effects of 10 μM forskolin on the currents produced by TREK-2b, TREK-2c and TREK-2c S353A.

Together, these studies may contribute to the endeavour of correlating heterogeneity of channel expression with heterogeneity of physiological properties of different populations of neurons.

The other splice variant, TREK-2b, was strongly expressed in the proximal tubule of human kidney. To elucidate the possible function of these channels in the kidney it is necessary to determine the subcellular localization of TREK-2b channels. If they are targeted to the basolateral membrane their strong outward rectification would be consistent with a role of these channels in the transepithelial transport of potassium ions.

Functional characteristics of TREK-2 channels

Using an algorithm that excluded the very short events we were able precisely to determine the current amplitudes of TREK-2b and TREK-2c channels at different potentials despite the rapid kinetics of the channels. In symmetrical K^+ solution, the single-channel current voltage relation of both splice forms was almost linear in the presence of external Ca^{2+} and Mg^{2+}. The slope conductance measured at negative potentials in the presence of divalent cations was in the range 150–200 pS. Since the longer events showed a roughly Gaussian distribution and were consistent with the histogram of the raw data (Fig. 5) it is very unlikely that the determination of the single-channel amplitude was distorted by the rapid kinetics. The elementary characteristics of the other splice variant, TREK-2a (hTREK-2a; Lesage *et al.* 2000*b*) and of the rat orthologue of TREK-2a (rTREK-2a; Bang *et al.* 2000), have only been studied in inside-out patches. Interestingly, the conductance of these channels at positive potentials (allowing outward currents) was found to be much smaller (100 pS for hTREK-2a; 68 pS for rTREK-2a) than the values reported here. The reasons for this discrepancy are not clear. In the absence of external divalent cations, the conductance of TREK-2b and TREK-2c at negative potentials increased to 250–300 pS. The molecular mechanisms underlying the marked dependence of inward currents on the presence of divalent external cations (Fig. 6), which is also found in TASK-3 (Rajan *et al.* 2000), are not yet known.

The K_{2P} channels are generally characterized by short openings interrupted by short closures, which results in the typical 'flickery' appearance of single-channel recordings. The mean open time of TREK-2b and TREK-2c at −84 mV could be described by a single time constant of about 130 μs. The closed time distribution at the same potential showed at least two components, of which the shorter one was about 110 μs. The whole-cell current voltage relation of TREK-2b and TREK-2c in normal physiological salt solution (containing 5 mM K^+) was outwardly rectifying (Fig. 7), similar to TREK-2a (Lesage *et al.* 2000*b*). This outward rectification is most likely the result of (i) the asymmetrical K^+ concentrations and (ii) the voltage dependence of open probability (Lesage *et al.* 2000*b*; Bang *et al.* 2000).

Regulation of TREK-2 channels

The amplitude of the whole-cell current carried by TREK-2 channels could be increased by volatile anaesthetics (isoflurane, halothane and chloroform) and by externally applied lipids (linoleic acid and arachidonic acid). In this respect there was no difference between the two novel splice forms TREK-2b and TREK-2c and the data published previously for TREK-2a (Lesage *et al.* 2000*b*). This was to be expected since the three splice variants differ only in their N-terminus. At position 7 of TREK-2b there is a putative PKC phosphorylation site that is not present in TREK-2a and TREK-2c. However, both TREK-2b and TREK-2c could be inhibited by PMA, a non-specific activator of PKC. Furthermore, removal of the putative phosphorylation site by mutagenesis (construct TREK-2b T7A) did not cause a significant change in the effects of PMA. Thus, the putative phosphorylation site at position 7 is either not functional or the phosphorylation at this position has no effect on current amplitude.

In contrast, we found that activation of PKA by forskolin produced a significant decrease in whole-cell current. When the putative phosphorylation site was removed (construct S364A) the inhibitory effect of forskolin disappeared. These findings suggest that phosphorylation by PKA at position 364 of TREK-2b and TREK-2c (which corresponds to S359 in hTREK-2a) can inhibit the outward current of TREK-2 channels.

Possible alternative splicing in other K_{2P} channels

In the GenBank database several entries from TREK-1 and TRAAK channels from different species can be found which differ substantially in their N-terminal regions. This may indicate alternative splicing in other members of the TREK/TRAAK subfamily as well. For human TREK-1, two putative splice forms can be found in the GenBank database: AF129399 and AF171068 encode a shorter variant that was characterized in several studies (Fink *et al.* 1996; Meadows *et al.* 2000), AF004711 encodes another longer splice form (named TPKC1) isolated from human brain that also harbours 15 extra amino acids at the N-terminal part (Bockenhauer *et al.* 2001). Interestingly, the TREK-1 isoform that we isolated from rat brain has a similar N-terminal extension (accession number AF385401). Unfortunately, a genomic sequence for the first human TREK-1/*KCNK2* exons on chromosome 1 is still not available. For TRAAK there are database entries for mouse, rat and human. A yet unpublished human TRAAK isoform (AF247042) is significantly longer (26 amino acids) than the mouse and rat cDNAs (AF056492 and AF302842); the published human sequence (Lesage *et al.* 2000*a*) may therefore represent a different splice form.

Conclusions

The diversity of potassium currents in different cell types is determined not only by the number of different channel genes, but also by alternative splicing and heteromer formation of different subunits (Luneau *et al.* 1991; Butler *et al.* 1993; Attali *et al.* 1993; Shuck *et al.* 1994; Derst *et al.* 2001; Pan *et al.* 2001). Diversity of the K_{2P} channel family is partly determined by the relatively large number or different genes: about 50 K_{2P} channel genes were found in *Caenorhabditis elegans* (Wei *et al.* 1996), twelve K_{2P} channel genes were found in *Drosophila melanogaster* (Littleton & Ganetzki, 2000) and the number of K_{2P} channels in the human genome is at least 14. The results reported here show that alternative splicing of TREK-2, and possibly other K_{2P} channels, can further increase channel diversity. The cell-specific expression of different splice forms may play an important role in determining the functional properties of various neuronal and non-neuronal cell types.

REFERENCES

Attali, B., Lesage, F., Ziliani, P., Guillemare, E., Honore, E., Waldmann, R., Hugnot, J. P., Mattei, M. G., Lazdunski, M. & Barhanin, J. (1993). Multiple mRNA isoforms encoding the mouse cardiac Kv1.5 delayed rectifier K^+ channel. *Journal of Biological Chemistry* **268**, 24283–24289.

Bang, H., Kim, Y. & Kim, D. (2000). TREK-2, a new member of the mechanosensitive tandem-pore K^+ channel family. *Journal of Biological Chemistry* **275**, 17412–17419.

Bockenhauer, D., Zilberberg, N. & Goldstein, S. A. N. (2001). KCNK2: reversible conversion of a hippocampal potassium leak into a voltage-dependent channel. *Nature Neuroscience* **4**, 486–491.

Butler, A., Tsunoda, S., McCobb, D. P., Wei, A. & Salkoff, L. (1993). mSlo, a complex mouse gene encoding "maxi" calcium-activated potassium channels. *Science* **261**, 221–224.

Chavez, R. A., Gray, A. T., Zhao, B. B., Kindler, C. H., Mazurek, M. J., Mehta, Y., Forsayeth, J. R. & Yost, C. S. (1999). TWIK-2, a new weak inward rectifying member of the tandem pore domain potassium channel family. *Journal of Biological Chemistry* **274**, 7887–7892.

Decher, N., Maier, M., Dittrich, W., Gassenhuber, J., Brüggemann, A., Busch, A. E. & Steinmeyer, K. (2001). Characterization of TASK-4, a novel member of the pH-sensitive, two-pore domain potassium channel family. *FEBS Letters* **492**, 84–89.

Derst, C., Karschin, C., Wischmeyer, E., Hirsch, J. R., Preisig-Muller, R., Rajan, S., Engel, H., Grzeschik, K. H., Daut, J. & Karschin, A. (2001). Genetic and functional linkage of Kir5.1 and Kir2.1 channel subunits. *FEBS Letters* **491**, 305–311.

Duprat, F., Lesage, F., Fink, M., Reyes, R., Heurteaux, C. & Lazdunski, M. (1997). TASK, a human background K^+ channel to sense external pH variations near physiological pH. *EMBO Journal* **16**, 5464–5471.

Fink, M., Duprat, F., Lesage, F., Reyes, R., Romey, G., Heurteaux, C. & Lazdunski, M. (1996). Cloning, functional expression and brain localization of a novel unconventional outward rectifier K^+ channel. *EMBO Journal* **15**, 6854–6862.

Fink, M., Lesage, F., Duprat, F., Heurteaux, C., Reyes, R., Fosset, M. & Lazdunski, M. (1998). A neuronal two P domain K^+ channel stimulated by arachidonic acid and polyunsaturated fatty acids. *EMBO Journal* **17**, 3297–3308.

Girard, C., Duprat, F., Terrenoire, C., Tinel, N., Fosset, M., Romey, G., Lazdunski, M. & Lesage, F. (2001). Genomic and functional characteristics of novel human pancreatic 2P domain K^+ channels. *Biochemical and Biophysical Research Communications* **282**, 249–256.

Goldstein, S. A., Bockenhauer, D., O'Kelly, I. & Zilberberg, N. (2001). Potassium leak channels and the KCNK family of two-P-domain subunits. *Nature Reviews Neuroscience* **2**, 175–184.

Gray, A. T., Zhao, B. B., Kindler, C. H., Winegar, B. D., Mazurek, M. J., Xu, J., Chavez, R. A., Forsayeth, J. R. & Yost, C. S. (2000). Volatile anesthetics activate the human tandem pore domain baseline K^+ channel KCNK5. *Anesthesiology* **92**, 1722–1730.

Karschin, C., Wischmeyer, E., Preisig-Müller, R., Rajan, S., Derst, C., Grzeschik, K.-H., Daut, J. & Karschin, A. (2001). Expression pattern in brain of TASK-1, TASK-3, and a tandem pore domain K^+ channel subunit, TASK-5, associated with the central auditory nervous system. *Molecular and Cellular Neuroscience* **18**, 632–648.

Kim, Y., Bang, H. & Kim, D. (2000). TASK-3, a new member of the tandem pore K^+ channel family. *Journal of Biological Chemistry* **275**, 9340–9347.

Kim, D., Fujita, A., Horio, Y. & Kurachi, Y. (1998). Cloning and functional expression of a novel cardiac two-pore background K^+ channel (cTBAK-1). *Circulation Research* **82**, 513–518.

Kim, D. & Gnatenco, C. (2001). TASK-5, a new member of the tandem-pore K^+ channel family. *Biochemical and Biophysical Research Communications* **284**, 923–930.

Lesage, F., Guillemare, E., Fink, M., Duprat, F., Lazdunski, M., Romey, G. & Barhanin, J. (1996*a*). TWIK-1, a ubiquitous human weakly inward rectifying K^+ channel with a novel structure. *EMBO Journal* **15**, 1004–1011.

Lesage, F. & Lazdunski, M. (2000). Molecular and functional properties of two-pore-domain potassium channels. *American Journal of Physiology* **279**, F793–801.

Lesage, F., Maingret, F. & Lazdunski, M. (2000*a*). Cloning and expression of human TRAAK, a polyunsaturated fatty acids-activated and mechano-sensitive K^+ channel. *FEBS Letters* **471**, 137–140.

Lesage, F., Reyes, R., Fink, M., Duprat, F., Guillemare, E. & Lazdunski, M. (1996*b*). Dimerization of TWIK-1 K^+ channel subunits via a disulfide bridge. *EMBO Journal* **15**, 6400–6407.

Lesage, F., Terrenoire, C., Romey, G. & Lazdunski, M., (2000*b*). Human TREK2, a 2P domain mechano-sensitive K^+ channel with multiple regulations by polyunsaturated fatty acids, lysophospholipids and Gs, Gi, and Gq protein-coupled receptors. *Journal of Biological Chemistry* **275**, 28398–28405.

Littleton, J. T. & Ganetzky, B. (2000). Ion channels and synaptic organization: analysis of the Drosophila genome. *Neuron* **26**, 35–43.

Luneau, C. J., Williams, J. B., Marshall, J., Levitan, E. S., Oliva, C., Smith, J. S., Antanavage, J., Folander, K., Stein, R. B., Swanson, R., Kaczmarek, L. K. & Buhrow, S. A. (1991). Alternative splicing contributes to K^+ channel diversity in the mammalian central nervous system. *Proceedings of the National Academy of Sciences of the USA* **88**, 3932–3936.

Maingret, F., Fosset, M., Lesage, F., Lazdunski, M. & Honoré, E. (1999*a*). TRAAK is a mammalian neuronal mechano-gated K^+ channel. *Journal of Biological Chemistry* **274**, 1381–1387.

MAINGRET, F., PATEL, A. J., LESAGE, F., LAZDUNSKI, M., HONORÉ, E. (1999*b*). Mechano- or acid stimulation, two interactive modes of activation of the TREK-1 potassium channel. *Journal of Biological Chemistry* **274**, 26691–26696.

MAINGRET, F., PATEL, A. J., LESAGE, F., LAZDUNSKI, M. & HONORÉ, E. (2000). Lysophospholipids open the two-pore domain mechano-gated K^+ channels TREK-1 and TRAAK. *Journal of Biological Chemistry* **275**, 10128–10133.

MEADOWS, H. J., BENHAM, C. D., CAIRNS, W., GLOGER, I., JENNINGS, C., MEDHURST, A. D., MURDOCK, P. & CHAPMAN, C. G. (2000). Cloning, localisation and functional expression of the human orthologue of the TREK-1 potassium channel. *Pflügers Archiv* **439**, 714–722.

MILLAR, J. A., BARRATT, L., SOUTHAN, A. P., PAGE, K. M., FYFFE, R. E. W., ROBERTSON, B. & MATHIE, A. (2000). A functional role for the two-pore domain potassium channel TASK-1 in cerebellar granule neurons. *Proceedings of the National Academy of Sciences of the USA* **97**, 3614–3618.

NEHER, E. (1992). Correction for liquid junction potentials in patch clamp experiments. In *Methods in Enzymology*, vol. 207, *Ion Channels*, ed. RUDY, B. & IVERSON, L.E., pp. 123–131. Academic Press, San Diego.

PAN, Z., SELYANKO, A. A., HADLEY, J. K., BROWN, D. A., DIXON, J. E. & MCKINNON, D. (2001). Alternative splicing of KCNQ2 potassium channel transcripts contributes to the diversity of M-currents. *Journal of Physiology* **531**, 347–358.

PATEL, A. J., HONORÉ, E., MAINGRET, F., LESAGE, F., FINK, M., DUPRAT, F. & LAZDUNSKI, M. (1998). A mammalian two pore domain mechano-gated S-like K^+ channel. *EMBO Journal* **17**, 4283–4290.

PATEL, A. J., HONORÉ, E., LESAGE, F., FINK, M., ROMEY, G. & LAZDUNSKI, M. (1999*a*). Inhalational anesthetics activate two-pore-domain background K^+ channels. *Nature Neuroscience* **2**, 422–426.

PATEL, A. J. & HONORÉ, E. (2001). Properties and modulation of mammalian 2P domain K^+ channels. *Trends in Neurosciences* **24**, 339–346.

PATEL, A. J., MAINGRET, F., MAGNONE, V., FOSSET, M., LAZDUNSKI, M. & HONORÉ, E. (1999*b*). TWIK-2, an inactivating 2P domain K^+ channel. *Journal of Biological Chemistry* **275**, 28722–28730.

RAJAN, S., WISCHMEYER, E., KARSCHIN, C., PREISIG-MÜLLER, R., GRZESCHIK, K.-H., DAUT, J., KARSCHIN, A. & DERST, C. (2001). THIK-1 and THIK-2, a novel subfamily of tandem pore domain K^+ channels. *Journal of Biological Chemistry* **276**, 7302–7311.

RAJAN, S., WISCHMEYER, E., LIU, G. X., PREISIG-MÜLLER, R., DAUT, J., KARSCHIN, A. & DERST, C. (2000). TASK-3, a novel tandem pore domain acid-sensitive K^+ channel. An etracellular histidine as pH sensor. *Journal of Biological Chemistry* **275**, 16650–16657.

REYES, R., DUPRAT, F., LESAGE, F., FINK, M., SALINAS, M., FARMAN, N. & LAZDUNSKI, M. (1998). Cloning and expression of a novel pH-sensitive two pore domain K^+ channel from human kidney. *Journal of Biological Chemistry* **273**, 30863–30869.

SALINAS, M., REYES, R., LESAGE, F., FOSSET, M., HEURTEAUX, C., ROMEY, G. & LAZDUNSKI, M. (1999). Cloning of a new mouse two-P domain channel subunit and a human homologue with a unique pore structure. *Journal of Biological Chemistry* **274**, 11751–11760.

SCHAFER, J. A., WATKINS, M. L., LI, L., HERTER, P., HAXELMANS, S. & SCHLATTER, E. (1997). A simplified method for isolation of large numbers of defined nephron segments. *American Journal of Physiology* **273**, F650–657.

SHUCK, M. E., BOCK, J. H., BENJAMIN, C. W., TSAI, T. D., LEE, K. S., SLIGHTOM, J. L. & BIENKOWSKI, M. J. (1994). Cloning and characterization of multiple forms of the human kidney ROMK potassium channel. *Journal of Biological Chemistry* **269**, 24261–24270.

SIROIS, J. E., LEI, Q., TALLEY, E. M., LYNCH, C. III & BAYLISS, D. A. (2000). The TASK-1 two-pore domain K^+ channel is a molecular substrate for neuronal effects of inhalation anesthetics. *Journal of Neuroscience* **20**, 6347–6354.

TALLEY, E. M., LEI, Q., SIROIS, J. E. & BAYLISS, D. A. (2000). TASK-1, a two-pore domain K^+ channel, is modulated by multiple neurotransmitters in motoneurons. *Neuron* **25**, 399–410.

TALLEY, E. M., SOLORZANO, G., LEI, Q., KIM, D. & BAYLISS, D. A. (2001). CNS distribution of members of the two-pore-domain (KCNK) potassium channel family. *Journal of Neuroscience* **21**, 7491–7505.

WEI, A., JEGLA, T. & SALKOFF, L. (1996). Eight potassium channel families revealed by the *C. elegans* genome project. *Neuropharmacology* **35**, 805–829.

Acknowledgements

This work was supported by the Deutsche Forschungsgemeinschaft (grants Da177/7-3 and Ka1175/1-3), by the Ernst-und-Berta-Grimmke Stiftung and by the P. E. Kempkes-Stiftung. We thank Regina Preisig-Müller and Sindhu Rajan for useful discussions. The excellent technical help of Tanja Haase, H. Wegener and Anette Hennighausen is gratefully acknowledged.

130917

POTASSIUM LEAK CHANNELS AND THE KCNK FAMILY OF TWO-P-DOMAIN SUBUNITS

Steve A. N. Goldstein, Detlef Bockenhauer, Ita O'Kelly and Noam Zilberberg

With a bang, a new family of potassium channels has exploded into view. Although KCNK channels were discovered only five years ago, they already outnumber other channel types. KCNK channels are easy to identify because of their unique structure — they possess two pore-forming domains in each subunit. The new channels function in a most remarkable fashion: they are highly regulated, potassium-selective leak channels. Although leak currents are fundamental to the function of nerves and muscles, the molecular basis for this type of conductance had been a mystery. Here we review the discovery of KCNK channels, what has been learned about them and what lies ahead. Even though two-P-domain channels are widespread and essential, they were hidden from sight in plain view — our most basic questions remain to be answered.

Departments of Pediatrics and Cellular and Molecular Physiology, Boyer Center for Molecular Medicine, Yale University School of Medicine, New Haven, Connecticut 06536 USA. Correspondence to S.A.N.G. e-mail: steve.goldstein@yale.edu

Potassium (K^+) leak currents have been described as essential to neuromuscular function for more than 50 years[1–4]. However, the existence of unique molecular transport entities responsible for leak currents (also called resting or background conductances) was questioned despite the fact that they were attributed prominent roles in the function of sympathetic ganglia[5,6], invertebrate axons[7], vertebrate myelinated axons[8–14] and cardiac myocytes[15–20]. We now understand that leak is not just seepage, but flux through dedicated pathways.

Leak currents exert control over excitability by shaping the duration, frequency and amplitude of action potentials, in part through their influence over the resting membrane potential (BOX 1). Increased K^+ leak currents stabilize cells at hyperpolarized voltages below the firing threshold of nerves and muscles, whereas leak suppression permits depolarization and excitation. In addition, although leak channels pass K^+ readily upon changes in membrane voltage, they operate under tight control of agents as disparate as molecular oxygen, cyclic nucleotides, noradrenaline, serotonin and GABA (γ-aminobutyric acid)[21–24]. But despite their significant duties and tight regulation, native leak currents have defied coherent description for years. In a multitude of events occurring in just milliseconds, leaks seemed largely invariant: they were readily ignored, easily camouflaged and even actively removed by 'subtraction' during electrophysiological recordings. But cloning and study of TOK1 from *Saccharomyces cerevisiae*[25–27], KCNK0 from *Drosophila melanogaster*[28–30] and 11 mammalian two-P-domain K^+ channel genes have established unequivocally that leaks are indeed much more than unchanging dribble through pathways devoted to other functions (TABLE 1).

Potassium channels with two P domains

Before 1995, K^+ channel subunits were identifiable by the presence of a single pore-forming P domain, characterized by the amino-acid signature motif TXGYG[31–40]. For example, voltage-gated K^+ channel (Kv) subunits have one P domain and six transmembrane (TM) segments (1P/6TM). The fourth transmembrane domain (S4) acts as voltage sensor; it has positively charged residues at every third or fourth position and moves with changes in membrane potential to trigger channel opening[41,42] (FIG. 1a). Similarly, inwardly rectifying K^+ channel (Kir) subunits also have one P domain, but only two transmembrane segments (1P/2TM). The outward currents through these channels are relatively

Box 1 | What is leak?

From the earliest days of electrophysiological recordings, a fixed conductance called the leak was used to explain the presence of a resting membrane potential from which action potentials emerged and to which they returned. In current parlance, 'leak' is still applied to fixed background currents present at rest and to currents that seem to rise instantly to a new steady level with voltage steps. Leaks can be non-selective (for example, when a membrane is damaged) or result from the movement of specific ions.

Even at rest, the plasma membrane of a living cell is bustling with activity: ions move in and out, and ionic and electrical transmembrane gradients are maintained. The ionic gradient is established by active transport systems (such as Na^+–K^+ pumps). These pumps expend cellular energy (ATP) to keep internal levels of Na^+ low and K^+ high. Ion channels dissipate the ionic gradient by opening water-filled pathways across the membrane that allow for free diffusion of selected ions. An open K^+ channel allows K^+ ions to flow out of the cell down the K^+ concentration gradient. This leaves behind negative counter ions, producing an excess of negative charge inside the cell that limits K^+ flux: net outflow of K^+ continues until the chemical energy favouring efflux is balanced by the electrostatic energy favouring K^+ influx. At equilibrium, chemical and electrostatic forces are equal, efflux equals influx and there is no net movement of K^+ ions. The Nernst potential is the membrane voltage that yields equilibrium for a particular ion at a given ionic gradient. For a hypothetical membrane that allows only K^+ to cross, the Nernst potential is the same as the equilibrium reversal potential for K^+ ions, E_K, and is described by EQN 1:

$$E_K = \frac{RT}{zF} \ln \frac{K_{ex}}{K_{in}} \quad (1)$$

where R is the gas constant, T is temperature in degrees Kelvin, z is the charge of the ion, F is Faraday's constant and K_{ex} and K_{in} the concentrations of K^+ in the external and internal compartments, respectively. For physiological K^+ ion concentrations at physiological temperature (37 °C), RT/zF is ~27 mV and E_K is ~−97 mV. Mammalian cells have resting membrane potentials of −60 to −80 mV because K^+ ions are not the only ions that move at rest: for example, leak of Na^+ and Cl^- moves the membrane towards their Nernst potentials (about +67 and −93 mV, respectively). The resting membrane potential is often close to E_K because more K^+ channels are open at rest than pathways for other ions.

Excitability depends on resting membrane potential because action potentials fire when the membrane voltage rises to a threshold level where voltage-gated channels open and subsequently become inactive. To fire again these voltage-gated channels must recover from inactivation by returning to a negative potential below threshold, that is, the resting membrane potential.

small owing to chronic obstruction by internal magnesium and POLYAMINES; when membrane voltage is negative with respect to the K^+ equilibrium potential (E_K), K^+ ions that move into the cell relieve pore blockade and inward ion flux is significant[42–45] (FIG. 1b). In both families of one-P-domain channels, four subunits assemble to form a central K^+-selective pathway across the membrane[46,47].

In 1995, the first example of a two-P-domain channel subunit – TOK1 – was found in the sequence database for the budding yeast *Saccharomyces cerevisiae*; TOK1 has eight predicted transmembrane segments (2P/8TM) and constituted the first example of a non-voltage-gated outward rectifier[25–27] (FIG. 1e). The following year *KCNK0* was cloned from the neuromuscular tissues of the adult fruitfly *Drosophila melanogaster* on the basis of its capacity to rescue K^+-transport-defective yeast cells[36]. KCNK0 subunits were also found to have two P domains but just four predicted transmembrane segments (2P/4TM) (FIG. 1d) and provided the first example of a canonical K^+-selective leak conductance channel. The first mammalian gene for a 2P/4TM subunit – *KCNK1* – was also identified in the same year[39,48] and, although it was later proved to be a non-functional channel[49–51], attention was focused and these previously inconspicuous channel genes came rushing into view.

So far, over 50 genes for 2P/4TM subunits have been recognized in sequence databases and 14 of them have been cloned, studied and formally designated (TABLE 1). Unfortunately, this frenzy of productivity has led to a nomenclature nightmare. So, there are identical subunits with multiple names; for example, TBAK1, TASK1, OAT1 and KCNK3 are the same subunit. In other cases, subunits are the product of non-homologous genes but share the same root name; for example, TASK1 (KCNK3) and TASK3 (KCNK9) are not significantly related to TASK2 (KCNK5). There are also identical genes with multiple names; for example, what some authors call *Kcnk6* (REF. 52) is officially *Kcnk8* (REFS 50,53). However, this is also unfortunate because *Kcnk8* should have been *Kcnk7*, as it is the mouse variant of the human gene *KCNK7* (REF. 54). There are also subunits named for functional attributes that later proved to be minor or inaccurately assessed. Moreover, the number of two-P-domain channels is expected to increase significantly on the basis of the presence of at least 42 potential genes for 2P/4TM subunits in the complete genomic sequence of the nematode *Caenorhabditis elegans*[25,54]. Indeed, one of them – *TWK-18* – has now been shown to have K^+ channel activity[55]. In an attempt to avoid this confusion, we now use a simplified terminology that is gene-based and in accord with HUGO (Human Genome Organization) assignations; for example, *KCNK0* gene and KCNK0 channel (TABLE 1).

Functional types of two-P-domain channel

A dozen two-P-domain channel genes have been shown to function in experimental cells so far, and three have yet to show reproducible activity despite the presence of their transcript in native cells (TABLE 1). *TOK1* and *KCO1* (REF. 56) (a plant 2P/4TM subunit) encode non-voltage-gated outward rectifiers. The animal isolates *KCNK0, 2, 3, 4, 5, 6, 9, 10, 13* and *TWK-18* encode K^+-selective leak channels; however, this does not seem to be their full functional repertoire, as at least one, KCNK2, can reversibly transform into a voltage-gated channel[57,58].

Outward rectifiers. TOK1 remains unique as the only 2P/8TM subunit. It functions as a non-voltage gated outward rectifier; that is, a channel that passes outward current in a K^+ concentration-dependent (and so E_K-dependent) fashion (FIG. 1c), reminiscent of inward rectifier channels but in the opposite direction (FIG. 1b). TOK1 currents show an apparently instantaneous increase followed by a slow rising phase in response to depolarization[25,28,59]. In yeast cells (which are not noted for their excitability), TOK1 channels are a target of K1 killer toxin, a peptide encoded by an RNA virus that mediates strain-environmental dominance by killing its virus-free neighbours[33]. External K1 toxin directly activates TOK1 channels, leading to increased K^+ flux and death of virus-free cells. Conversely, internal K1 toxin blocks TOK1

POLYAMINES: Organic compounds that contain two or more amino groups. Putrescine, spermine and spermidine are prime examples.

Table 1 | **The two-P-domain potassium channels**

Gene[a]	Subunit names[b]	Species (chromosome)[c]	Expression mRNA! (**protein shown)	Phenotype[d]	Regulatory influences[e]	Accession number[f,g]	References
TOK1	TOK1	*S. cerevisiae* (X)		Outward	K1 Tx η, VA η	U28005	25–35
KCNK0	KCNK0 dORK1	*D. melanogaster* (1–10A1–2)	CNS,SM, GU	Open	PKη	U55321	36–38
KCNK1	KCNK1 TWIK1 hOHO	*H. sapiens* (1q42–43) *M. musculus* (8) *R. norvegicus*	CVR, CNS, GU, GI CVR, CNS**, GU	None		U76986	48–50, 105,106
KCNK2	KCNK2 TREK1 TPKC1	*H. sapiens* (1q41) *M. musculus* *R. rattus*	CNS, GI CVR, CNS**, GU, SM	Open or voltage-dependent	PK ι, AA η, MS η, VA η Temperature η	AF00471	49,50,57, 58,69–72
KCNK3	KCNK3 OAT1 TASK1	*H. sapiens* (7p24.1–23.3) *M. musculus* (5B) *R. rattus*	CVR, CNS, GU, GI CVR** CVR, CNS**	Open	pHo ι, AA ι LA ι, VA η	AF065163	61,75–66
KCNK4	KCNK4 TRAAK	*H. sapiens* (11q13) *M. musculus* (5)	CNS, GU CNS**	Open	AA η, MS η	AF247042	92,107–109
KCNK5	KCNK5 TASK2	*H. sapiens* (6p21.31–33) *M. musculus*	GU, GI UB	Open	pHo ι, VA η	AU026559	87,110
KCNK6	KCNK6 TOSS TWIK2	*H. sapiens* (19q13.1) *R. norvegicus*	CVR, CNS, GU, GI	Open	AA η, VA ι	AF134149	50,53, 111,112
KCNK7	KCNK7	*H. sapiens* (11q13)	CVR, CNS, GU, GI,	None		AF110522	52
KCNK8	Kcnk8	*M. musculus* (19,2B)	(**retina)			AF158234	51
KCNK9	KCNK9 TASK3	*H. sapiens* (8q24.3)	UB	Open	pHo ι, AA ι	AF212828	60,113,114
KCNK10	KCNK10 TREK2	*H. sapiens* (14q31) *R. norvegicus*	CNS, GU, GI	Open	AA η	AF279890	115,116
KCNK11		Reserved					
KCNK12	KCNK12 THIK2	*H. sapiens* (2p22–21) *R. rattus*	CVR, CNS, GU, GI	None		AF287302	73
KCNK13	KCNK13 THIK1	*H. sapiens* (14q24.1–3) *R. rattus*	UB	Open	AA η	AF287303	73
TWK-18	TWK-18	*C. elegans* (X)	Body wall muscle	Open	Temperature η	AAC32861	55
KCO1	KCO1	*A. thaliana*		Outward	Internal Ca^{2+} η	X97323	56

[a]Names for mammalian clones assigned by HUGO. *KCNK* and *Kcnk* represent human and mouse isolates, respectively. The 42 potential KCNK-like genes in *Caenorhabditis elegans*, including the first functional isolate (*TWK-18*), have not received KCNK designations.
[b]KCNK and Kcnk represent protein isolates and are accompanied by other names used in the literature.
[c]Based on Northern blot or rt-PCR studies and categorized by system as CVR, cardiovascular; CNS, central nervous system; GU, genitourinary; GI, gastrointestinal; SM, skeletal muscle and integument; UB, ubiquitous.
[d]*A. thaliana*, *Arabidopsis thaliana*; *D. melanogaster*, *Drosophila melanogaster*; *H. sapiens*, *Homo sapiens*; *R. norvegicus*, *Rattus norvegicus*; *R. rattus*, *Rattus rattus*; *S. cerevisiae*, *Saccharomyces cerevisiae*.
[e]Outward, non-voltage gated outward rectifier; open, open rectifier.
[f]K1 Tx, K1 killer toxin; VA, volatile anaesthetic; PK, protein kinase; AA, arachidonic acid; pHo, lowered external pH; LA, local anaesthetic; MS, mechanical stretch. The criteria for listing as stimulatory (η) or suppressive (ι) were as follows: VA, ≥30% change to clinical concentrations of chloroform (≤0.8 mM), halothane (≤0.2 mM) and/or isoflurane (≤0.3 mM); PK, ≥ threefold change to activation or suppression of one or more protein kinase systems; AA, ≥50% change in response to ≤100 μM, pHo, ≥10% change within one unit of physiological pH (7.4); LA, ≥50% change in response to clinical concentration of lidocaine (≤300 μM) or bupivacaine (≤200 μM); MS, ≥ twofold increase in response to ≤–60 mm Hg, temperature, Q_{10} >4.
[g]In human if available.

MACROSCOPIC CURRENTS
The sum of the ionic currents measured simultaneously from a large population of channels.

Q_{10}
The ratio of reaction rates for a 10°C increase in temperature.

channels, opposing the effect of external toxin and conferring immunity to virus-positive cells[35]. Moreover, overexpression of *TOK1* can rescue K^+-transport-defective yeast cells[32], whereas overactive channel mutants kill normal cells[59]. Why K^+ homeostasis is crucial for yeast cell survival is uncertain, as resting potential and nutrient uptake in yeast cells are primarily dependent on a transmembrane gradient for protons rather than for K^+, as is the case in mammalian cells (BOX 1).

KCO1, a 2P/4TM channel from *Arabidopsis thaliana*, is also an outward rectifier but it responds both to changes in E_K and in cytoplasmic Ca^{2+} levels[56]. The mechanism responsible for non-voltage-gated outward rectification (BOX 2) seems to involve both conformational changes of the protein and ion occupancy of the pore[22,26,28,31].

Open rectifiers — KCNK0. KCNK channels operate like K^+-selective holes in an electric field; that is, they show the attributes expected for leak channels. KCNK0 was the first clone to show the phenotype: MACROSCOPIC CURRENTS that seemed to be instantaneous, independent of voltage and selective for K^+ (REF. 36). Moreover, KCNK0 channels showed a behaviour called 'Goldman–Hodgkin–Katz rectification' or 'open rectification', as their conduction properties approximated predictions of constant-field current equations for free electrodiffusion through an open ion-selective pore[1,3]. In other words, KCNK0 currents change in a linear fashion as a function of voltage when the K^+ concentration is identical across the membrane. But when the concentration of K^+ is high intracellularly and low extracellularly (as occurs in

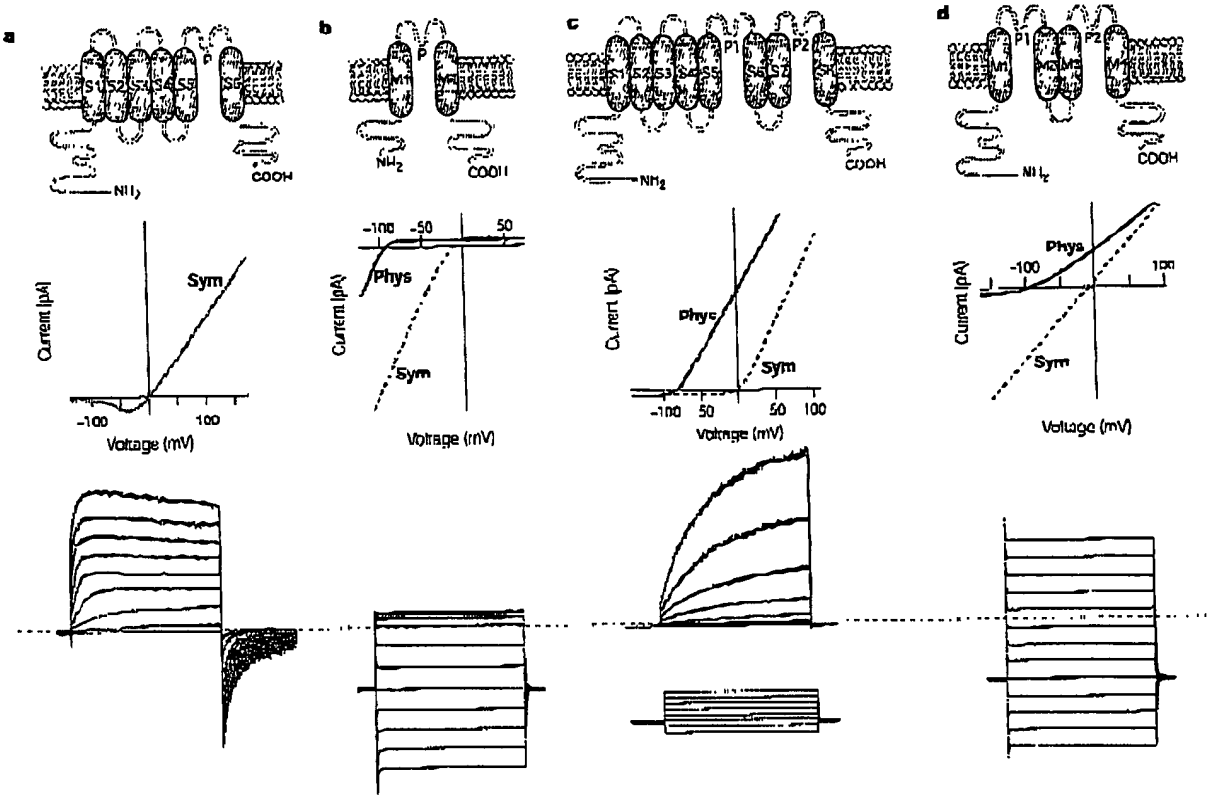

Figure 1 | **Potassium channels: membrane topology and current–voltage relationships.** Subunits are drawn with the external solution upwards. Graphs represent ideal examples. If the relationship is sensitive to changes in E_K, two conditions have been drawn: symmetric (sym, dashed) and physiological (phys, solid) K^+ concentration. Currents are drawn based on channels studied in symmetric conditions with 500 ms pulses to voltages of –80 to 60 mV (c, bottom panel), the dashed line corresponds to 0 mV. **a** | Voltage-gated K^+ channel (Kv) subunits have a one-P/six transmembrane domain (1P/6TM) predicted topology and are noted for their positively charged fourth transmembrane segment (S4) that acts as a sensor for changes in membrane potential. Some Kv channels are activated by depolarization (as shown here), whereas others open in response to hyperpolarizing stimuli. The current trace is based on KCNQ1 and reveals a delay before current begins to flow, which reflects the time it takes for the channels to enter into the open state after the voltage change. **b** | Inwardly rectifying K^+ channel (Kir) subunits have one P domain and two transmembrane segments (1P/2TM). Kir channels pass small outward currents owing to chronic blockade by intracellular cations; large inward currents pass when voltage is negative to E_K and the pore is unblocked. The current trace is based on Kir4.2 and reveals no delay before current begins to flow because unblock kinetics are faster than the resolution of the recording. **c** | TOK1, a non-voltage-gated, outwardly rectifying K^+ channel from *Saccharomyces cerevisiae* that has a 2P/8TM predicted topology. The channel passes outward current when membrane voltage is positive relative to E_K. The trace reveals a fast and a slow phase to current development after a change in voltage. **d** | KCNK channels have a predicted 2P/4TM-subunit topology. The channels are open rectifiers and allow the passage of large outward currents under conditions of high internal and low external K^+ (BOX 2). The current trace is based on KCNK0. It shows a nearly linear CURRENT–VOLTAGE RELATIONSHIP under symmetrical K^+, and reveals no delay before current starts to flow because the channels are open before the voltage step.

mammalian cells), a larger outward current is observed (FIG. 1d). Indeed, even KCNK channels that pass larger inward than outward single-channel currents in SYMMETRIC K^+ mediate primarily outward currents under physiological ionic conditions[50]; open rectification was an expected attribute of cloned K^+ leak channels (BOX 2).

Characterization of single KCNK0 channels has helped to define the basis for open rectification by showing, as expected, that leak currents accrue from channels that are open at rest[30]. So, voltage-gated K^+ channels show a pause before current flows because they are closed before a stimulating voltage step; the delay reflects the time it takes the channel to move into the open conformation[41,42]. Conversely, single KCNK0 channels show bursts of activity that last for minutes (punctuated by long-lasting closures) at all voltages: as a result, the channels are often open before a voltage step and ready to pass current without delay[38] (FIG. 2a). Whereas all KCNK channels are expected to leak in this fashion, the various isolates have already begun to reveal their individual differences. For example, currents through KCNK0 rise instantaneously to a stable new level (FIGS 1a, 2a) whereas ion flow through Kcnk3 shows additional voltage- and time-dependent responses to changes in potential[51].

Studies of single KCNK0 channels have also shown that leak pores conduct ions like one-P-domain channels[34,38], showing rapid and selective ion flux through a pathway that holds multiple ions simultaneously[27,43–44]. So, KCNK0 channels show attributes that herald ion–channel and ion–ion interactions in a multi-ion

SYMMETRIC IONIC CONDITIONS
Conditions in which the concentration of a particular ion is the same on both sides of a membrane.

CURRENT–VOLTAGE RELATIONSHIP
The changes in ionic current as a function of membrane voltage.

Box 2 | Why do channels rectify?

Potassium channels preferentially pass current in one direction (rectify) for three reasons:

- Unequal ion concentration. Current flows more easily from a side of high permeant ion concentration. This form of rectification, called Goldman–Hodgkin–Katz (or open) rectification, is seen with native currents[27,30] and cloned leak channels[26,28] (FIG. 1d), and explains why KCNK channels pass outward current under physiological ionic conditions. So, KCNK0 has a linear single channel current–voltage relationship under symmetric conditions[28], whereas KCNK9 shows mild inward rectification[60]. Nonetheless, both channels pass significant currents only in the outward direction across the physiological voltage range under native ionic conditions of high internal and low external K^+. Although the underlying assumptions of electrodiffusion theory are inaccurate (ions do not move independently of each other or the pore), this theory predicts some of the observed nonlinear current–voltage relationships surprisingly well[28,38].
- Gating. Channels can rectify if they only open in a voltage range that favours outward or inward current. For example, some voltage-gated K^+ channels show voltage-dependent outward rectification because they open with depolarization to voltages where outward K^+ flux is favoured (FIG. 1a). Unlike TOK1, these channels do not shift their activation voltage with E_K. Other depolarization-activated channels are inward rectifiers because they inactivate so rapidly once they open that they only pass large currents on recovery from inactivation at negative voltages where inward flux is favoured[45]. Still other voltage-gated channels show inward rectification because they are opened by steps to hyperpolarized voltages[59].
- Block. Some channels rectify because they are blocked in a voltage-dependent fashion. For example, inward rectifiers of the Kir class allow for the passage of inward current because internal magnesium and polyamines obstruct them when membrane voltage is positive to E_K. The channels are unblocked at hyperpolarized potentials below E_K, allowing significant inward K^+ flux[43–45] (FIG. 1b).

pore[38]: nonlinear concentration-dependent changes in unitary conductance (FIG. 2b), ANOMALOUS MOLE-FRACTION BEHAVIOUR, pore occlusion by barium and a classical RELATIVE PERMEABILITY SERIES. This result was not surprising: the cloning of KCNK channels revealed that they used the same pore-forming motif as one-P-domain channels. However, significant differences are likely to exist between the pores of one-P and two-P-domain channels[37]. In the case of one-P-domain channels, four matching P loops are assembled to form the pore, whereas the two P domains in KCNK subunits are not identical[23,24].

Finally, studies of single KCNK0 channels have shown that leak channels are not always open. KCNK0 activity is linked strongly to protein kinase action: single channels open when kinases are active (open probability, Po ~1) and close when they are suppressed (Po <0.05)[37] (FIG. 2c). This does not herald all-or-none inflexibility: KCNK0 activity is finely tuned through integration of signals from multiple second-messenger pathways that involve protein kinases A, C and G. These pathways determine the frequency and duration of the long-lasting closed state[37]. The regulatory domain of KCNK0 seems to reside in its ~700 residue carboxyl terminus, as the region can be deleted to produce active but unregulated ~300 residue 2P/4TM channels (FIG. 2c) that contain the KCNK0 pore and its gate[37].

Like KCNK0 (and most classical one-P-domain K^+ channels[56]), the level of activity of other cloned KCNK channels is also strictly regulated. Notable influences include kinase-dependent pathways, arachidonic acid, membrane stretch, external pH and temperature (TABLE 1).

Phenotypic flexibility: KCNK2. Expressed robustly in the central nervous system (CNS), especially in the hippocampus, whole-cell KCNK2 currents are increased by arachidonic acid, mechanical stretch and volatile anaesthetics and diminished by lowered temperature via a protein kinase A (PKA)-dependent pathway[10,57,58,69–72]. Exploring the basis for PKA effects, we were surprised to find that regulation of KCNK2 could produce something other than more or less leak. Single KCNK2 channels show unexpected and dynamic functional versatility: reversible inter-conversion from a leak to voltage-dependent phenotype[57,58]. Thus, KCNK2 is an open rectifier when the single canonical PKA consensus site is mutated to alanine (or bears no phosphate), passing large currents both inwards and outwards in symmetrical conditions (FIG. 3a). Conversely, channels altered to aspartate at the site (or phosphorylated) pass more outward current even in symmetrical K^+ owing to voltage-dependent changes in their open probability (FIG. 3b). These channels show a half-maximal activation voltage >0 mV that does not change with E_K (REFS 57, 58) and, so, are like classical voltage-gated channels (FIG. 1a; BOX 2) rather than the two-P-domain outward rectifiers TOK1 and KCO1 (FIG. 1c). This phenotypic alchemy is expected to enhance neuronal excitability as leak currents inhibit depolarization towards firing threshold, whereas channels activated at supra-threshold potentials do not interfere with rise to threshold but do facilitate recovery and repetitive re-firing.

The non-functional genes. The products of *KCNK1, 7/8* and *12* remain silent despite reaching the plasma membrane[73]. We have proposed, therefore, that for these proteins to become functional channels, they require a hitherto unidentified accessory subunit, pore-forming subunit or regulatory influence[10,41]. So far, their expression with functional KCNK subunits has failed to provide evidence for heteromeric co-assembly[21,22,73], but the possibility that non-pore-forming subunits are required for the function of these proteins has received genetic support in *C. elegans*. A 2P/4TM channel subunit encoded by the *SUP-9* gene is found in the same cells as two genetically interacting proteins that are predicted to reach the membrane and that lack P domains (REF. 74 and L. Pérez de la Cruz and H. R. Horvitz, personal communication).

Assigning KCNK channels to native leaks: KCNK3

Studies that seek to correlate KCNK genes and native currents are beginning to emerge in the literature, but such endeavours are difficult. Indeed, studies of one-P-domain channels have shown the common challenges to include, first, non-identical channels that behave similarly, and second, identical channels that behave differently as a function of their environment (for example, experimental versus native cells, two different cells in the same tissue, and the same cell type in health and disease). Such confounding variation results from altered gene expression, mRNA processing, subunit composition and channel modulation, and is also likely to slow identification of the physiological correlates of KCNK channels.

ANOMALOUS MOLE-FRACTION BEHAVIOUR
When two or more ions simultaneously reside inside a channel, their movement through the pore is dependent on each other. When channel conductance is measured as a function of the concentration ratio of two different ionic species and the conductance goes through a minimum rather than changing linearly as the ratio changes, then it is said to show anomalous mole-fraction behaviour.

RELATIVE PERMEABILITY SERIES
A given ion channel can allow the passage of related ionic species, although not all with the same ease. Potassium channels can be grouped by their relative permeability for monovalent cations at equilibrium.

The process of establishing a correlation begins with a suspicion born of similarities between a native current and a cloned channel. It must then be confirmed that the channel protein is expressed in the cells of interest and, later, a direct biophysical comparison, ideally at the single channel level, should be done. In the case of K^+ leak currents, we begin from our expectations and encounter the first problem. Leak currents should be instantaneous, stable and serve to suppress excitation because they shift the resting membrane potential towards E_K, a potential that is negative relative to the firing threshold of nerves and muscles (BOX 1). However, KCNK channels are not the only channel type to manifest these attributes: many classical one-P-domain channels also open in the hyperpolarized voltage range, influence resting membrane potential and contribute to K^+ leak (BOX 3).

However, the task is not insurmountable, particularly when studies are facilitated by judicious use of the available pharmacological tools. Thus, the most extensively studied mammalian genes, rat *Kcnk3* and mouse *Kcnk3* (REFS 61,75–86) seem to mediate currents in several tissues. These include: cardiac background currents (I_{K_2}), neurotransmitter-inhibited currents in central neurons, neuronal currents altered by volatile anaesthetics and, perhaps, oxygen sensing by the CAROTID BODY[84], and the action of ANGIOTENSIN II on adrenal cells[85].

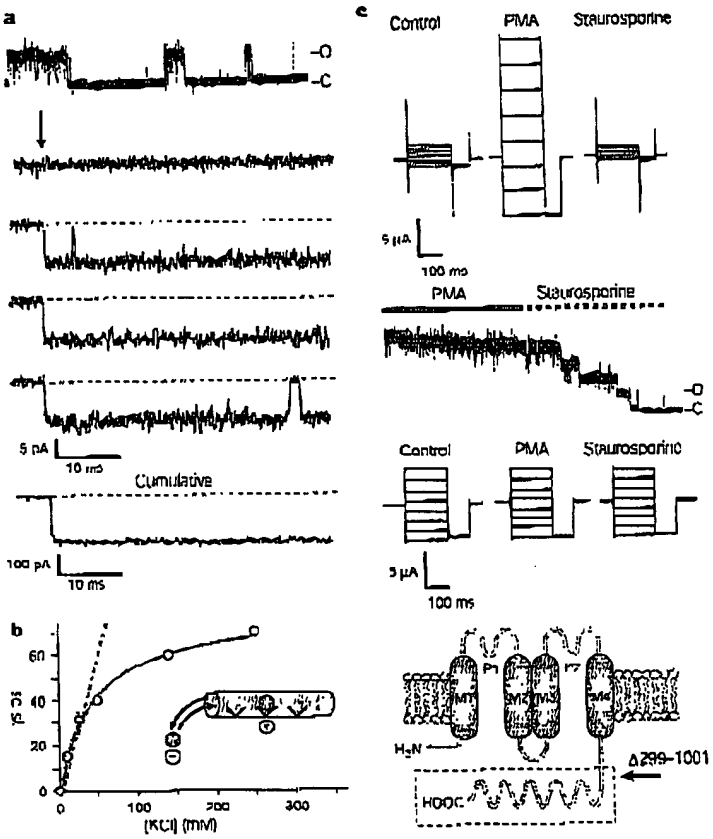

Figure 2 | **KCNK0 single channels open and close, show multi-ion attributes and are regulated.** KCNK0 channels were studied by expression in *Xenopus* oocytes. a | Top. Single KCNK0 channel recorded in an on-cell patch at 60 mV for 5 minutes with 140 mM KCl at the extracellular face of the channel; open state 3.3 pA. Bottom. Channel behaviour in response to a step from 0 to −120 mV (arrow). The first trace shows the response when the channel was closed (C) before the step; the next three traces show the response observed when the channel was open (O) before the pulse. (The dashed line is the 0 mV current level). Cumulative indicates an ensemble of 40 traces. b | KCNK0 single-channel conductance saturates with increasingly symmetrical K^+ (circles). Inset. Model of a multi-ion pore showing that ions entering a channel might find it occupied; as the new ion can not traverse the pore until the resident ion leaves, its movement is not independent (dashed line in top panel) and shows a saturating velocity. c | Top. Macroscopic KCNK0 currents measured by two-electrode voltage clamp in 20 mM K^+ with or without 50 nM PMA (phorbol-12-myristate-13-acetate) or 2 μM staurosporine. The cell was held at −80 mV and depolarized by 250 ms steps from −150 to 60 mV in 30 mV increments followed by 75 ms at −150 mV. Second panel. Four KCNK0 channels recorded in an on-cell patch at 60 mV with PMA in the bath and then staurosporine. Third panel. Macroscopic current traces for a cell expressing a channel without the carboxy-terminal 700 residues under conditions as in the top panel. Bottom. Model of a KCNK0 subunit showing the two functional domains, one pore-forming and the other regulatory. (Recordings adapted with permission from REFS 37,38.)

Cardiac I_{K_2}. Kcnk3 is an open rectifier noted for its inhibition by external protons across the physiological pH range (FIG. 4a). In the mouse, Kcnk3 is expressed throughout the heart with prominence in the ventricles[61] (FIG. 4b). This channel shows low basal open probability (<0.05), brief transitions to the open state, blockade by acidification of the extracellular medium in a K^+-sensitive fashion, and decremental changes in activity in response to its most common regulators[61]. In cardiac myocytes, I_{K_2} influences the amplitude and duration of the action-potential plateau and, consequently, the duration of myocardial contraction[19]. On the basis of their common distribution and biophysical attributes, it seems likely that Kcnk3 channels contribute to native I_{K_2} currents in mouse heart[61,81].

Neurotransmitter-inhibited leak channels. Inhibition of resting K^+ leak currents is a widespread mechanism by which serotonin, noradrenaline, substance P, glutamate, thyrotropin-releasing hormone (TRH) and acetylcholine (acting through muscarinic receptors) enhance neuronal excitability in the nervous system[11]. This is crucial to the regulation of 'state-switching' in cortical and thalamic neurons, which seems to mediate transitions between sleep and wakefulness, and perhaps attentiveness[12]. Two groups have now associated KCNK3 with these transmitter-sensitive currents in rat hypoglossal motoneurons[83] and cerebellar granule cells[82]. Hypoglossal motoneurons express the *KCNK3* transcript (FIG. 4c) and show KCNK3-like currents that are inhibited by lowered pH or by five different neurotransmitters known to operate through receptors that typically use the $\alpha_{q/11}$ G proteins. Once blocked by lowered pH, the native channels are no longer sensitive to the transmitters (FIG. 4d). Moreover, expression of the receptor for TRH with KCNK3 channels in experimental cells can reconstitute the phenomenon: TRH inhibits cloned KCNK3 currents unless they are previously suppressed by acidification[83] (FIG. 4d).

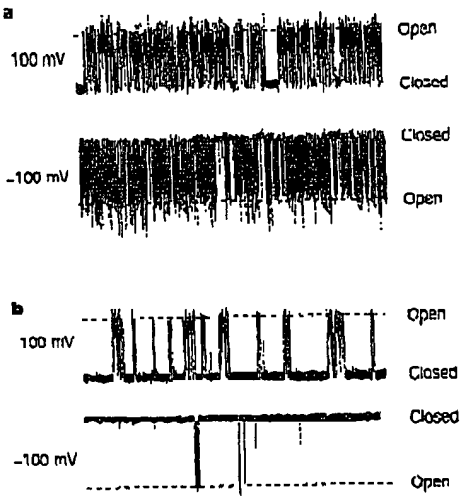

Figure 3 | **KCNK2: a leak pore that can also operate as a voltage-gated channel.** Inside-out patches were excised from oocytes expressing the channels and studied with symmetric 100 mM KCl; 2 s shown. Open state (dashed line) 7.8 pA at 100 mV and −8.5 pA at −100 mV; sampled 20 kHz, filtered 2 kHz (REFS 57,58). **a** | Single KCNK2-S348A channels have the same open probability across a wide range of potentials as expected for a non-voltage-dependent leak pore. **b** | Single KCNK2-S348D channels show a greater open probability at 100 than −100 mV (~100-fold[57,58]).

Box 3 | Do other K^+ channels leak?

Yes. Any channel open at rest will contribute to background K^+ current. Classical one-P-domain channels that leak include:

- Kir subunits. The one-P/two transmembrane domain (1P/2TM) inward rectifiers act to stabilize cells near E_K because their activity is dependent on inward flux of K^+ and relief from chronic channel block. An example is the acetylcholine-induced current in the heart, I_{KACh}, which is crucial for heart-rate control[100].
- Kv subunits. Some of these 1P/6TM subunits form channels that are active at hyperpolarized potentials when on their own[98]. Others leak when associated with accessory subunits. For example, MinK-related peptide 2 (MiRP2) assembles with the Shaw family isolate Kv3.4 to form subthreshold K^+ channels in skeletal muscle that set the resting membrane potential and are associated in mutant form with inherited periodic paralysis[101].
- KCNQ subunits. These 1P/6TM subunits form mixed complexes of KCNQ2/3 and KCNQ3/4 that show a relatively hyperpolarized activation threshold (~−60 mV). They contribute to M CURRENTS in sympathetic neurons and the central nervous system, and are inhibited by muscarinic receptor activation and are associated with familial epilepsy[89–91]. KCNQ1 subunits gain prominent expression in the ear and heart and are associated with inherited deafness and arrhythmia[81,102]. MiRP2–KCNQ1 complexes have been shown to allow for the passage of K^+ ions at rest in experimental cells[103,104].

Action of anaesthetics. Soon after they were identified, KCNK channels were considered prime candidates as native targets for anaesthetics[21,30]. The idea was attractive because anaesthetics enhance leak currents in neural tissue (and therefore decrease excitability) and, at the same time, the presence of KCNK channels in the heart could explain the depressive side effects of anaesthetics. Several KCNK clones are sensitive to local and volatile anaesthetics (TABLE 1). Moreover, native KCNK3-like[86] and KCNK5-like channels[87] have been shown to respond at clinically relevant concentrations. KCNK3-expressing hypoglossal and locus coeruleus neurons (FIG. 4c) show halothane-induced, pH-sensitive membrane hyperpolarization that leads to decreased spiking activity[86] (FIG. 4e). Inhibition of hypoglossal and locus coeruleus neurons is thought to contribute to halothane-induced immobilization and to the analgesic and hypnotic actions of halothane, respectively.

These are compelling results, but caution is in order. One and two-P-domain K^+ channels that show comparable attributes are widely expressed in the heart and brain. Cardiac myocytes contain rapidly activating, non-inactivating, voltage-dependent K^+ channels formed by 1P/6TM Kv subunits. These channels contribute to K^+ flux during the plateau of the cardiac action potential[89]. Similarly, voltage-dependent M channels formed by 1P/6TM KCNQ subunits might accompany neuronal, muscarine-inhibited KCNK3-like channels[92] as KCNQ channels are also suppressed by muscarine and external acidification, and contribute to resting K^+ flux owing to their activation at hyperpolarized potentials[89–91] (BOX 3). Furthermore, KCNK channels themselves show overlapping attributes and expression patterns. For example, KCNK2, KCNK3 and KCNK4 are neurotransmitter-inhibited resting currents that are co-expressed in several regions of the nervous system, although they do have distinguishable regulatory profiles[80,92,93] (TABLE 2). For instance, serotonin inhibits all three channels, but KCNK2 (like *Aplysia californica* sensory neuron S channels[21,94]) is suppressed via cyclic AMP and PKA, whereas KCNK3 and KCNK4 are responsive via another signalling pathway.

Many unanswered questions

Two-P-domain channels have been discovered at a remarkable rate over the past five years. This has produced a marvellous collection of KCNK genes waiting to be studied that seem well matched to the multitude of orphan channels without intrinsic voltage dependence that have been found in native cells[6,95]. Some long-standing issues have been addressed, but our most pressing questions remain to be answered. What roles do KCNK channels have in physiology and disease? Are they targets for common drugs? Where are their gates (and do they resemble the gates of one-P-domain channels as we suspect[60,33,34,37,55])? How does KCNK2 sense voltage? Will KCNK channels other than KCNK2 show phenotypic versatility? Do two-P-domain channels

CAROTID BODY
A chemoreceptor organ located above the bifurcation of the common carotid artery. It monitors changes in blood O_2 and CO_2 content and pH, thus helping to control respiratory activity.

ANGIOTENSIN II
Vasoconstrictor octapeptide that acts on the zona glomerulosa of the adrenal cortex to increase aldosterone production and, consequently, to stimulate sodium uptake by the kidney.

M CURRENT
Cationic current modulated by the activation of muscarinic receptors that participates in determining the subthreshold excitability of neurons and their responsiveness to synaptic input. The underlying channel is thought to consist of KCNQ potassium channel subunits.

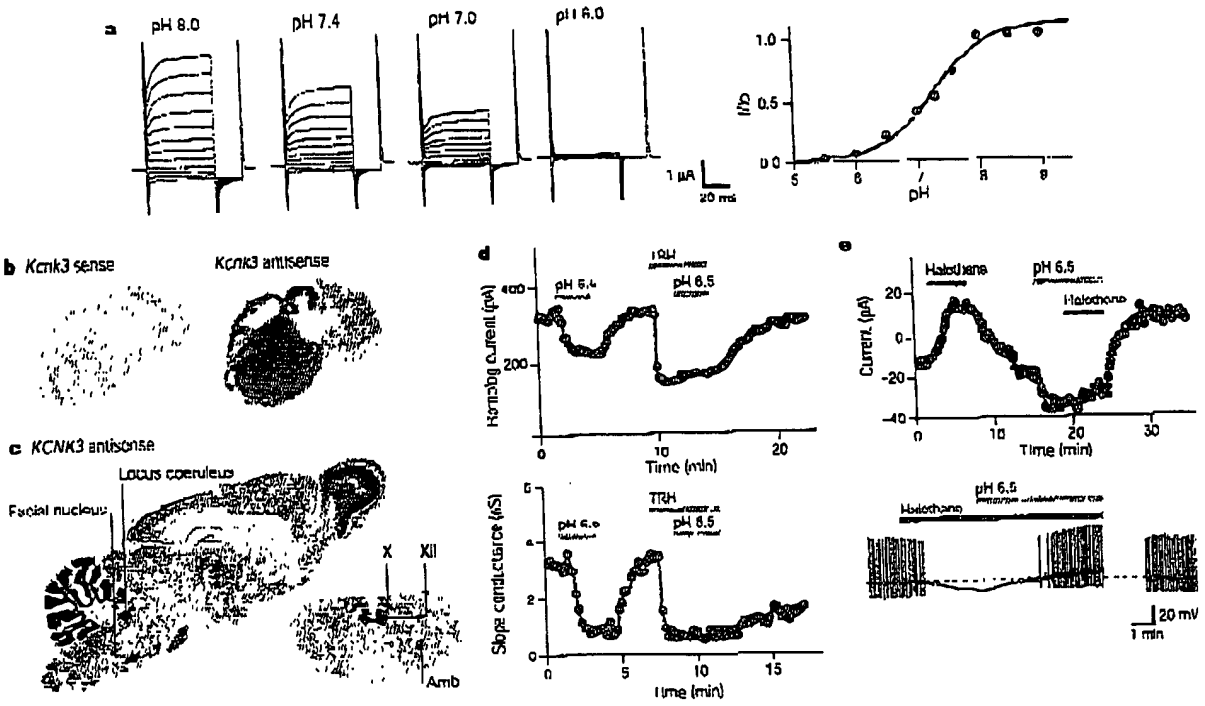

Figure 4 | **KCNK3 channels: molecular correlation with native cardiac and neuronal currents.** **a** | Cloned KCNK3 channels are inhibited by external protons at physiological pH. Two-electrode voltage clamp protocol: oocyte membrane potential was held at −80 mV and pulsed from −120 to +45 mV in 15 mV voltage steps for 50 ms, followed by a 20 ms step to −120 mV. A cell exposed to varying pH with 5 mM KCl bath solution is shown. The plot shows dependence of current at 0 mV on bath pH (mean ± SEM) for groups of five cells normalized to pH 8.0. The solid line represents a fit giving a pKa of 7.24 ±0.03 and a Hill coefficient of 1.02 ±0.06. **b** | *In situ* hybridization of mouse heart with an ^{35}S-labelled antisense probe to mouse *Kcnk3* shows a strong signal for message in ventricle and a weak signal in atria. **c** | *In situ* hybridization of rat brain with a ^{32}P-labelled antisense probe to rat *KCNK3* cDNA shows a strong signal for message in brainstem motoneurons — the nucleus ambiguus (Amb), and the facial, vagal (X), and hypoglossal nuclei (XII) — and in the locus coeruleus. **d** | Thyrotropin-releasing hormone (TRH) inhibits both KCNK3-like current in hypoglossal motoneurons and cloned KCNK3 channels in HEK 293 cells that also express the TRH receptor. Top: Hypoglossal motoneurons were exposed to low pH solution before and after changes in holding current induced at −60 mV by 1–2 µM TRH. Bottom: Slope conductance from ramp currents measured in HEK 293 cells expressing both KCNK3 and the TRH receptor when exposed to low pH solution before and after 0.1 µM TRH. TRH acted to inhibit the channel fully so that further effect was not observed by re-acidification. **e** | Halothane (0.3 mM) hyperpolarizes neurons of the rat locus coeruleus, suppressing firing by activating a KCNK3-like current. Top: Holding current of a cell at −60 mV is increased by halothane; the effect was inhibited by lowered pH. Bottom: Current clamp recording shows halothane-induced hyperpolarization and spike suppression that is reversed by acidification. (Panels **a** and **b** adapted with permission from REF. 61 © (2000) American Society for Biochemistry and Molecular Biology. Panels **c** and **d** adapted with permission from REF. 83 © (2000) Elsevier Science Ltd. Panel **e** adapted with permission from REF. 86 © (2000) Society for Neuroscience.)

function as dimers (crosslinking through a non-conserved cysteine indicates that this might be the case[56])? Do both P domains contribute directly to pore formation? Will lack of identity between first and second P domains in KCNK channel subunits yield variations in gating or in ion selectivity[57]? Do KCNK subunits form heteromers? What kind of alchemy will bring the non-functional KCNK variants to life?

Conclusion

Fifty years after K^+-selective leak channels were first described, their genes have been found. They are numerous and widespread. The genes encode unique channel subunits with two pore-forming P domains. Whereas fungi and plants contain variants that operate as non-voltage dependent outward rectifiers, animals carry at least 50 genes for 2P/4TM subunits (the KCNK channels) that function as open rectifiers primarily passing outward current under physiological K^+ concentrations. Studies of single KCNK channels have confirmed that leak currents result from channels open at rest but have also shown that leak channels are not always open. Instead, like their native counterparts, the activity of KCNK channels is subject to strict regulation. As expected from classical studies, KCNK channels seem to control the excitability of nerves and muscles and, perhaps, to mediate the effects of volatile anaesthetics. Thus, neurotransmitter-mediated inhibition of resting K^+ flux has an excitatory influence, whereas increased activity with anaesthetic exposure stabilizes cells at rest. Regulation of one KCNK isolate has been observed to reversibly produce leak or voltage-dependent function.

behaviours that stabilize cells or facilitate repetitive excitation, respectively. There is much yet to learn about KCNK channels now that they are visible. Like dark matter in the universe, the more we understand, the greater their influence seems to be.

Links

DATABASE LINKS TOK1 | *KCNK0* | *KCNK1* | KCNK2 | KCNK3 | Kcnk3 | KCNK4 | KCNK5 | KCNK6 | *KCNK7* | *Kcnk8* | KCNK9 | *KCO1*

1. Goldman, D. E. Potential, impedance, and rectification in membranes. *J. Gen. Physiol.* **27**, 37–60 (1943).
2. Hodgkin, A. L. & Katz, B. The effect of sodium ions on the electrical activity of the giant axon of the squid. *J. Physiol.* **108**, 37–77 (1949).
3. Hodgkin, A. L. & Huxley, A. F. A quantitative description of membrane current and its application to conduction and excitation in nerve. *J. Physiol.* **117**, 500–544 (1952).
References 1–3 are classical works on currents that mediate excitable membrane function (including a resting leak).
4. Adams, D. J., Smith, S. J. & Thompson, S. H. Ionic currents in molluscan soma. *Annu. Rev. Neurosci.* **3**, 141–167 (1980).
5. Jones, S. W. On the resting potential of isolated frog sympathetic neurons. *Neuron* **3**, 159–161 (1989).
6. Koyano, K., Tanaka, K. & Kuba, K. A patch-clamp study on the muscarine-sensitive potassium channel in bullfrog sympathetic ganglion cells. *J. Physiol.* **454**, 231–248 (1992).
7. Chang, D. C. Is the K+ permeability of the resting membrane controlled by the excitable K+ channel? *Biophys. J.* **50**, 1095–1100 (1986).
8. Schmidt, H. & Stampfli, R. The effect of tetraethylammonium chloride on single Ranvier's nodes. *Pflügers Arch. Gesamte Physiol. Menschen Tiere* **287**, 311–325 (1966).
9. Hille, B. Potassium channels in myelinated nerve. Selective permeability to small cations. *J. Gen. Physiol.* **61**, 669–686 (1973).
10. Baker, M., Bostock, H., Grafe, P. & Martius, P. Function and distribution of three types of rectifying channel in rat spinal root myelinated axons. *J. Physiol.* **383**, 45–67 (1987).
11. Nicoll, R. A., Malenka, R. C. & Kauer, J. A. Functional comparison of neurotransmitter receptor subtypes in mammalian central nervous system. *Physiol. Rev.* **70**, 513–565 (1990).
12. McCormick, D. A. & Bal, T. Sleep and arousal: thalamocortical mechanisms. *Annu. Rev. Neurosci.* **20**, 185–215 (1997).
13. Koh, D. S., Jonas, P. Brau, M. E. & Vogel, W. A TEA-insensitive fluctuating potassium channel active around the resting potential in myelinated nerve. *J. Membr. Biol.* **130**, 149–162 (1992).
14. Wu, J. V. Rubinstein, C. T. & Strieger, F. Single-channel characterization of multiple types of potassium channels in demyelinated *Xenopus* axons. *J. Neurosci.* **13**, 5153–5163 (1993).
15. Apkon, M. & Nerbonne, J. M. Are there multiple types of depolarization-activated K+ channels in adult ventricular myocytes? *Biophys. J.* **60**, 1036a (1991).
16. Yue, D. T. & Marban, E. A novel cardiac potassium channel that is active and conductive at depolarized potentials. *Pflügers Arch.* **413**, 127–133 (1988).
17. Bryte, W. A. & Nerbonne, J. M. Two functionally distinct 4-aminopyridine-sensitive outward K+ currents in rat atrial myocytes. *J. Gen. Physiol.* **100**, 1041–1067 (1992).
18. Wang, Z., Fermini, B. & Nattel, S. Sustained depolarization-induced outward current in human atrial myocytes. Evidence for a novel delayed rectifier K+ current similar to Kv1.5 cloned channel currents. *Circ. Res.* **73**, 1061–1076 (1993).
19. Backx, P. H. & Marban, E. Background potassium current active during the plateau of the action potential in guinea pig ventricular myocytes. *Circ. Res.* **72**, 890–900 (1993).
20. Van Wagoner, D. R., Pond, A. L., McCarthy, P. M., Trimmer, J. S. & Nerbonne, J. M. Outward K+ current densities and Kv1.5 expression are reduced in chronic human atrial fibrillation. *Circ. Res.* **80**, 772–781 (1997).
21. Siegelbaum, S. A., Camardo, J. S. & Kandel, E. R. Serotonin and cyclic AMP close single K+ channels in *Aplysia* sensory neurones. *Nature* **299**, 413–417 (1982).
22. Shen, K. Z., North, R. A. & Surprenant, A. Potassium channels opened by noradrenaline and other transmitters in excised membrane patches of guinea-pig submucosal neurons. *J. Physiol. (Lond.)* **446**, 581–600 (1992).
23. Buckler, K. J. A novel oxygen-sensitive potassium current in rat carotid body type I cells. *J. Physiol.* **498**, 649–662 (1997).
24. Wegner, R. G. & Dekin, M. S. cAMP modulates an S-type K+ channel coupled to $GABA_A$ receptors in mammalian respiratory neurons. *Neuroreport* **8**, 1667–1670 (1997).
25. Kerschun, K. A., Jones, W. J., Sellers, A. J., Kaczmarek, L. K. & Goldstein, S. A. N. A new family of outwardly-rectifying potassium channel proteins with two pore domains in tandem. *Nature* **376**, 690–695 (1995).
26. Zhou, X. L., Vallant, B., Loukin, S. H., Kung, C. & Saimi, Y. YKC1 encodes the depolarization-activated K+ channel in the plasma membrane of yeast. *FEBS Lett.* **373**, 170–176 (1995).
27. Reid, J. D. *et al.* The *S. cerevisiae* outwardly-rectifying potassium channel (DUK1) identifies a new family of channels with duplicated pore domains. *Receptors Channels* **4**, 51–62 (1996).
References 25–27 describe the discovery of TOK1, the first cloned two-P-domain channel, the first cloned non-voltage gated outward rectifier and the first channel with a predicted two-P/eight-transmembrane domain subunit topology.
28. Vergani, P., Mucaga, T., Jarvis, S. M. & Blair, M. R. Extracellular K+ and Ba^{2+} maintain voltage-dependent inactivation of the outward-rectifying K+ channel encoded by the yeast gene TOK1. *FEBS Lett.* **405**, 337–344 (1997).
29. Yost, C. S., Gray, A. T., Winegar, D. D. & Leonoudakis, D. Baseline K+ channels as targets of general anesthetics: studies of the action of volatile anesthetics on TOK1. *Toxicol. Lett.* **100**, 293–300 (1998).
30. Gray, A. T., Winegar, B. D., Leonoudakis, D. J., Forsayeth, J. R. & Yost, C. S. TOK1 is a volatile anesthetic stimulated K+ channel. *Anesthesiology* **88**, 1076–1084 (1998).
31. Vergani, P., Hamilton, D., Jarvis, S. & Blair, M. R. Mutations in the pore regions of the yeast K+ channel YKC1 affect gating by extracellular K+. *EMBO J.* **17**, 7180–7190 (1998).
32. Hamm, C., Zhou, X. L., & Kung, C. Potassium uptake through the TOK1 K+ channel in the budding yeast. *J. Membr. Biol.* **168**, 149–157 (1999).
33. Ahmed, A. *et al.* A molecular target for viral K1 killer toxin: TOK1 potassium channels. *Cell* **99**, 283–291 (1999).
Identification of TOK1 as a target for viral K1 killer toxin.
34. Loukin, S. H. & Saimi, Y. K+-dependent composite gating of the yeast K+ channel, Tok1. *Biophys. J.* **77**, 3060–3070 (1999).
35. Sesti, F., Shih, T., Nikolaeva, N. & Goldstein, S. A. N. The basis for immunity to killer toxin: channel block. *Biophys. J.* **80**, 443a (2001).
36. Goldstein, S. A. N., Price, L. A., Rosenthal, D. N. & Pausch, M. H. ORK1, a potassium-selective leak channel with two pore domains cloned from *Drosophila melanogaster* by expression in *Saccharomyces cerevisiae*. *Proc. Natl Acad. Sci. USA* **93**, 13256–13261 (1996).
37. Tiberbend, N., Ilan, N., Gonzalez-Colaso, R. & Goldstein, S. A. N. Opening and closing of KCNK0 potassium leak channels is tightly regulated. *J. Gen. Physiol.* **116**, 721–734 (2000).
38. Ilan, N. & Goldstein, S. A. N. KCNK0: single, cloned nonsaxon leak channels are multi-ion pores. *Biophys. J.* **80**, 241–254 (2001).
References 36–38 describe KCNK0, the first cloned example of a canonical leak channel (an open rectifier) and the first functional channel with a predicted two-P/four-transmembrane domain subunit topology.
39. Yellen, G., Jurman, M. E., Abramson, T. & MacKinnon, R. Mutations affecting internal TEA blockade identify the probable pore-forming region of a K+ channel. *Science* **251**, 939–942 (1991).
40. Heginbotham, L., Lu, Z., Abramson, T. & MacKinnon, R. Mutations in the K+ channel signature sequence. *Biophys. J.* **66**, 1061–1067 (1994).
41. Sigworth, F. J. Voltage gating of ion channels. *Q. Rev. Biophys.* **27**, 1–40 (1994).
42. Yellen, G. The moving parts of voltage-gated ion channels. *Q. Rev. Biophys.* **31**, 239–295 (1998).
43. Vandenberg, C. A. Inward rectification of a potassium channel in cardiac ventricular cells depends on internal magnesium ions. *Proc. Natl Acad. Sci. USA* **84**, 2560–2564 (1987).
44. Jan, L. Y. & Jan, Y. N. Potassium channels and their evolving gates. *Nature* **371**, 119–122 (1994).
45. Lopatin, A. N., Makhina, E. N. & Nichols, C. G. Potassium channel block by cytoplasmic polyamines as the mechanism of intrinsic rectification. *Nature* **372**, 366–369 (1994).
46. MacKinnon, R. Determination of the subunit stoichiometry of a voltage-activated potassium channel. *Nature* **350**, 232–235 (1991).
47. Doyle, D. A. *et al.* The structure of the potassium channel: molecular basis of K+ conduction and selectivity. *Science* **280**, 69–77 (1998).
48. Lesage, F. *et al.* TWIK-1, a ubiquitous human weakly inward rectifying K+ channel with a novel structure. *EMBO J.* **15**, 1004–1011 (1996).
Reference 48 and reference 105 describe KCNK1, the first mammalian two-P/four-transmembrane domain clone now recognized to be in part of a so far non-functional group.
49. Goldstein, S. A. N., Wang, K. W., Ilan, N. & Pausch, M. Sequence and function of the two P domain potassium channels: implications of an emerging superfamily. *J. Mol. Med.* **76**, 13–20 (1998).
50. Pountney, D. J. *et al.* Identification and cloning of TWIK-originated similarity sequence (TOSS): a novel human 2 pore K+ channel principal subunit. *FEBS Lett.* **458**, 191–196 (1999).
51. Duckenhauer, D., Nimmakayalu, M. A., Ward, D. C., Gaitanaki, S. A. N. & Gallaghe, P. G. Genomic organization and chromosomal localization of the murine 2 P domain potassium channel gene Kcnk6: conservation of gene structure in 2 P domain potassium channels. *Gene* (in the press).
52. Salinas, M. *et al.* Cloning of a new mouse two-P domain channel subunit and a human homologue with a unique pore structure. *J. Biol. Chem.* **274**, 11751–11760 (1999).
53. Chavez, R. A. *et al.* TWIK-2, a new weak inward rectifying member of the tandem pore domain potassium channel family. *J. Biol. Chem.* **274**, 7887–7892 (1999).
54. Wang, Z. W., Kunkel, M. T., Wei, A., Butler, A. & Salkoff, L. Genomic organization of nematode 4TM K+ channels. *Ann. NY Acad. Sci.* **868**, 286–303 (1999).
55. Kunkel, M. T., Johnstone, D. B., Thomas, J. H. & Salkoff, L. Mutants of a temperature-sensitive two-P domain potassium channel. *J. Neurosci.* **20**, 7517–7524 (2000).
Describes the identification of TWIK-1B, the first functional two-P/four-transmembrane domain clone of at least 42 potential variants in *C. elegans*.
56. Czempinski, K., Zimmermann, S., Ehrhardt, T. & Muller-Rober, B. New structure and function in plant K+ channels: KCO1, an outward rectifier with a steep Ca^{2+} dependency. *EMBO J.* **16**, 2565–2575 (1997).
57. Bockenhauer, D., Zilberberg, N. & Goldstein, S. A. N. A hippocampal potassium leak pore into a voltage-dependent channel by phosphorylation. (submitted)
58. Bockenhauer, D. & Goldstein, S. A. N. Excitement creating a voltage-dependent potassium channel from a leak. *Biophys. J.* **80**, 193a (2001).
References 57 and 58 show that regulation of cloned and hippocampal KCNK2 reversibly yields open rectifier or voltage-dependent K+ channel function.
59. Loukin, S. H. *et al.* Random mutagenesis reveals a region important for gating of the yeast K+ channel Ykc1. *EMBO J.* **16**, 4817–4825 (1997).
60. Kim, Y., Bang, H. & Kim, D. TASK-3, a new member of the tandem pore K+ channel family. *J. Biol. Chem.* **275**, 9340–9347 (2000).
61. Lopes, C. M. B., Gallagher, P. G., Buck, M. E., Butler, M. H. & Goldstein, S. A. N. Proton block and voltage gating are potassium-dependent in the cardiac leak channel Kcnk3. *J. Biol. Chem.* **275**, 16969–16978 (2000).
References 61 and references 76–81 describe the cloning and characterization of KCNK3, a pH-sensitive open rectifier.
62. Hille, B. & Schwarz, W. Potassium channels as multi-ion single-file pores. *J. Gen. Physiol.* **72**, 409–442 (1978).
63. Yellen, G. Ionic permeation and blockade in Ca^{2+}-activated K+ channels of bovine chromaffin cells. *J. Gen. Physiol.* **84**, 157–186 (1984).
64. Neyton, J. & Miller, C. Discrete Ba^{2+} block as a probe of ion occupancy and pore structure in the high-conductance

Ca^{2+}-activated K^+ channel. *J. Gen. Physiol.* **92**, 569–586 (1988).

66. Heginbotham, L. & MacKinnon, R. Conduction properties of the cloned Shaker K^+ channel. *Biophys. J.* **65**, 2089–2096 (1993).
66. Lu, Z. & MacKinnon, R. A conductance maximum observed in an inward-rectifier potassium channel. *J. Gen. Physiol.* **104**, 477–488 (1994).
67. Chapman, M. L., Krouse, H. S. & VanDongen, A. M. J. GYGD pore motifs in neighbouring potassium channel subunits interact to determine ion selectivity. *J. Physiol.* **530**, 21–33 (2001).
68. Levitan, I. B. Modulation of ion channels by protein phosphorylation and dephosphorylation. *Annu. Rev. Physiol.* **56**, 193–212 (1994).
69. Fink, M. *et al.* Cloning, functional expression and brain localization of a novel unconventional outward rectifier K^+ channel. *EMBO J.* **15**, 6854–6862 (1996).
Describes the identification of KCNK2, the first functional two-P/four-transmembrane domain clone from a mammal.
70. Maingret, F. TREK-1 is a heat-activated background K^+ channel. *EMBO J.* **19**, 2483–2491 (2000).
71. Maingret, F., Fosset, M., Lesage, F., Lazdunski, M. & Honore, E. Lysophospholipids open the two-pore domain mechano-gated K^+ channels TREK-1 and TRAAK. *J. Biol. Chem.* **275**, 10128–10133 (2000).
72. Meadows, H. J. *et al.* Cloning, localization and functional expression of the human orthologue of the TREK-1 potassium channel. *Pflugers Arch. Eur. J. Physiol.* **439**, 714–722 (2000).
73. Rajan, S. *et al.* THIK-1 and THIK-2, a novel subfamily of tandem pore domain K^+ channels. *J. Biol. Chem.* (in the press).
74. Trimmer, J. S. & Horvitz, H. R. unc-93(e1500): A behavioral mutant of *Caenorhabditis elegans* that defines a gene with a wild-type null phenotype. *Genetics* **96**, 147–164 (1980).
75. Duprat, F. *et al.* TASK, a human background K^+ channel to sense external pH variations near physiological pH. *EMBO J.* **16**, 5464–5471 (1997).
76. Leonoudakis, D. *et al.* An open rectifier potassium channel with two pore domains in tandem cloned from rat cerebellum. *J. Neurosci.* **18**, 868–877 (1998).
77. Kim, D., Fujita, A., Horio, Y. & Kurachi, Y. Cloning and functional expression of a novel cardiac two-pore background K^+ channel (cTBAK-1). *Circ. Res.* **82**, 513–518 (1998).
78. Lopes, C. M. B., Gallagher, P. G., Wong, C., Buck, M. & Goldstein, S. A. N. OAT1 is an open, acid-sensitive, two P domain K^+ channel from mouse heart. *J. Biophys.* **74**, A14 (1998).
79. Kindler, C. H., Yost, C. S. & Gray, A. T. Local anesthetic inhibition of baseline potassium channels with two pore domains in tandem. *Anesthesiology* **90**, 1092–1102 (1999).
80. Mangurian, N. A., Bmy-Ward, P., Goldstein, S. A. N. & Gnagstret, I. G. Assignment of the 2 P domain, acid-sensitive potassium channel gene OAT1 (KCNK3) to human chromosome 20q13. 3-p24. 1 and murine chromosome band 5B by *in situ* hybridization. *Cytogen. Cell Genet.* **86**, 242–243 (1999).
81. Kim, Y., Bang, H. & Kim, D. TBAK-1 and TASK-1, two-pore K^+ channel subunits: kinetic properties and expression in rat heart. *Am. J. Physiol.* **277**, H1658–H1670 (1999).
82. Millar, J. A. *et al.* A functional role for the two-pore domain potassium channel TASK-1 in cerebellar granule neurons. *Proc. Natl Acad. Sci. USA* **97**, 3614–3618 (2000).
83. Talley, E. M., Lei, Q., Sirois, J. E. & Bayliss, D. A. TASK-1, a two-pore domain K^+ channel, is modulated by multiple neurotransmitters in motoneurons. *Neuron* **25**, 399–410 (2000).
84. Buckler, K. J., Williams, B. A. & Honore, E. An oxygen-, acid- and anaesthetic-sensitive TASK-like background potassium channel in rat arterial chemoreceptor cells. *J. Physiol. (Lond.)* **525**, 135–142 (2000).
85. Czirjak, G., Fischer, T., Spat, A., Lesage, F. & Enyedi, P. TASK (TWIK-related acid sensitive K^+ channel) is expressed in glomerulosa cells of rat adrenal cortex and inhibited by angiotensin II. *Mol. Endocrinol.* **14**, 863–874 (2000).
86. Sirois, J. E., Lei, Q., Talley, E. M., Lynch, C. & Bayliss, D. A. The TASK-1 two-pore domain K^+ channel is a molecular substrate for neuronal effects of inhalation anesthetics. *J. Neurosci.* **20**, 6347–6354 (2000).
References 81–86 along with reference 61 describe KCNK3-like native currents; evidence for a contribution to cardiac I_{to}, neurotransmitter-inhibited resting currents and the action of inhaled anaesthetics in the nervous system.
87. Gray, A. T. *et al.* Volatile anesthetics activate the human tandem pore domain baseline K^+ channel KCNK5. *Anesthesiology* **92**, 1727–1730 (2000).
88. Nerbonne, J. M. Molecular basis of functional voltage gated K^+ channel diversity in the mammalian myocardium. *J. Physiol.* **525**, 285–298 (2000).
89. Brown, D. A. & Adams, P. R. Muscarinic suppression of a novel voltage-sensitive K^+ current in a vertebrate neuron. *Nature* **283**, 673–676 (1980).
90. Wang, H. S. *et al.* KCNQ2 and KCNQ3 potassium channel subunits: molecular correlates of the M-channel. *Science* **282**, 1890–1893 (1998).
91. Jentsch, T. J. Neuronal KCNQ potassium channels: physiology and role in disease. *Nature Rev. Neurosci.* **1**, 21–30 (2000).
92. Patel, A. J. *et al.* A mammalian two pore domain mechano-gated S-like K^+ channel. *EMBO J.* **17**, 4283–4290 (1998).
93. Maingret, F., Fosset, M., Lesage, F., Lazdunski, M. & Honore, E. TRAAK is a mammalian neuronal mechano-gated K^+ channel. *J. Biol. Chem.* **274**, 1381–1387 (1999).
94. Klein, M. & Kandel, E. R. Mechanism of calcium current modulation underlying presynaptic facilitation and behavioral sensitization in *Aplysia*. *Proc. Natl Acad. Sci. USA* **77**, 6912–6916 (1980).
95. O'Kelly, I., Stephens, R. H., Peers, C. & Kemp, P. J. Potential identification of the O2-sensitive K^+ current in a human neuroepithelial body-derived cell line. *Am. J. Physiol.* **276**, L95–L104 (1999).
96. Lesage, F. *et al.* Dimerization of TWIK-1 K^+ channel subunits via a disulfide bridge. *EMBO J.* **15**, 6400–6407 (1996).
97. Dodge, F. A. & Frankenhaeuser, B. Membrane currents in isolated frog nerve fibre under voltage clamp conditions. *J. Physiol.* **143**, 76–90 (1958).
98. Campbell, D. T. & Hille, B. Kinetic and pharmacological properties of the sodium channel of frog skeletal muscle. *J. Gen. Physiol.* **67**, 309–323 (1976).
99. Anderson, J. A., Huprikar, S. S., Kochian, L. V., Lucas, W. J. & Gaber, R. F. Functional expression of a probable *Arabidopsis thaliana* potassium channel in *Saccharomyces cerevisiae*. *Proc. Natl Acad. Sci. USA* **89**, 3736–3740 (1992).
100. Krapivinsky, G. *et al.* The G-protein-gated atrial K^+ channel IKACh is a heteromultimer of two inwardly rectifying K^+-channel proteins. *Nature* **374**, 135–141 (1995).
101. Abbott, G. W. MiRP2 forms potassium channels in skeletal muscle with Kv3.4 and is associated with periodic paralysis. *Cell* **104**, 217–231 (2001).
102. Splawski, I. *et al.* Spectrum of mutations in long-QT syndrome genes. KVLQT1, HERG, SCN5A, KCNE1 and KCNE2. *Circulation* **102**, 1178–1185 (2000).
103. Schroeder, B. C. A constitutively open potassium channel formed by KCNQ1 and KCNE3. *Nature* **403**, 196–199 (2000).
104. Melman, Y. F., Domenech, A., de la Luna, S. & McDonald, T. V. Structural determinants of KvLQT1 control by the KCNE family of proteins. *J. Biol. Chem.* (in the press).
105. Orias, M., Velazquez, H., Tung, R., Ilse, G. & Desir, G. V. Cloning and localization of a double-pore K channel, KCNK1: exclusive expression in distal nephron segments. *Am. J. Physiol.* **273**, F883–F896 (1997).
106. Lesage, F. *et al.* The structure, function and distribution of the mouse TWIK-1 K^+ channel. *FEBS Lett.* **402**, 28–32 (1997).
107. Fink, M. *et al.* 1998 A neuronal two P domain K^+ channel stimulated by arachidonic acid and polyunsaturated fatty acids. *EMBO J.* **17**, 3297–3308 (1998).
108. Reyes, R. *et al.* Immunolocalization of the arachidonic acid and mechanosensitive baseline mink potassium channel in the nervous system. *Neuroscience* **95**, 893–901 (2000).
109. Lesage, F., Maingret, F. & Lazdunski, M. Cloning and expression of human TRAAK, a polyunsaturated fatty acids-activated and mechano-sensitive K^+ channel. *FEBS Lett.* **471**, 137–140 (2000).
110. Reyes, R. *et al.* Cloning and expression of a novel pH-sensitive two pore domain K^+ channel from human kidney. *J. Biol. Chem.* **273**, 30863–30869 (1998).
111. Gray, A. T., Kindler, C. H., Sampson, E. R. & Yost, C. S. Assignment of KCNK8 encoding the human weak inward rectifier potassium channel TWIK-2 to chromosome band 19q13.1 by radiation hybrid mapping. *Cytogenet. Cell Genet.* **84**, 190–191 (1999).
112. Patel, A. J. *et al.* TWIK-2, an inactivating 2P domain K^+ channel. *J. Biol. Chem.* **275**, 28722–28730 (2000).
113. Chapman, C. C. *et al.* Cloning, localization and functional expression of a novel human, cerebellum specific, two pore domain potassium channel. *Mol. Brain Res.* **82**, 74–83 (2000).
114. Rajan, S. *et al.* TASK-3, a novel tandem pore domain acid-sensitive K^+ channel — an extracellular histidine as pH sensor. *J. Biol. Chem.* **275**, 16650–16657 (2000).
115. Berg, H., Kim, Y. & Kim, D. TREK-2, a new member of the mechanosensitive tandem-pore K^+ channel family. *J. Biol. Chem.* **275**, 17412–17419 (2000).
116. Lesage, F., Terrenoire, C., Romey, G. & Lazdunski, M. Human TREK2, a 2P domain mechano-sensitive K^+ channel with multiple regulations by polyunsaturated fatty acids, lysophospholipids, and Gs, Gi, and Gq protein-coupled receptors. *J. Biol. Chem.* **275**, 28398–28405 (2000).

Acknowledgements

This work was supported by grants to S.A.N.G. from the National Institutes of Health. We are grateful to our many colleagues who have shared their thoughts during the preparation of this review: D. A. Bayliss (University of Virginia), M. P. Blair (University of Glasgow), C. G. Chapman (SBPMRD), J. Daut (Universität Marburg), A. T. Gray (University of California, San Francisco), H. R. Horvitz (MIT), D. Kim (Chicago Medical School), A. Mathie (Imperial College of Science, Technology & Medicine, London), I. Perez de la Cruz (MIT), D. J. Pountney (New York University), L. Salkoff (Washington University, St. Louis), E. Talley (University of Virginia), J. White (HUGO) and S. Yost (University of California, San Francisco).

THE JOURNAL OF BIOLOGICAL CHEMISTRY
Vol. 275, No. 37, Issue of September 15, pp. 28398–28405, 2000
Printed in U.S.A.

Human TREK2, a 2P Domain Mechano-sensitive K^+ Channel with Multiple Regulations by Polyunsaturated Fatty Acids, Lysophospholipids, and G_s, G_i, and G_q Protein-coupled Receptors*

Received for publication, March 9, 2000, and in revised form, June 22, 2000
Published, JBC Papers in Press, July 3, 2000, DOI 10.1074/jbc.M002822200

Florian Lesage, Cécile Terrenoire, Georges Romey, and Michel Lazdunski‡

From the Institut de Pharmacologie Moléculaire et Cellulaire, CNRS-UPR 411, 660 route des Lucioles, Sophia Antipolis, 06560 Valbonne, France

Mechano-sensitive and fatty acid-activated K^+ belong to the structural class of K^+ channel with two pore domains. Here, we report the isolation and the characterization of a novel member of this family. This channel, called TREK2, is closely related to TREK1 (78% of homology). Its gene is located on chromosome 14q31. TREK2 is abundantly expressed in pancreas and kidney and to a lower level in brain, testis, colon, and small intestine. In the central nervous system, TREK2 has a widespread distribution with the highest levels of expression in cerebellum, occipital lobe, putamen, and thalamus. In transfected cells, TREK2 produces rapidly activating and non-inactivating outward rectifier K^+ currents. The single-channel conductance is 100 picosiemens at +40 mV in 150 mM K^+. The currents can be strongly stimulated by polyunsaturated fatty acid such as arachidonic, docosahexaenoic, and linoleic acids and by lysophosphatidylcholine. The channel is also activated by acidification of the intracellular medium. TREK2 is blocked by application of intracellular cAMP. As with TREK1, TREK2 is activated by the volatile general anesthetics chloroform, halothane, and isoflurane and by the neuroprotective agent riluzole. TREK2 can be positively or negatively regulated by a variety of neurotransmitter receptors. Stimulation of the G_s-coupled receptor 5HT4sR or the G_q-coupled receptor mGluR1 inhibits channel activity, whereas activation of the G_i-coupled receptor mGluR2 increases TREK2 currents. These multiple types of regulations suggest that TREK2 plays an important role as a target of neurotransmitter action.

Potassium channel subunits containing two pore domains form a novel class of background K^+ channels. These K_{2P} channels have unique pharmacological and functional properties (1–10). They are active at all membrane potentials and display very rapid kinetics of activation and deactivation, and no inactivation. Their widespread tissue distribution suggests that one of their major physiological role is the setting of the resting membrane potential in many different cell types. However, background K^+ channels with specific functional and regulatory properties, as well as unique tissue distribution, have now been cloned. These channels could be involved in more specific functions such as epithelial K^+ transport and regulation of neuronal and muscular excitability (11).

Various K^+ currents have been recorded *in vivo* from neuronal, cardiac, and smooth muscle cells that form a subfamily of background K^+ currents sensitive to fatty acids (12–15). Recently, fatty acid-activated K^+ channels have been cloned from mouse and human (2, 6, 16). These channels, named TREK1[1] (TWIK-related K^+ channel) and TRAAK (TWIK-related arachidonic acid-stimulated K^+ channel), produce quasi-instantaneous currents that are outwardly rectifying in physiological K^+ gradient. These channels have a low basal activity compared with TASK background channels (3–5). However, they can be strongly activated by application of arachidonic acid. This effect is specific of unsaturated fatty acids. Oleate, linoleate, eicosapentaenoate, and docosahexaenoate all strongly activate TREK1 and TRAAK, whereas saturated fatty acids such as palmitate, stearate, and arachidate are ineffective (6, 17). Another efficient way for activating these channels is the application of a stretch to the cell membrane (17, 18). Both channels are activated by shear stress, cell swelling, and negative pressure. They are mechano-sensitive K^+ channels. Compared with TRAAK, TREK1 has additional features. TREK1 is inhibited by activators of protein kinases C (PKC) and A (PKA). The site for PKA phosphorylation has been localized in the cytoplasmic carboxyl-terminal part of the channel (17). TREK1 but not TRAAK is opened by internal acidification (19). Lowering pH_i shifts the pressure-activation relationships toward positive values and leads to channel opening at atmospheric pressure. TREK1 but not TRAAK is activated by inhalational general anesthetics, halothane and isoflurane, at concentrations used in human general anesthesia (16). Finally, TREK1 and TRAAK have different tissue distributions, the expression of TRAAK being more restricted to neuronal cells than TREK1 (2, 6, 20).

This article describes the cloning, the genomic organization, the localization, and the functional characterization of a novel human K^+ channel with two pore domains. The molecular and functional properties of this channel indicates that it too belongs to the particular subclass of mechano-sensitive and unsaturated fatty acid-activated K^+ channels. TREK2 is more related to TREK1 than to TRAAK, and like TREK1, it is activated by general anesthetics at clinical concentrations. TREK2 is modulated by different types of neurotransmitter receptors.

* This work was supported by CNRS and the Association Française contre les Myopathies (AFM). The costs of publication of this article were defrayed in part by the payment of page charges. This article must therefore be hereby marked "*advertisement*" in accordance with 18 U.S.C. Section 1734 solely to indicate this fact.

The nucleotide sequence(s) reported in this paper has been submitted to the GenBank™/EBI Data Bank with accession number(s) AF279890.

‡ To whom correspondence should be addressed. Tel.: 33 (0) 4 93 95 77 02 or 03; Fax: 33 (0) 4 93 95 77 04; E-mail: ipmc@ipmc.cnrs.fr.

[1] The abbreviations used are: TREK, TWIK-related K^+ channel; TWIK, Tandem of P domains in a Weak Inward rectifying K^+ channel; TRAAK, TWIK-related arachidonic acid-stimulated K^+ channel; TASK, TWIK-related acid-sensitive K^+ channel; PKC, protein kinase C; PKA, protein kinase A; RACE, rapid amplifications of cDNA ends; PCR, polymerase chain reaction; kb, kilobase(s); contig, group of overlapping clones.

EXPERIMENTAL PROCEDURES

Cloning of TREK2—Sequences of two P-domain K^+ channels were used to search homologs in public DNA data bases by using the tBlastn alignment program and TREK1 as the query sequence (21). This led to the identification of a genomic sequence (EMBL accession number AL133279.1), which showed significant similarities with TREK1. To characterize the corresponding full-length cDNA, 5′- and 3′-rapid amplifications of cDNA ends (RACE)-PCR was performed on adult human brain cDNAs ligated with adaptors (22). Two antisense primers for 5′-RACE (5′-ACTGCCGAGGTCCCAGTGGCTGCTGTT-3′ and 5′-TCTGGCTGCTCTCAAAGGGCTGCT-3′) and two sense primers for 3′-RACE (5′-GACGATCCCTGCTGTCATCTT-3′ and 5′-TTGCAGCTGTCCTCAGTAGATCG-3′) were derived from genomic sequences. Two successive RACE reactions were performed by using anchor primers 5′-TAGAATCGAGGTCGACGGTATC-3′ and 5′-GATTTAGGTGACACTATAGAATCGA-3′. The amplified products were subcloned into pGEMt easy (Promega), and eight clones of each product were sequenced (Applied Biosystems model 373A). The entire coding sequence was amplified from human brain cDNA by PCR using a low error-rate DNA polymerase and then subcloned into the pIRES-CD8 vector to give pIRES-CD8.TREK2. Inserts from two different independent PCR ligation experiments were sequenced on both strands and found to be identical.

Analysis of TREK1, TREK2, and TRAAK Distributions—For reverse transcription-PCR experiment, multiple tissue cDNA panels were used as templates according to the manufacturer's protocol (CLONTECH). Primers were: TREK2, sense primer 5′-CAGCCCTTTGAGAGCAGCC-3′, antisense primer 5′-AAGATGACAGCAGGGATCGTC-3′; TRAAK, 5′-GAGGCCCGGCCAGG GGATCCTG-3′ and 5′-CTCAGTGCTCACCACCATCG-3′; and TREK1, 5′-GGATTTGGAAACATCTCACCACGCACA-3′ and 5′-GATCCACCTGCAACG TAGTC-3′. PCR conditions were 32 cycles of 30 s at 94 °C, 30 s at 55 °C, and 30 s at 72 °C. PCR products were separated by electrophoresis, transferred onto nylon membranes, and probed with ^{32}P-labeled primers (TREK2, 5′-ACTGCCGAGGTCCCAGTGGCTGCTGTT-3′; TRAAK, 5′-TCAGGCTGCCAGCTGGACTG-3′; TREK1, 5′-TAGCTGATCTCCAACTCCAGCCAAG-3′). For Northern blot analysis, multiple tissue Northern blots from CLONTECH were probed with the ^{32}P-labeled insert of pIRES-CD8.TREK2 in Ultrahyb hybridization buffer (Ambion) at 50 °C for 18 h then washed stepwise at 55 °C to a final stringency of 0.2 ×SSC (1× SSC = 0.15 M NaCl and 0.015 M sodium citrate), 0.3% SDS. Blots were then dehybridized according to the manufacturer's protocol and reprobed with TREK1 and TRAAK following the same procedure. A 0.7-kb *Bam*HI fragment from pCD8.hTREK1 and the insert from pIRES-CD8.hTRAAK were used as probes. Autoradiograms were exposed 24 h at −70 °C on BioMax films by using a Transcreen-HE Intensifying Screen (Eastman Kodak Co.).

Electrophysiology in Transfected COS Cells—COS cells were seeded at a density of 20,000 cells/35-mm dish 24 h before transfection. Cells were transiently transfected by the classical DEAE-dextran method with 0.2 μg of pIRES-CD8.TREK2 with or without mGluR1, mGluR2, or 5HT4sR expression vectors (a generous gift of Drs. J. P. Pin and A. Dumuis, Montpellier, France). Transfected cells were visualized 48 h after transfection using the anti-CD8 antibody-coated beads method. For whole-cell experiments, the patch electrode solution (INT) contained 150 mM KCl, 3 mM $MgCl_2$, 5 mM EGTA, and 10 mM HEPES, adjusted to pH 7.3 with KOH; the external solution (EXT) contained 150 mM NaCl, 5 mM KCl, 3 mM $MgCl_2$, 1 mM $CaCl_2$, and 10 mM HEPES, adjusted to pH 7.4 with NaOH. For outside-out patch recordings, the pipette solution was the INT solution, and the external solution was either the EXT solution (5 mM K^+) or a K^+-rich EXT solution that contained 150 mM KCl instead of 150 mM NaCl. For inside-out patch recordings, pipettes were filled with the EXT solution, and the bathing solution was the INT solution buffered either at pH 7.3 or at pH 5.6 in the internal acidosis experiments. Cells were continuously superfused with a microperfusion system during the experiment (0.2 ml/min) done at room temperature. A RK400 patch-clamp amplifier was used for whole-cell and single-channel recordings (Bio-Logic, Claix, France). Single-channel data were low pass-filtered at 5 KHz and digitized at 50 KHz using a DAT recorder (Bio-Logic, Claix, France). pClamp software was used to analyze whole-cell data and Biopatch software (Bio-Logic) to analyze single-channel data.

Concentrations of volatile anesthetics were adjusted from saturated solutions (15.3 mM isoflurane, 17.5 mM halothane, and 66.6 mM chloroform) in saline at room temperature (16). Mechanical stimulation was applied through an open loop pressure-generating system and monitored at the level of the patch pipette by a calibrated pressure sensor (17).

RESULTS

Molecular Cloning of TREK2—DNA sequences produced in the frame of the human genome sequencing program are rapidly accumulating in the public high throughput genomic sequences (HTGS) data base. Searches of this data base using the Blast sequence alignment program (21) led to the identification of human sequences restrained to a single genomic contig. The analysis of these sequences suggested the presence of introns and exons forming a gene coding for a novel K_{2P} subunit. Oligonucleotides were deduced from the potential exon sequences and used to clone cDNA fragments from human brain by using RACE-PCR. The sequence deduced from these cDNAs is 2730 base pairs long and contains an open reading frame of 1617 nucleotides, predicting a 538-amino acid polypeptide (Fig. 1*A*). This protein has the same overall structure than the previously cloned K_{2P} subunits. It displays four membrane-spanning segments (M1 to M4), two P domains (P1 and P2), and an extended loop between M1 and P1. The dendrogram shown in Fig. 1*C* clearly indicates that this subunit is more related to TREK1 and TRAAK than to other K_{2P} subunits. Therefore, this novel K_{2P} subunit was named TREK2 (gene *KCNK10* in the human genome organization (HUGO) nomenclature). TREK2 shares 63% identity and 78% homology with TREK1. The homology level falls to 69% with TRAAK and to 50–55% with the other K_{2P} subunits.

TREK2 Gene Organization and Location—The genomic organization of TREK2 was deduced from the alignment of the cloned cDNAs with the genomic sequences available in the high throughput genomic sequences (HTGS) DNA data base. The open reading frame is composed of six introns and seven exons. The amino terminus of TREK2 is encoded by exon 1, the M1 domain by exon 2, M2 by exon 4, M3 by exon 5, and M4 by exon 6. The third exon codes for the carboxyl-terminal part of the M1P1 interdomain, and the seventh one encodes the large carboxyl terminus of the channel (Fig. 1*A*). The length of introns 2–6 varies from 1.8 kb to 35 kb (Fig. 1*B*). The first exon being out of the genomic contig, the size of the first intron is not known. At this point, it cannot be excluded that the 5′-untranslated sequence corresponds to more than one exon. This organization is different than TWIK1 and TASK3 gene organizations. TWIK1 contains three exons separated by two large introns (23), and TASK3 contains only one short intron (10). However, genomic organization of TREK2 is very close to the genomic organization of both TRAAK (24) and TREK1 channel[2] genomic organizations. Introns 2 to 6 are found in the same positions. This observation confirms that these three channels are closely related and suggests that they have arisen by gene duplication from a common ancestor. A particular feature found in TWIK1, TASK1, TREK1, TREK2, TRAAK, TASK2, and TASK3 genes is the presence of a conserved intron in the sequence coding the P1 domain (third intron in the TREK2 gene). The intron site is between the first and the second nucleotides of the codon coding for the first glycine residue of the pore signature sequence G(Y/F/L)G. An intron in the same position is found in 20 genes among the 36 examined that encode potential K_{2P} channels in the nematode *Caenorhabditis elegans* (25) and in 8 genes among 11 in the *Drosophila*, as determined by analyzing its recently released genomic sequences. The significance of this conserved intron position is not known; however, it is worth noting that this intron has been conserved in mammals, where it might eventually have the same role as in the nematode. The analysis of genomic contig bearing the TREK2 gene showed that this sequence

[2] F. Lesage, C. Terrenoire, G. Romey, and M. Lazdunski, unpublished results.

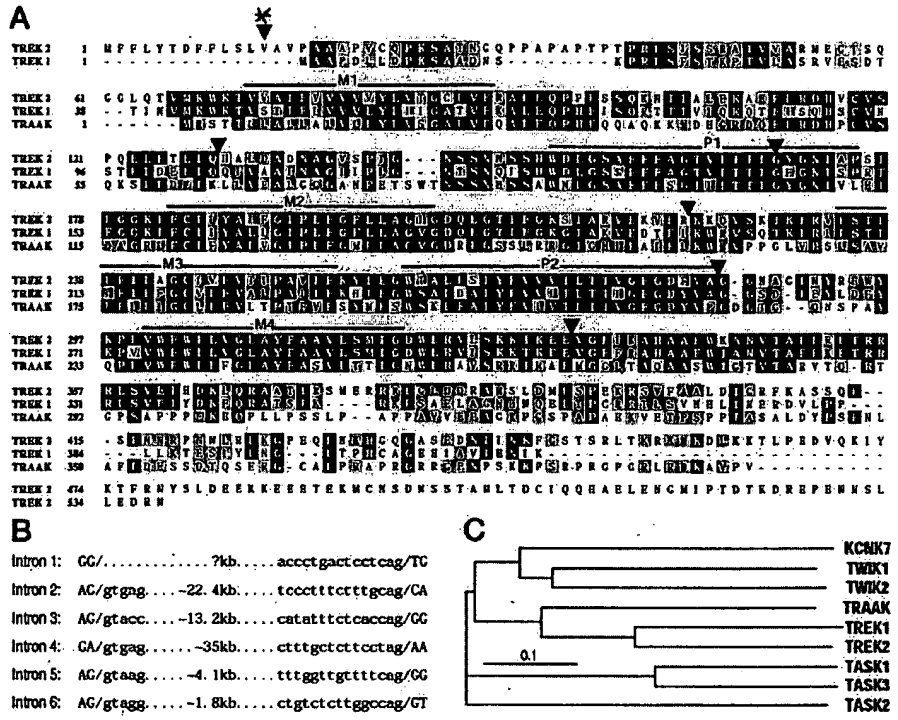

FIG. 1. **Sequence and genomic organization of TREK2.** *A*, alignment of TREK2, TREK1, and TRAAK channels. Relative positions of introns are indicated by *arrows*. M1 to M4 membrane-spanning segments and P1 and P2 pore-domains are indicated. The *star* shows the point of divergence between the TREK2 channel sequences from rat and human. *B*, sequences at the boundaries exon-intron. Exonic sequence is in *uppercase*. The sizes of introns are indicated. *C*, the dendrogram of K_{2P} channels cloned in human was established with ClustalW and Treeview.

contains two sequence tag sites, D14S1058 and WI-6710. WI-6710 has been placed on the WICGR radiation hybrid map 308.53 centiRay from the top of the Chr14 linkage group, and D14S1058 has been mapped by Genethon 86.3 centimorgan from the top of the Chr14 linkage group. These results are in agreement and indicate that the chromosomal location of TREK2 gene is 14q31. This location is different from those of TREK1 (1q41) (26) and TRAAK (11q13) (24).

Tissue Distribution of TREK2—The expression of TREK2 in various adult human tissues was examined by reverse transcription-PCR analysis. As shown in Fig. 2*A*, TREK2 is abundantly expressed in kidney and pancreas and more moderately in testis, brain, colon, and small intestine. Only very faint signals were obtained in liver, heart, prostate, and thymus. This expression pattern contrasts with the TREK1 and TRAAK tissue distributions (Fig. 2*A*). Some tissues express only one of these channels: for instance, pancreas and colon (TREK2), placenta (TRAAK), and ovary (TREK1). Other tissues do not express these channels or only to modest levels: heart, skeletal muscle, lung, peripheral blood leukocytes, and spleen. Finally, some tissues express two or three of these related channels: brain, testis, and small intestine. Distributions of TREK1, TREK2, and TRAAK in the different areas of the human brain were analyzed by Northern blot. As shown in Fig. 2*B*, the TREK2 probe detected two transcripts of 4 and 7.5 kb. TREK2 is mainly expressed in cerebellum, occipital lobe, putamen, and thalamus and to lower levels in the other examined areas. No expression was detected in amygdala and spinal cord. The 4-kb transcript is expressed at a higher level than the 7.5-kb transcript except in occipital lobe and cerebellum. As expected from the previous studies on TREK1 and TRAAK expression in rodent central nervous system (2, 6, 20), these two channels have a widespread distribution in the human brain. The 2-kb TRAAK transcript and the 2.7- and 3.3-kb TREK1 transcripts are well expressed in areas where TREK2 is mainly expressed: putamen and thalamus. In the brain cortex (occipital, frontal, and temporal lobes), TRAAK is also highly expressed. Finally, TREK1 is the only channel of this family to be expressed in the spinal cord.

Biophysical Properties of TREK2—TREK2-transfected COS cells display noninactivating currents (Fig. 3*A*) that are not present in control cells (not shown). The activation kinetics of TREK2 current are rapid. Depolarization pulses induce a two-step current composed of instantaneous and delayed components (Fig. 3*A*). The current-voltage (I-V) relationship is outwardly rectifying, and almost no inward currents were recorded in an external medium containing 5 mM K^+ (Fig. 3*B*). When cells are bathed in a K^+-rich solution (150 mM), an inward current is revealed, and the reversal potential becomes 0 mV, as expected for a K^+-selective channel. However, the I-V relationship is not linear and does not strictly fit the Goldman-Hodgkin-Katz equation for an open K^+-selective pore. The current has a tendency to saturate at very negative potentials. Two-step activation kinetics and outward rectification in symmetrical K^+ conditions have also been found for the TREK1 current (2, 17). Moreover, like TREK1, TREK2 outward currents are more important in 150 mM K^+ than in 5 mM K^+ for depolarizations higher than +50 mV. This effect is unusual since an increase of external K^+ lowers the chemical driving force for outward K^+ flux and would be expected to decrease rather than increase the currents. For TREK1, this effect has been attributed to a stimulating effect of external K^+, as found for other types of K^+ channels (27, 28). In addition, TREK1 has been shown to be sensitive to external Na_e^+ (Na_e^+). When Na_e^+ was substituted by *N*-methyl-D-glucamine, TREK1 activity was strongly decreased (2). TREK2 is only partially inhibited by removing Na_e^+ (23% of inhibition, $n = 5$, not shown). Single-channel properties of TREK2 are illustrated in Fig. 3, *C* and *D*. Basal channel activity in outside-out patches is characterized by a flickery bursting behavior (Fig. 3*C*). In physiological K^+ conditions, the I-V relationship is outwardly rectifying, and almost no inward currents were recorded as in whole-cell recording. In symmetrical conditions, inward currents were recorded in addition to outward currents, with single-channel conductances of 128 picosiemens at −40 mV and 100 picosiemens at +40 mV ($n = 5$) (Fig. 3, *C* and *D*). It is interesting to note that the single-channel I-V relationship is inwardly rectifying because the single-channel conductance in-

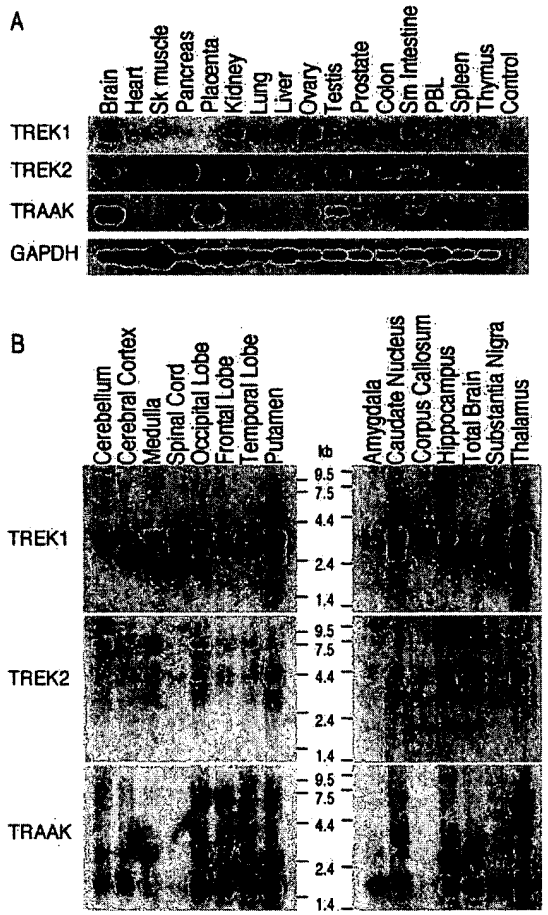

FIG. 2. **Expression of TREK2 in adult human.** *A*, tissue distribution analysis by reverse transcription-PCR. The amplified products were analyzed by Southern blot using specific internal primers as probes. To check the integrity of cDNAs, a glyceraldehyde-3-phosphate dehydrogenase fragment was amplified. *sk. muscle*, skeletal muscle; *sm intestine*, small intestine; *PBL*, peripheral blood leukocytes. *B*, localization in the brain by Northern blot analysis. Blots were hybridized at high stringency with specific probes. Each *lane* contains 2 μg of poly(A)$^+$RNA.

creases for negative potentials. However, the channel open probability at negative potentials is lower than at positive potentials (P_o = 0.26 at -40 mV and P_o = 0.45 at +40 mV, n = 5), and this explains why the currents are outwardly rectifying in the whole-cell configuration.

Stretch and pH Sensitivity of TREK2 Currents—In addition to being modulated by polyunsaturated fatty acids, TREK2, as TREK1, is stimulated by a stretch of the membrane as well as by acidification of the intracellular medium. Fig. 4*A* shows that application of a negative pressure in the inside-out configuration induces a strong activation of TREK2 activity that is reversible. The activation is graded in the function of the applied pressure (Fig. 4*B*). As shown for TREK1 and TRAAK (17, 18), stretch-induced TREK2 channel activity can be elicited at both negative and positive potentials, and the level of activation increases with depolarization (Fig. 4*C*). Fig. 4*D* shows that intracellular acidification induces a strong increase of TREK2 channel activity. This effect is reversible and is observed at all membrane potentials (Fig. 4*E*). A similar effect has been previously described for TREK1 (19). Acidification of the extracellular medium has no effect on the whole cell TREK2 current (less than 20% of inhibition at pH 6.5) (not shown).

Pharmacological Properties—TREK2 currents are insensitive to tetraethylammonium (10 mM) and Ba^{2+} (1 mM). Quinidine inhibited the currents (50% of inhibition at 100 μM) (not shown). Like TREK1, TREK2 is stimulated by application of the inhalational anesthetics chloroform, halothane, and isoflurane (Fig. 5, *A* and *B*). At a clinical dose of halothane (29), TREK2 is markedly activated (1.4 ± 0.1-fold increase at 0.25 mM, n = 10, at +100 mV). The maximal halothane effect is nearly obtained at 0.5 mM (2.6 ± 0.3-fold increase, n = 10, at +100 mV). The efficiency of anesthetics is different between TREK1 and TREK2. For TREK2, halothane (2.3 ± 0.3-fold increase at 1 mM, n = 6, at 0 mV) is more efficient than isoflurane (1.9 ± 0.1-fold increase at 1 mM, n = 6) and chloroform (1.8 ± 0.1-fold increase at 1 mM, n = 7). For TREK1, chloroform is more effective than halothane and isoflurane at the same concentrations (1 mM) (16). Fig. 5, *C* and *D*, show that TREK2 is also activated by application of the neuroprotective drug riluzole. As for TREK1, this activation is transient and is followed by a decrease of the activity corresponding to an inhibition. In the case of TREK1, this is due to an increase of the intracellular cAMP and a phosphorylation of the channel by PKA (30).

Activation of TREK2 by Fatty Acids and Inhibition by Intracellular cAMP—Fig. 6*A* illustrates the strong stimulating effect of 10 μM arachidonic acid on TREK2 current (8.4 ± 1.9-fold increase at 0 mV, n = 6). This effect is reversible (not shown). Like TREK1, TREK2 is activated by other polyunsaturated fatty acids, docosahexaenoic and linoleic acids, and by lysophosphatidylcholine but not by the saturated fatty acid palmitic acid (Fig. 6, *B* and *C*) (17, 31). TREK2 is also activated by 10 μM lysophosphatidylinositol (5.1 ± 0.6-fold increase at 0 mV, n = 8). Application of the permeant chlorophenylthio-cAMP (500 μM) led to 50% inhibition of TREK2 activity at 0 mV (50 ± 5, n = 8) (Fig. 6*D*). A similar inhibition is obtained by application of a mixture of 1 mM 3-isobutyl-1-methylxanthine, 10 μM forskolin to increase the intracellular cAMP level (72 ± 10% of inhibition, n = 8). This suggests that TREK2 as TREK1 is inhibited by PKA phosphorylation (16).

Regulation of TREK2 by Co-expression with G_s-, G_i-, and G_q-coupled Neurotransmitter Receptors—TREK2 was co-expressed with 5HT4sR, a G_s-coupled receptor. The stimulation of the receptor by application of 5-hydroxytryptamine is associated with a decrease of TREK2 activity, as expected for a receptor positively coupled to adenylate cyclase (Fig. 7*A*). Conversely, activation of the co-expressed G_i-coupled mGluR2 receptor by glutamate leads to a stimulation of TREK2 activity (Fig. 7*B*). The decrease of TREK2 activity by the stimulation of 5HT4sR is rapidly reversed after washing (Fig. 7*A*), whereas the TREK2 increase associated with mGluR2 is much slower to reverse (more than 10 min) (Fig. 7*B*). A third type of G-protein-coupled receptor was co-expressed with TREK2. This receptor is the G_q-coupled mGluR1 receptor. Activation of mGluR1 by application of glutamate led to an inhibition of TREK2 activity that is rapidly reversed by washing (Fig. 7*C*). The G_q protein is commonly associated with activation of phospholipase C and the consequent production of diacylglycerol and inositol 1,4,5-trisphosphate. Ultimately, diacylglycerol leads to activation of PKC and inositol 1,4,5-trisphosphate to an increase of intracellular Ca^{2+}. However, neither the application of the PKC-activator phorbol 12-myristate 13-acetate (100 nM) nor the addition of Ca^{2+} in the recording pipette (1 μM) was able to induce an inhibition of TREK2 (not shown).

DISCUSSION

Characterization of a Novel Channel—TREK2 is a novel member of the fatty acid-activated and mechano-sensitive K^+ channel family that includes TREK1 and TRAAK. Like these channels, TREK2 is not blocked by tetraethylammonium and Ba^{2+} and is stimulated by polyunsaturated fatty acids, such as

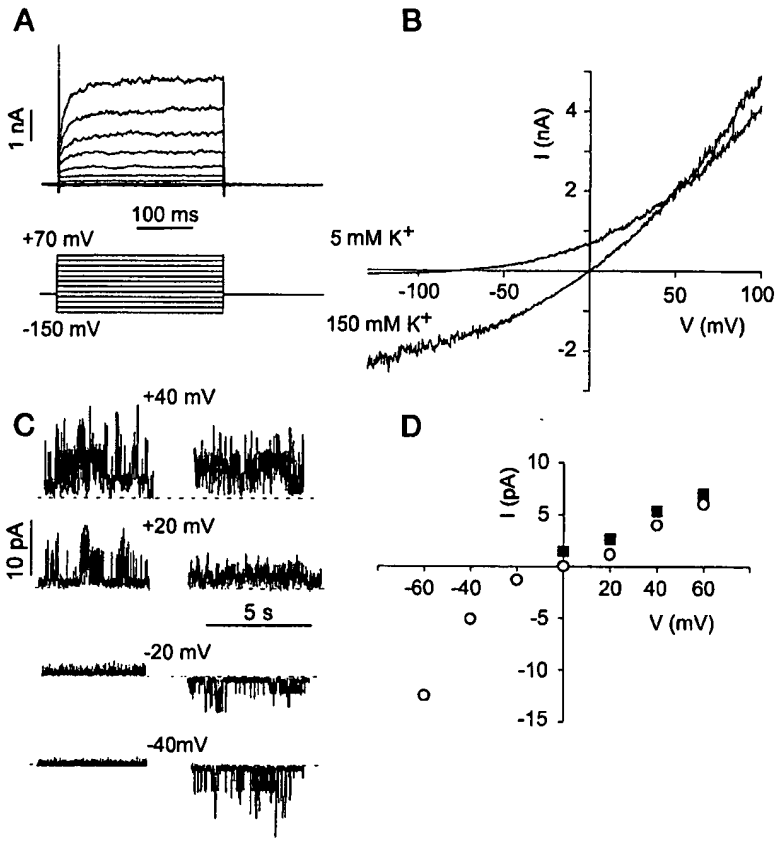

FIG. 3. **Biophysical properties of TREK2 currents.** *A*, whole-cell configuration. Superimposed current traces elicited by voltage steps from −150 mV to +70 mV by increments of 20 mV. *B*, current-voltage (I-V) relationships in physiological (5 mM K^+) and symmetrical (150 mM K^+) K^+ gradients (800-ms voltage ramps from −130 to +100 mV from a holding potential of −80 mV). *C*, steady-state single-channel activities at the indicated potentials. Outside-out patch mode in physiological (*left traces*) and symmetrical (*right traces*) K^+ conditions. *D*, single-channel I-V curves of TREK2 obtained from outside-out patches in physiological (*filled square*) and symmetrical (*open circle*) K^+ conditions. Mean of five examined patches. Single-channel conductance was 128 picosiemens at −40 mV and 100 picosiemens at +40 mV when measured in symmetrical K^+ conditions.

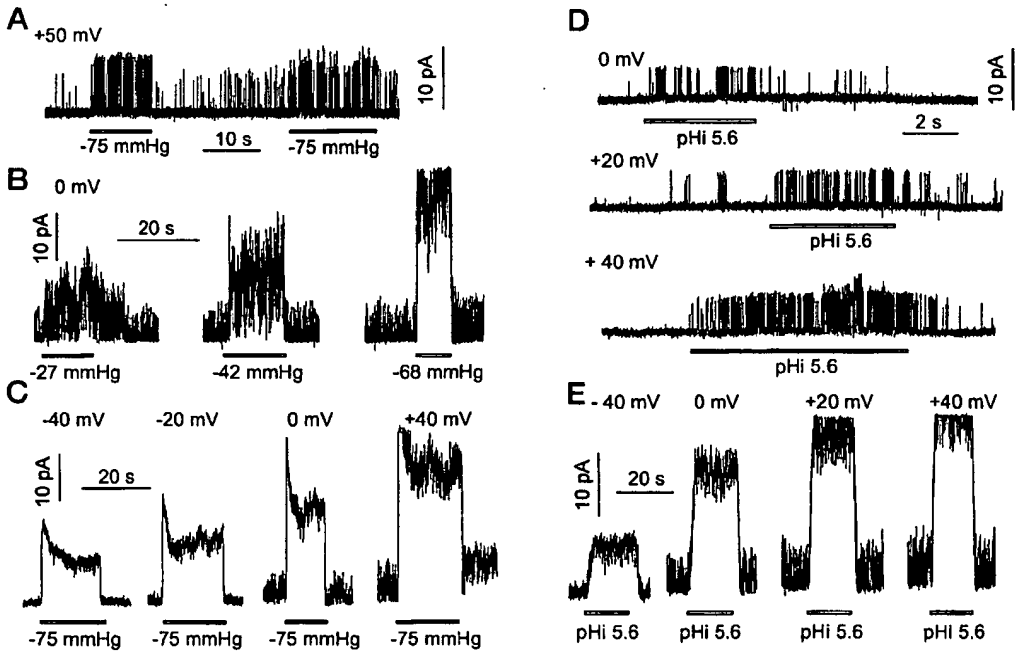

FIG. 4. **Activation of TREK2 by a stretch of the membrane and by internal acidosis.** *A*, reversible activation of TREK2 by membrane stretch in an inside-out patch exhibiting a low basal activity at +50 mV. *B*, effects of increasing stretch stimulation (in mm of Hg) on TREK2 activation in an multi-channel inside-out patch held at 0 mV. *C*, multi-channel inside-out patch. Effects of membrane voltage (as indicated) on TREK2 activation by the same membrane stretch (−75 mm of Hg). *D*, reversible activation of TREK2 by internal acidosis (pH_i 5.6) in a patch displaying a low basal activity. The maximum TREK2 activation is obtained in depolarized conditions. *E*, multi-channel inside-out patch. Voltage dependence of activation by internal acidosis at pH 5.6 is shown. In *A* and *B*, the control value of pH_i was kept at 7.3.

arachidonic, docosahexaenoic, and linoleic acids, by lysophospholipids and by application of a negative pressure to the cell membrane. In addition, TREK2 shares with these channels the same gene organization, indicating that the three genes probably derive from a common ancestral gene. However, TREK2 is more related to TREK1 than to TRAAK. TREK2 and TREK1

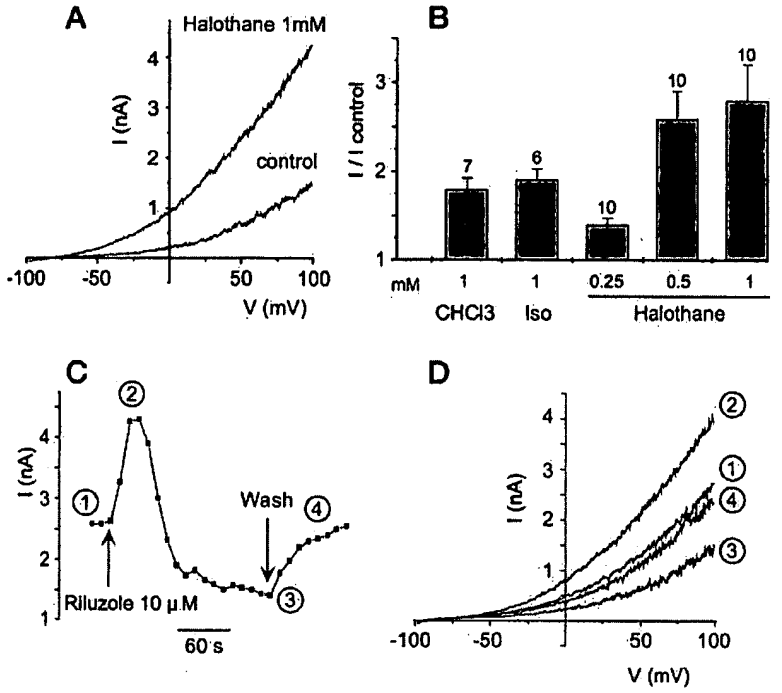

FIG. 5. **Activation of TREK2 by volatile anesthetics and riluzole.** *A*, halothane (1 mM) stimulates TREK2 channel activity elicited in the whole-cell configuration. The I-V curves were obtained with a voltage-ramp protocol of 800-ms duration starting from a holding potential of −80 mV. *B*, activation of TREK-2 channel activity by chloroform ($CHCl_3$), isoflurane (*Iso*), and halothane. The number of cells in each experimental condition is indicated above the *bar*. *C*, transient activation of TREK2 by riluzole. Evolution of the current under control conditions (*1*), after a 20-s application of riluzole (*2*), after a 3-min application of riluzole (3), and after a 1-min wash (4). The voltage-clamp protocol consists of the same ramp as in *A* applied every 10 s. The current was monitored at +100 mV. *D*, corresponding I-V curves of the experiment shown in *C*.

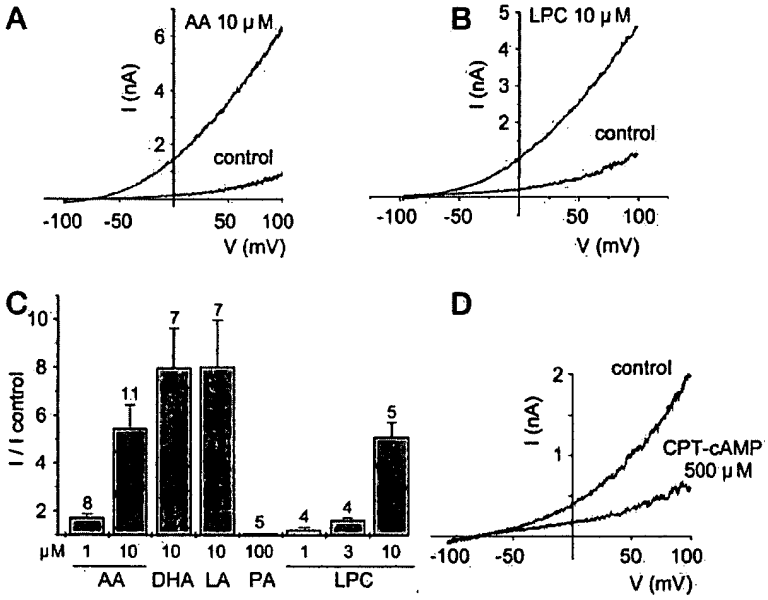

FIG. 6. **Activation of TREK2 by polyunsaturated fatty acids and lysophosphatidylcholine and inhibition by cAMP.** *A*, activation by arachidonic acid (*AA*) of the whole-cell TREK2 current. The I-V curves were obtained with a voltage-ramp protocol of 800-ms duration starting from a holding potential of −80 mV. *B*, activation by lysophosphatidylcholine (*LPC*). The protocol was as in *A*. *C*, effect of fatty acids on TREK2. *DHA*, docosahexaenoic acid; *LA*, linoleic acid; *PA*, palmitic acid. *D*, regulation of TREK2 channel activity by cAMP. Inhibition of the current after external application of 500 µM chlorophenylthio-cAMP (CPT-cAMP). The voltage protocol was as in *A*.

have unique functional and pharmacological properties that are not shared by TRAAK; they are negatively regulated by agents that activate PKA, positively regulated by acidification of internal medium, and strongly activated by volatile general anesthetics. Like TREK1, TREK2 is also transiently activated by riluzole, whereas TRAAK is permanently activated. For TREK1, the inhibition that follows activation by riluzole has been related to an increase of intracellular cAMP and a consequent inhibitory PKA phosphorylation of the channel (30). In molecular terms, TREK2 is also more related to TREK1, not only if one considers the overall sequence homology but also the distribution of this homology along the sequences. TRAAK, TREK1, and TREK2 have a conserved domain that extends from M1 to M4. Between TREK1 and TREK2, the homology level remains high after M4 and continues over 50 residues. This post-M4 carboxyl-terminal part is crucial for TREK1 channel sensitivity to fatty acids and stretch but also to PKA and pH_i (17, 16, 19). The high level of conservation in this domain between TREK1 and TREK2 explains why these channels have closely related mechanisms of regulation. Interestingly, the PKA site, which is implicated in the negative regulation by phosphorylation of TREK1 (17), is conserved in TREK2 (serine 359), suggesting that TREK2 is negatively regulated by PKA in the same way as TREK1. In TREK1, the cytoplasmic amino terminus is not important for the channel activity and for its mechanical and chemical regulations (17, 16, 19). This is also the case for TREK2 because a truncated TREK2 beginning at methionine 55 apparently conserves its properties after the removal of the first 54 residues by mutagenesis (not shown). While this manuscript was being reviewed, the cloning of a novel channel from rat has been published on line (32). This channel is clearly the rat ortholog of

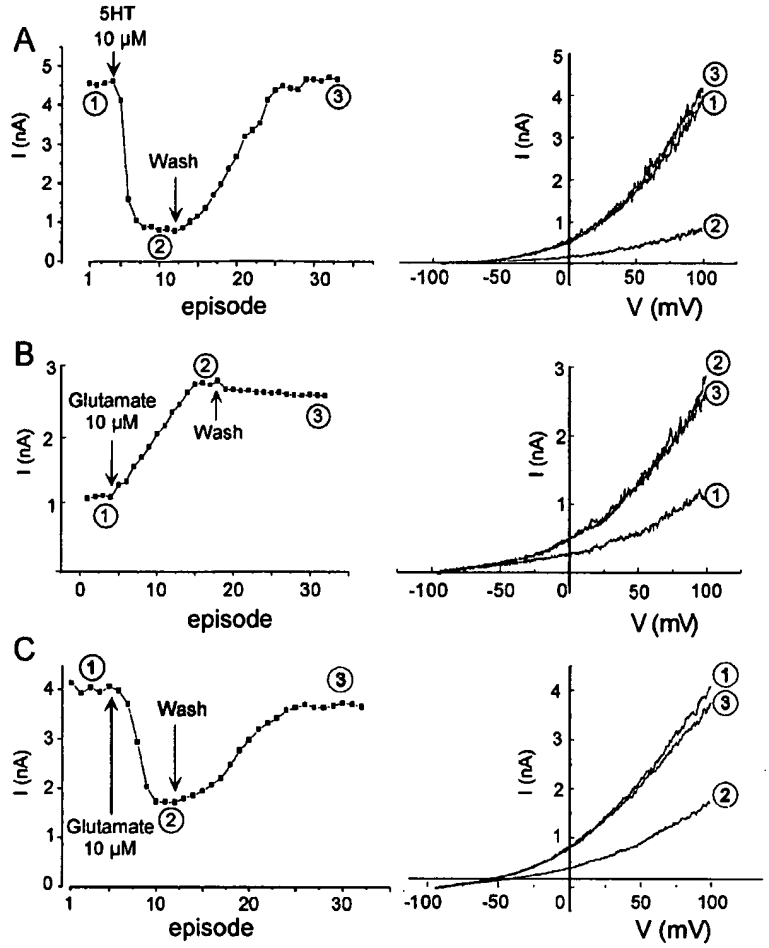

FIG. 7. **Regulation of TREK2 by G-protein-coupled receptors.** *Left*, evolution of the whole-cell TREK2 current under control conditions (*1*) at the steady-state effect after receptor activation (*2*) and after wash (3). The voltage-clamp protocol consists of a voltage-ramp of 800-ms duration starting from a holding potential of −80 mV applied every 10 s. The current was monitored at +100mV. *Right*, corresponding I-V curves of the experiments shown on the *left*. The TREK2 channel was co-expressed together with 5HT4sR (*A*), mGluR2 (*B*), or mGluR1 (*C*) receptors. The receptors were activated by application of 5-hydroxytryptamine (*5HT*) for 5HT4sR and glutamate for mGluR1 and 2. No effect on TREK2 current were seen after 5-hydroxytryptamine and glutamate applications on COS cells transfected with only TREK2.

human TREK2. These channels have a similar tissue distribution, except in the kidney, where TREK2 is not expressed in the rat although it is highly expressed in the human. In addition, they share many common functional properties such as single channel conductance and sensitivity to polyunsaturated fatty acids and stretch. However, despite of a high sequence identity (more than 70%), the cytoplasmic amino-terminal part encoded by the first exon (Fig. 1*A*) is clearly unrelated between these two channels, suggesting alternative splicing from a single gene.

What Could Be the Physiological role of TREK2?—In neurons cultured from mesencephalic and hypothalamic areas of rat brain, several arachidonic acid-activated and mechano-sensitive K^+ currents have been characterized (15). Their functional properties are very similar to the properties of TREK-related channels. Three different native currents have been identified in neurons with I-V relationships being slightly outwardly rectifying or linear or slightly inwardly rectifying in high symmetrical K^+ conditions. Under the same conditions, the I-V relationship of TREK1 is slightly outwardly rectifying, and the I-V relationship of TRAAK is linear. These results together with the fact that TREK1 and TRAAK are expressed in brain areas that contain neurons expressing the native currents suggested that both cloned channels contribute to these native currents. None of the channels cloned until now corresponded to the third type of current with an inward rectification. From the Northern blot analysis, it appears that TREK2 is expressed in the same brain areas as TREK1. Since TREK2 produces currents whose I-V relationship is slightly inwardly rectifying, we propose that TREK2 could form or contribute to the formation of this third type of native arachidonic acid-activated and mechano-sensitive current with inward rectification. These channels are expected to play a role in the control of neuronal excitability and, particularly, in the control of the resting membrane potential if they are active at rest *in vivo*. The level of TREK2 activity can be regulated by the three different types of G-protein-coupled receptors. This indicates that TREK2 activity in neurons is probably fine-tuned by a variety of neurotransmitters and that TREK2 could play a role similar to the role of the K_{2P} channel TASK1. In cerebellar granule cells and hypoglossal motoneurons, TASK1 has a central importance in controlling cell excitability, and the modulation of its activity by a variety of neurotransmitters acting via G_q-coupled receptors profoundly alters both resting membrane potential and excitability (33, 34). It is interesting to note that the signal transduction pathway by which G_q-coupled receptor inhibits TASK1 does not involve PKC or Ca^{2+} (33, 34), as also observed for TREK2. A major difference between TASK1 and TREK2 is that TREK2 is also regulated via G_i- and G_s-coupled receptors. TREK2 will probably turn out to be an important channel in charge of tuning neuronal excitability in response to a variety of neurotransmitters and hormones. The isolation and the characterization of TREK2 constitute an additional step toward the understanding of this particular class of K^+ channels, which probably plays a wide variety of important physiological roles in the brain and other tissues (11) and that, because it is a target of volatile anesthetics (Ref. 16 and this article) and riluzole, a neuroprotective drug (6, 30), might have an important impact in medicine.

Acknowledgments—We are grateful to Drs. J. Bockaert, J. P. Pin, and A. Dumuis for providing us with the G-protein-coupled receptor expression vectors. We thank Valérie Lopez for secretarial assistance.

REFERENCES

1. Lesage, F., Guillemare, E., Fink, M., Duprat, F., Lazdunski, M., Romey, G., and Barhanin, J. (1996) *EMBO J.* **15,** 1004–1011
2. Fink, M., Duprat, F., Lesage, F., Reyes, R., Romey, G., Heurteaux, C., and Lazdunski, M. (1996) *EMBO J.* **15,** 6854–6862
3. Duprat, F., Lesage, F., Fink, M., Reyes, R., Heurteaux, C., and Lazdunski, M. (1997) *EMBO J.* **16,** 5464–5471
4. Leonoudakis, D., Gray, A. T., Winegar, B. D., Kindler, C. H., Harada, M., Taylor, D. M., Chavez, R. A., Forsayeth, J. R., and Yost, C. S. (1998) *J. Neurosci.* **18,** 868–877
5. Kim, D., Fujita, A., Horio, Y., and Kurachi, Y. (1998) *Circ. Res.* **82,** 513–518
6. Fink, M., Lesage, F., Duprat, F., Heurteaux, C., Reyes, R., Fosset, M., and Lazdunski, M. (1998) *EMBO J.* **17,** 3297–3308
7. Reyes, R., Duprat, F., Lesage, F., Fink, M., Salinas, M., Farman, N., and Lazdunski, M. (1998) *J. Biol. Chem.* **273,** 30863–30869
8. Salinas, M., Reyes, R., Lesage, F., Fosset, M., Heurteaux, C., Romey, G., and Lazdunski, M. (1999) *J. Biol. Chem.* **274,** 11751–11760
9. Kim, Y., Bang, H., and Kim, D. (2000) *J. Biol. Chem.* **275,** 9340–9347
10. Rajan, S., Wischmeyer, E., Liu, G. X., Preisig-Müller, R., Daut, J., Karschin, A., and Derst, C. (2000) *J. Biol. Chem.* **275,** 16650–16657
11. Lesage, F., and Lazdunski, M. (1999) in *Potassium Ion Channels: Molecular Structure, Function, and Diseases* (Kurachi, Y., Jan, L. Y., and Lazdunski, M., ed) Vol. 46, pp. 199–222, Academic Press, Inc., San Diego, CA
12. Premkumar, L. S., Gage, P. W., and Chung, S. H. (1990) *Proc. R. Soc. Lond. B. Biol. Sci.* **242,** 17–22
13. Ordway, R. W., Singer, J. J., and Walsh, J. V., Jr. (1991) *Trends Neurosci.* **14,** 96–100
14. Kim, D., and Clapham, D. E. (1989) *Science* **244,** 1174–1176
15. Kim, D. H., Sladek, C. D., Aguadovelasco, C., and Mathiasen, J. R. (1995) *J. Physiol. (Lond.)* **484,** 643–660
16. Patel, A. J., Honoré, E., Lesage, F., Fink, M., Romey, G., and Lazdunski, M. (1999) *Nature Neurosci.* **2,** 422–426
17. Patel, A. J., Honoré, E., Maingret, F., Lesage, F., Fink, M., Duprat, F., and Lazdunski, M. (1998) *EMBO J.* **17,** 4283–4290
18. Maingret, F., Fosset, M., Lesage, F., Lazdunski, M., and Honoré, E. (1999) *J. Biol. Chem.* **274,** 1381–1387
19. Maingret, F., Patel, A. J., Lesage, F., Lazdunski, M., and Honoré, E. (1999) *J. Biol. Chem.* **274,** 26691–26696
20. Reyes, R., Lauritzen, I., Lesage, F., Etaiche, M., Fosset, M., and Lazdunski, M. (2000) *Neuroscience* **95,** 893–901
21. Altschul, S. F., Gish, W., Miller, W., Myers, E. W., and Lipman, D. J. (1990) *J. Mol. Biol.* **215,** 403–410
22. Waldmann, R., Bassilana, F., de Weille, J., Champigny, G., Heurteaux, C., and Lazdunski, M. (1997) *J. Biol. Chem.* **272,** 20975–20978
23. Arrighi, I., Lesage, F., Scimeca, J. C., Carle, G. F., and Barhanin, J. (1998) *FEBS Lett.* **425,** 310–316
24. Lesage, F., Maingret, F., and Lazdunski, M. (2000) *FEBS Lett.* 137–140
25. Wang, Z. W., Kunkel, M. T., Wei, A., Butler, A., and Salkoff, L. (1999) *Ann. N. Y. Acad. Sci.* **868,** 286–303
26. Lesage, F., and Lazdunski, M. (1998) *Genomics* **51,** 478–479
27. Carmeliet, E. (1989) *Pfluegers Arch.* **414,** Suppl. 1, S88–S92
28. Pardo, L. A., Heinemann, S. H., Terlau, H., Ludewig, U., Lorra, C., Pongs, O., and Stühmer, W. (1992) *Proc. Natl. Acad. Sci. U. S. A.* **89,** 2466–2470
29. Lopes, C. M., Franks, N. P., and Lieb, W. R. (1994) *Nature* **367,** 607–614
30. Duprat, F., Lesage, F., Patel, A. J., Fink, M., Romey, G., and Lazdunski, M. (2000) *Mol. Pharmacol.* **57,** 906–912
31. Maingret, F., Patel, A. J., Lesage, F., Lazdunski, M., and Honoré, E. (2000) *J. Biol. Chem.* **275,** 10128–10133
32. Bang, H., Kim, Y., and Kim, D. (2000) *J. Biol. Chem.* **275,** 17412–17419
33. Millar, J. A., Baratt, A. P., Southan, A. P., Page, K. M., Fyffe, R. E. W., Robertson, B., and Mathie, A. (2000) *Proc. Natl. Acad. Sci. U. S. A.* **97,** 3614–3618
34. Talley, E. M., Lei, Q., Sirois, J. E., and Bayliss, D. A. (2000) *Neuron* **25,** 399–410

CHEMICON® INTERNATIONAL
a division of Serologicals® Corporation

RABBIT ANTI-TREK2 POLYCLONAL ANTIBODY

CATALOG NUMBER: AB5933

LOT NUMBER: xxxxxxx

QUANTITY: 50 µL

BACKGROUND: Mechano-sensitive and fatty acid-activated K channels belong to the structural class of K channel with two pore domains (2P domains) TREK2 is a novel member of this family. This channel is closely related to TREK1 (78% of homology). TREK2 in human is abundantly expressed in pancreas and kidney and to a lower level in brain, testis, colon, and small intestine. In the central nervous system, TREK2 has a widespread distribution with the highest levels of expression in cerebellum, occipital lobe, putamen, and thalamus. In transfected cells, TREK2 produces rapidly activating and non-inactivating outward rectifier K currents. The currents can be strongly stimulated by polyunsaturated fatty acid such as arachidonic, docosahexaenoic, and linoleic acids and by lysophosphatidylcholine. The channel is also activated by acidification of the intracellular medium. TREK2 is blocked by application of intracellular cAMP. As with TREK1, TREK2 is activated by the volatile general anesthetics chloroform, halothane, and isoflurane and by the neuroprotective agent riluzole. TREK2 can be positively or negatively regulated by a variety of neurotransmitter receptors. Stimulation of the Gs-coupled receptor 5HT4sR or the Gq-coupled receptor mGluR1 inhibits channel activity, whereas activation of the Gi-coupled receptor mGluR2 increases TREK2 currents. These multiple types of regulations suggest that TREK2 plays an important role as a target of neurotransmitter action.

SPECIFICITY: TREK2 (Kcnk10)

IMMUNOGEN: Synthetic peptide from rat TREK2.

APPLICATIONS: Western blotting: 1:500-1:1,000
Optimal working dilutions must be determined by the end user.

SPECIES REACTIVITIES: Rat. Other species have not been tested.

FORMAT: Rabbit serum

PRESENTATION: Liquid with 0.05% sodium azide.

STORAGE/HANDLING: Maintain at -20°C in undiluted for up to 6 months. Avoid repeated freeze/thaw cycles.

RELATED REFERENCE: Bang, H., et al., *PNAS.USA* (1987) **84** (8):2532-2536.

Important Note: *During shipment, small volumes of product will occasionally become entrapped in the seal of the product vial. For products with volumes of 200 µL or less, we recommend gently tapping the vial on a hard surface or briefly centrifuging the vial in a tabletop centrifuge to dislodge any liquid in the container's cap.*

For research use only; not for use as a diagnostic.

USA & Canada • Phone: +1(800) 437-7500 • Fax: +1 (909) 676-9209 • Europe +44 (0) 23 8026 2233
Australia +61 3 9839 2000 • Germany +49-6192-207300 • ISO Registered worldwide
www.chemicon.com • custserv@chemicon.com • techserv@chemicon.com

CHEMICON® INTERNATIONAL
a division of Serologicals® Corporation

APPLICATION NOTES FOR AB5933

WESTERN BLOT

Solubilized brain extract was examined by SDS-PAGE (4-40% tris-glycine gel) under reducing conditions. The gel was transferred to a nitrocellulose membrane and blocked overnight at room temperature with casein blocking buffer. Following blocking, primary antibody was added for 4 hours at room temperature. Membranes were then washed and incubated with alkaline phosphatase conjugated secondary antibody (CHEMICON catalog number AP108A) for 45 minutes at room temperature. After washing the membranes were treated with BCIP/NBT substrate reagents (CHEMICON catalog number ES006 to visualize immobilized protein.

For research use only; not for use as a diagnostic.

USA & Canada • Phone: +1(800) 437-7500 • Fax: +1 (909) 676-9209 • Europe +44 (0) 23 8026 2233
Australia +61 3 9839 2000 • Germany +49-6192-207300 • ISO Registered worldwide
www.chemicon.com • custserv@chemicon.com • techserv@chemicon.com